IN THE UNITED STATES PATENT AND TRADEMARK OFFICE

In re Application of	)	
	)	
G. WANG et al.	)	Art Unit: **3777**
	)	
Application No. **10/791,140**	)	Examiner: **Peter Luong**
	)	
Filing Date: **March 2, 2004**	)	Confirmation No.: **3175**
	)	
For: **SYSTEMS AND METHODS FOR BIOLUMINESCENT COMPUTED TOMOGRAPHIC RECONSTRUCTION**	)	

DECLARATION UNDER 37 C.F.R. §1.132

Commissioner for Patents
P.O. Box 1450
Alexandria, VA 22313-1450

Ballard Spahr LLP
Customer No. 23859

April 20, 2011

Dear Sir:

I, Ge Wang, Ph.D., a citizen of the United States, residing at 1222 Redbud Road, Blacksburg, VA 24060, hereby declare that:

(1) I am the Samuel Reynolds Pritchard Professor at the Virginia Tech – Wake Forest University School of Biomedical Engineering & Sciences. I received my Ph.D. at the State University of New York at Buffalo.

(2) I am a Fellow of the American Institute for Medical and Biological Engineering (AIMBE) (for seminal contributions to the development of single-slice spiral, cone-beam spiral, and micro CT), a Fellow of the Institute of Electrical and Electronics Engineers (for contributions to x-ray tomography); a Fellow of the International Society for Optical Engineering (for specific achievements in bioluminescence tomography and x-ray computed tomography), and a Fellow of the Optical Society of America (for pioneering contributions to development of bioluminescence tomography).

(3) I am the Director of the Biomedical Imaging Division at Virginia Tech – Wake Forest University School of Biomedical Engineering and Sciences, and the Director of the Institute of Critical Technology & Applied Science Center for Biomedical Imaging at Virginia Tech. Detailed professional experience is presented in **Exhibit A**.

(4) University of Iowa Research Foundation is the assignee of the above-identified application. From 2004-2006, I was the Director of the Center for X-ray & Optical Tomography at the University of Iowa, and a Professor at the Department of Radiology of the University of Iowa.

(5) I am an inventor of the invention embodied in the above-referenced patent application, and I have read and understand the application. The following is a summary of information related to imaging of soft condensed matter and, more specifically to imaging based on bioluminescence, which provide evidence of the inoperability of the art cited in the outstanding Office action issued for the instant application.

(6) Bioluminescence is the production and emission of light by a living organism ***without external light excitation***. Bioluminescence is generated through chemical reactions. Light emitted through bioluminescence spans the visible and infrared portions of the spectrum of electromagnetic radiation. In contrast, fluorescence is the production of light in response to an ***excitation with external light*** supplied by an external light source. In the absence of such excitation, light cannot be produced.

The foregoing distinction amongst bioluminescence and fluorescence is widely recognized amongst researchers as evidenced by dedicated, separate treatment of each topic in the literature. See, for example, **Exhibit B** [V. Ntziachristos et al., *Looking and listening to light: the evolution of whole-body photonic imaging,* Nature Biotechnology **23**, 313-320 (2005)] and **Exhibit C** [G. Choy et al., *Comparison of noninvasive fluorescent and bioluminescent small animal optical imaging*, BioTechniques **35**, 1022-1030 (2003)], which discloses (page 1022, col. 2:1-11):

> Typical of fluorescent imaging, acquisition of GFP signal relies on excitation by an external light source. Bioluminescence imaging, on the other hand, is based on the endogenous production of light by the expression of the enzyme luciferase. This enzyme, found in fireflies

> and other bioluminescent organisms, produces light upon reacting with the substrate luciferin in the presence of oxygen and ATP.

In addition, the foregoing distinction amongst bioluminescence and fluorescence results has various implications related to implementation of imaging systems. For example, a bioluminescence imaging system has no external source of light excitation. The associated reconstruction process of a bioluminescent source thus relies on a radiative transport equation or an approximation thereof, wherein such equation or the approximation thereof does not incorporate term(s) describing an external light source for excitation. In contrast, a formalism for reconstruction of a light source in a fluorescence imaging system requires incorporation of term(s) describing the external light source for excitation that enables fluorescence. For another example, in a bioluminescence imaging system, a light detection camera has a dynamic range substantively different from that in a fluorescence imaging system.

(7) Bioluminescence imaging generally is more sensitive than fluorescence imaging, as shown in the abstract of **Exhibit C**:

> Bioluminescent luciferase imaging was shown to be more sensitive than fluorescent GFP imaging. Luciferase-expressing tumors were detected as early as 1 day after tumor cell inoculation, whereas GFP-expressing tumors were not detected until 7 days later.

Bioluminescence imaging and fluorescence imaging are exploited complementarily rather than mutually exclusively.

(8) Features recited in independent claims 1 and 16 of the instant patent application are directed to fusion of three-dimensional (3D) tomographic modalities. As evidenced by **Exhibit B** at page 318, col. 2:12-14, fusion of tomographic modalities for 3D reconstruction of a bioluminescent source distribution in a small animal was unavailable prior to the disclosure set forth in the instant patent application. Such a synergistic combination is important to enable ***correction of optical heterogeneity*** inside an animal's anatomy so that ***the 3D reconstruction of bioluminescent sources***, rather than reconstruction of tissue properties, can be accurate and reliable. To the best of my knowledge, the combination of ***bioluminescence imaging and X-ray CT/micro-CT*** was not exploited for molecular and cellular imaging of soft condensed matter by persons of ordinary skill in the art at the time the invention claimed in the instant patent application was made.

(9) Without the benefit of the disclosure of the instant patent application, transition from fluorescence reconstruction to bioluminescence tomography (BLT) is non-obvious because bioluminescence reconstruction is significantly more challenging. (See, for example, **Exhibit B** at page 31, col. 2:1-6.) In particular, yet not exclusively, collection of optical data for fluorescence reconstruction can exploit multiple patterns of external light excitation; for example, a laser beam can be incident at different locations on the body surface of an animal. As a result, for each of the light excitation patterns, it is possible to record one set of optical views (or optical datasets) around the animal. Multiple optical datasets of such type can be exploited as input to a 3D reconstruction method. In contrast, when bioluminescent optical data, or bioluminescent views, are collected for 3D bioluminescence reconstruction, such data are passively observed around an animal or an object and only a single optical dataset can be recorded around the animal or the object, as opposed to the multiple optical datasets that can be gathered in the case of fluorescence tomography. Fluorescence reconstruction can be performed in a purely optical manner when data from micro-CT is unavailable. The rather limited amount of data in the case of bioluminescence tomography renders 3D bioluminescent reconstruction uniquely challenging. The non-obvious contribution of the present invention is accomplishing bioluminescence tomography by mitigating the lack of multiple optical datasets by including a wealth of anatomical and optical information derived from the fusion of bioluminescence imaging and other modalities of imaging soft tissue. In addition, the combination of micro-CT and bioluminescence imaging is specifically disclosed and claimed (see claim 26) in the instant patent application. The invention embodied and claimed in the instant patent application permits 3D bioluminescence reconstruction through the fusion of two or more imaging modalities.

The non-obvious distinction that would have prevented a person of ordinary skill in the art to modify fluorescence tomography to arrive at the invention claimed in the instant patent application is that fluorescence tomography is an ***active imaging mode***, reliant on controllable external light excitation and that utilizes ***multiple optical datasets***, whereas bioluminescence tomography is a ***passive imaging mode*** without controllable external light excitation and that utilizes ***a single set of bioluminescent views around a probed living organism***.

(10) The primary document (Warren et al) cited in the outstanding Office action is an inoperable reference, as evidenced by statements (6) through (9) conveyed herein. In particular,

Warren et al. is entitled "Combined ultrasound and fluorescence spectroscopy for physico-chemical imaging of atherosclerosis," and generally discloses (see, e.g., Abstract) "[t]his paper describes a combined ultrasonic and spectroscopic system for remotely obtaining physico-chemical images of normal arterial tissue and atherosclerotic plaque." In addition, Warren et al. discloses (see Abstract), inter alia:

> Despite variations in detector-tissue separation, R, fluorescence powers corresponding to pixels in the image are converted to the same set of calibrated units using distance estimations from A-mode ultrasound reflection times. An empirical model, validated by Monte Carlo simulation of light propagation in tissue, is used to describe changes in fluorescence power a function of R. Fluorescence spectra of normal and atherosclerotic human aorta obtained with this system are presented as a function of R.

Other passages of Warren et al. make it readily apparent that spectroscopy disclosed in Warren et al. relates to fluorescence spectroscopy.

Pursuant MPEP §716.07, it is noted that steps a person of ordinary skill would take in attempting to achieve the claimed invention set forth in the instant patent application include modifying Warren et al. to perform bioluminescence detection rather than fluorescence. Since bioluminescence does not rely on an external light excitation, the person of ordinary skill in the art would disable the continuous-wave (CW) Argon Ion Laser (see FIG. 2 in Warren et al.) that serves as the source of external light excitation (see page 124, Sec. III, in Warren et al.) and permits fluorescence spectroscopy. Yet, in view of statement (6), removal of such source of external light excitation precludes generation of emitted light, or fluorescence. Thus, without fluorescence in Warren et al., "remotely obtaining physico-chemical images of normal arterial tissue and atherosclerotic plaque" (Abstract; Warren et al.) is no longer feasible. Therefore, Warren et al. is rendered inoperable.

In addition, and pursuant to MPEP §716.07, it is submitted that steps a person of ordinary skill in the art would take to achieve the claimed invention set forth in the instant patent application also would include incorporation of bioluminescent material into a sample probed in Warren et al. Since Warren et al. is directed to fluorescence spectroscopy rather than bioluminescence spectroscopy, and in view of statement (6), a formalism for reconstruction of a light source in a fluorescence imaging system such as that of Warren et al. requires incorporation

of term(s) describing the external light source for excitation that enables fluorescence. Yet, such terms would be absent when the external excitation light source in Warren et al. is removed. Therefore, even when the person of ordinary skill in the art incorporates bioluminescent material into a sample probed in Warren et al., reconstruction of such light source will be inoperable because terms describing external light sources will be removed by the person of ordinary skill in the art.

(11) As described herein, the claimed subject matter in the instant patent application is distinguishable from art cited in the record. Yet, various claimed aspects in the instant patent application further define over such art. As an example, the claimed feature of "***at least one of the finite-element method, the mesh-free method and the Monte Carlo method***" is not taught by the cited art. Art cited in the record (Warren et al.) only teaches fluorescence imaging and uses neither one of: finite element/mesh-free or Monte Carlo methods for 3D reconstruction. Rather, the cited art discloses application of a Monte Carlo method to validate a simple correction model.

As a result of the contributions to the field of bioluminescence tomography provided by the various aspects disclosed in the instant patent application, the finite element method is now utilized almost exclusively for 3D bioluminescence source reconstruction in the field.

(12) The invention embodied in the instant patent application is directed to a long-felt need recognized by those of ordinary skill in the art. Pursuant to MPEP §716.04, evidence in support of such statement is provide by federal funding in the amount of $1,963,610 awarded by the National Institutes of Health/National Institute of Biomedical Imaging and Bioengineering (NIH/NIBIB) under Grant No. R21/33 EB1685 during the period beginning on March 2003 and ending February 2010. (See page 2 of **Exhibit A**.) Such substantive financial support readily indicates that that invention can satisfy the long-felt need and it also shows unsuccessful efforts by others to solve the problem of soft tissue imaging. In addition, financial support of such magnitude conveys that mere modification of the art available at the time the invention was made would not arrive at the invention embodied in the instant patent application.

(13) The leading companies commercializing equipment for imaging soft tissue with bioluminescence are only recently exploring the possibility of utilizing the imaging modality

based on the fusion approach disclosed in the present patent application, as evidenced by the correspondence presented in **Exhibit D**. This fact evidences unsuccessful efforts by others to solve the problem of soft tissue imaging. Moreover, this fact indicates that without the benefit of the invention embodied in the present patent application, 3D reconstruction of bioluminescent sources is likely to be commercially unviable.

I declare that all statements made herein of my own knowledge and belief are true and that all statements made on information and belief are believed to be true, and further, that the statements are made with the knowledge that willful false statements are punishable by fine or imprisonment, or both, under section 1001 of Title 18 of the United States Code, and that such willful false statements may jeopardize the validity of the application or any patent issuing thereon.

Date: 4-14-2011

Ge Wang, Ph.D.

Ge Wang, PhD
Pritchard Professor, Director
SEBE Division & ICTAS Center for Biomedical Imaging
VT-WFU School of Biomedical Engineering & Sciences
Virginia Polytechnic Institute & State University
ICTAS Building, Stanger Street, Blacksburg, VA 24061, USA

Phone: (540) 231-0620 (O)
Email: ge-wang@ieee.org
Web: www.imaging.sbes.vt.edu

Executive Summary

Publication Highlight

- *First paper on spiral/helical cone-beam CT (1991), which solves the "long object problem" and has become a main mode of CT scanners and remains a primary research area. Now, most CT scanners use the spiral/helical cone-beam scanning mode and perform >100-million scans annually in USA.*
- *First paper on overall superiority of spiral/helical fan-beam CT (1994), which shows that helical fan-beam CT produces better longitudinal resolution than conventional CT. This work was remarked as "the state of the art in spiral CT" by Dr. Kalender (Radiology 197:578-580, 1995)*
- *First paper on bioluminescence tomography (2004), which is an emerging molecular imaging modality*
- *First paper on interior tomography (2007), which solves the long-standing "interior problem" (theoretically exact reconstruction of an interior region of interest (ROI) from local projections through the ROI only), and can reduce radiation dose, handle large objects, and achieve ultrafast scan speed*
- *First paper on the a-index (2010), which formulates an axiomatic way to assign relative credits for a paper or other forms of teamwork*
- *More than 280 peer-reviewed journal papers and numerous other articles since 1992 (of which 39 in IEEE journals, 1 in PRL and 1 in PNAS. According to http://portal.isiknowledge.com, Dr. Ge Wang's h-factor is 30 in 2010 (doubled over the past 4+ years))*

Peer Recognition

- *Various awards (including the Oxford Univ. PhD Scholarship for the Sino-UK PhD Program in 1988)*
- *2006 Inverse Problems highlighted article on bioluminescence tomography theory*
- *2007 Inverse Problems highlighted article on cone-beam lambda tomography*
- *2009 Phys. Med. Biol. featured & highlighted article on triple-source CBCT*
- *2010 Phys. Med. Biol. featured article on optical Monte-Carlo simulation*
- *2010 Phys. Med. Biol. featured article on fluorescence molecular tomography*
- *Fellow of AIMBE (03/01/02, "for seminal contributions to single-slice / cone-beam spiral, micro-CT")*
- *Fellow of IEEE (01/01/03, "for contributions to x-ray tomography")*
- *Fellow of SPIE (01/01/07, "for achievements in bioluminescence tomography and x-ray CT")*
- *Fellow of OSA (10/12/09, "for pioneering contributions to bioluminescence tomography")*

Grant Support

- *$16M as PI/Contact PI*
- *$26M as Co-PI/Co-investigator*

Research Leadership

- *Director, CT Lab/Center for X-ray & Optical Tomography, College of Medicine, U. of Iowa, 1996-2006*
- *Director, Biomedical Imaging Division, SBES, College of Engineering, Virginia Tech, 2006-Now*
- *Director, ICTAS (Institute of Critical Technology & Applied Science) Center for Biomedical Imaging, College of Engineering, Virginia Tech, 2009-Now*

Professional Service

- *Founding Editor-in-Chief for International Journal of Biomedical Imaging*
- *Associate Editor for IEEE Trans. Medical Imaging, and other journals*
- *Chair, Co-Chair, Session Chair, members of numerous conference committees and review panels*

Grant Support (Total amount as PI/Contact PI: $16 millions; Total amount as Co-PI /Co-investigator: $26 millions)

Attracted as the PI or Contact PI

Title	Agency	Amount	FTE	Period
Spiral CT of the temporal bone	Whitaker (BME Program)	$166,731	50	12/93-11/96
Spiral CT deblurring for in-situ cochlear implant study	NIH/NIDCD (R03 DC02798)	$77,000	10	08/95-07/97
Unraveling the GI tract by spiral CT	NIH/NIDDK (R29 DK50184)	$543,628	50	04/96-03/01
Computed tomography	Marconi/Philips (MMS110100)	$100,000	10	12/00-11/01
Bioluminescent imaging	Univ. of Iowa	$75,000	5	10/02-09/03
Stereology for volume measurement	Univ. of Iowa	$20,000	5	10/02-09/03
Spiral CT for cochlear implantation	NIH/NIDCD (R01 DC03590)	$1,069,777	30	04/99-03/04
CT fluoroscopy	GE (GPN 1-78021-01)	$320,000	10	06/02-08/06
Micro-CT R&D	Univ. of Iowa	$400,000	5	10/01-09/06
Cone-beam methods for X-ray CT	NIH/NIBIB (R01 EB002667)	$1,408,525	30	10/03-09/10
Development and integration of bioluminescent CT	NIH/NIBIB (R21/33 EB1685)	$1,963,610	25	03/03-02/10
Bolus-chasing CT angiography using adaptive control techniques	NIH/NIBIB (R21/33 EB4287)	$1,404,387	30	04/04-03/10
Siemens equipment grant - A VolumeZoom 4-slice scanner	Siemens		5	04/06-03/07
Biomedical Imaging	*Virginia Tech*	*$600,000*	*10*	*11/06-10/10*
Development and evaluation of innovative biomedical imaging techniques	*Toshiba*	*$120,000*	*10*	*04/08-11/09*
Acquisition of a 500nm resolution nano-CT scanner	*NIH/NCRR (S10 RR025667)*	*$500,000*	*10*	*12/08-12/09*
Temperature-modulated bioluminescence tomography	*NIH/NCI (R21 CA127189)*	*$319,071*	*10*	*07/07-06/10*
Hologic equipment grant - An x-ray breast imaging system	*Hologic*	*$300,000*	*5*	*01/10-12/10*
Cardiac CT: Advanced Architectures and Algorithms	*NIH/NIBIB (R01 EB011785)**	*$1,913,186*	*20*	*07/09-06/12*
Next-generation nano-CT system	*NSF/MRI (0923297)*	*$1,360,206*	*10*	*08/09-07/12*
Matching fund to the above NSF/MRI grant	*VT+Xradia*	*$827,445*	*5*	*08/09-07/12*
Optical molecular tomography for regenerative medicine	*NIH/NHLBI (R01 HL098912)**	*$2,923,321*	*25*	*12/09-11/14*
	Subtotal	**$16,411,887**		
	Note: "*" indicates "Contact PI".			

Attracted as a Co-Investigator or Co-PI

Title	Agency	Amount	FTE	Period
Virtual colonic imaging with VoxelView™	Vital Images	$10,000	5	03/96-12/96
Strategies to optimize benefit from cochlear implant	NIH/NIDCD (R01 DC00581)	$801,956	12	12/93-11/97
Computerized stereological quantization of pediatric tumor volume	Soc Ped Rad	$5,000	5	07/98-06/99
Image-based dose planning in intracavitary brachytherapy	NIH/NCI (R01 CA75371)	$1,313,584	8	12/97-11/00
Reconstruction algorithm for discrete computed tomography	Univ. of Iowa	$10,000	5	12/02-12/03
A comprehensive program to investigate craniofacial and dental anomalies	NIH/NIDCR (R01 DE13076)	$1,499,865	5	08/99-07/04
Image and model based analysis of lung diseases (I)	NIH/NHLBI (R01 HL64368)	$8,270,875	20	12/99-11/04
Feasibility study of elasto-mammography	UI Informatics Initiatives*	$50,000	5	02/04-01/05
Micro-CT for variable spatial-temporal resolution	NIH/NCRR (S10 RR019242)*	348,900	5	04/04-03/05
Lung image database with pathologic correlates	NIH/NHLBI (R01 CA91085)	$1,400,000	5	04/01-03/06
Establishing a national computing center and NSF tier-2C program	Univ. of Iowa*	$115,000	5	05/05-04/06
Fluorescence-enhanced elasto-optical tomography	USAMRAA*	$106,416	5	07/05-06/07
Large-scale parallel Katsevich algorithm for 3D CBCT image reconstruction	NIH/NIBIB (EB006412)*	$221,250	10	07/06-06/08
Mouse modeling techniques for bioluminescence tomography	NIH/NIBIB (R03 EB006036)*	$150,000	5	09/06-08/08
Image and model based analysis of lung diseases (II)	NIH/NHLBI (R01 HL064368)	$10,206,902	20	07/05-06/10
X-ray grating-based imaging	*Virginia Tech**	*$100,000*	*5*	*05/07-04/08*
Bioluminescence imaging for inflammation research	*Virginia Tech**	*$50,000*	*5*	*05/07-04/08*
Implantable μ-Oncologists	*Virginia Tech**	*$100,000*	*5*	*10/07-06/08*
Holley scaffold	*Virginia Tech**	*$300,000*	*5*	*04/08-03/09*
Bone healing grafts fabricated by nano-scale assembly	*Virginia Tech*	*$50,000*	*5*	*10/07-09/09*
Bone tissue engineering: Effects of dynamic perfusion	*NIH/NIAMS (R21 AR055200)*	*$365,353*	*5*	*03/08-02/10*
Data redundancy based motion artifact reduction for head CT	*NIH/NIBIB (R03 EB007288)**	*$157,000*	*5*	*09/07-08/10*
Modeling the photon propagation for optical molecular imaging	*NIH/NIBIB (R03 EB008476)**	*$158,000*	*5*	*09/08-08/10*
In vivo tomographic imaging of fluorescence proteins	*NIH/NCI (R21 CA135151)**	*$352,000*	*5*	*06/09-05/11*
Bone Scaffolds for Heat Shock Protein Induced Regeneration and Healing	*NSF/ CBET (1067654)**	*$321,987*		
	Subtotal	**$26,142,101**		
	Note: "*" indicates "Co-PI".			

Education

- **BE**, 1982, Dept. of ECE, Xidian Univ., P. R. China (the best radar signal processing specialty in China)
- **MS**, 1985, Institute of Remote Sensing Applications, Graduate School of Academia Sinica (the first and most preeminent graduate school in China); Thesis: Texture analysis of satellite images
- **MS**, 1991, Dept. of ECE, State Univ. of New York at Buffalo; Thesis: Preliminary studies on cone-beam reconstruction (Advisors: Cheng PC, Lin TH)
- **PhD**, 1992, Dept. of ECE, State Univ. of New York at Buffalo; Dissertation: Cone-beam X-ray Microtomography (UMI# 9317362)

Employment

- Instructor, 84-86, Dept. of ECE, Graduate School of Academia Sinica, Beijing, China
- Assist. Prof., 86-88, Dept. of ECE, Graduate School of Academia Sinica, Beijing, China
- RA, 88-89, Dept. of Geog. & Environmental Studies, Tasmania Univ., Australia
- RA, 89-92, Dept. of ECE, State Univ. of New York at Buffalo, Buffalo
- Instructor, 92-93, Mallinckrodt Institute of Radiology, Washington Univ., St. Louis
- Assist. Prof., 94-96, Mallinckrodt Institute of Radiology (arguably, the best radiology department in USA), Washington Univ., St. Louis (Mentor: Vannier MV)
- Assoc. Prof., 97-02, Dept. of Radiology, Univ. of Iowa
- Prof., 02-06, Dept. of Radiology, College of Medicine, Univ. of Iowa
- Director of the CT Lab, 97-06, Dept. of Radiology, Univ. of Iowa
- Adjunct Prof., -06, Dept. of BME (00-), Dept. of Math (02-), Dept. of ECE (02-), Dept. of Civil Engineering (04-), Univ. of Iowa
- Director of the Center for X-ray & Optical Tomography, 04-06, Univ. of Iowa
- Pritchard Prof., 06-Now, College of Engineering (9 months), Virginia Tech
- Adjunct Prof., 06-Now, Dept. of Math, Dept. of ECE, Virginia Tech
- Prof., 06-Now, Dept. of Radiology & Dept. of BME, School of Medicine (3 months), Wake Forest Univ.
- Director of the Biomedical Imaging Division, 06-Now, Virginia Tech – Wake Forest University (VT-WFU) School of Biomedical Engineering and Sciences (SBES), Virginia Tech
- Adjunct Prof., 08-Now, Regenerative Medicine, Wake Forest Institute of Regenerative Medicine
- Director of the ICTAS (Institute of Critical Technology & Applied Science) Center for Biomedical Imaging, 09-Now, Virginia Tech

Honors and Awards

- 1988 Oxford Univ. PhD Scholarship for the Sino-UK PhD Program (Robotics)
- 1988 Univ. Postgraduate Research Scholarship (Remote Sensing). Univ. of Tasmania, Australia
- 1990 Travel Award. International Symposium on X-ray Microscopy, London, UK
- Travel Award. Scanning 1992, Atlantic City, NJ
- Travel Award. Scanning 1993, Orlando, FL
- 1996 Hounsfield Award. Society of Computed Body Tomography and Magnetic Resonance
- 1997 Giovanni DiChiro Award for Outstanding Scientific Research. Journal of Computer Assisted Tomography
- 1999 Marquis Who's Who in Science and Engineering (2000-2001)
- 1999 AAPM/IPEM Medical Physics Travel Award. The American Association of Physicists in Medicine (AAPM) and the Institute of Physics and Engineering in Medicine (IPEM), 1999 (The award is for promotion of interaction between medical physicists in USA and UK. One medical physicist is awarded in USA annually. The awardee is expected to lecture in UK for 2-3 weeks)
- IEEE Senior Member (effective from 1/1/2000)
- Cum Laude award from the SPIE Medical Imaging Conference, 2000
- Outstanding Scientists of the 21st Century (2001), International Biographical Centre, Cambridge CB2 3QP, England
- 2001 RSNA Research Trainee Prize for work entitled "Blind Deblurring of Spiral CT Images" by Jiang M in collaboration with Wang G, Skinner MW, Rubinstein JT, Vannier MW. RSNA, 2001

- ***Fellow of the American Institute for Medical and Biological Engineering*** *(AIMBE) (inducted in the National Academy of Sciences on 3/1/ 2002, with the citation "For seminal contributions to the development of single-slice spiral, cone-beam spiral, and micro CT.")*
- ***Fellow of the Institute of Electrical and Electronics Engineers*** *(effective 1/1/2003, with the citation "For contributions to x-ray tomography")*
- ***Outstanding International Educator****, the University of Iowa International Programs, 2003*
- ***2004 Herbert M. Stauffer Award for Outstanding Basic Science Paper*** *in Academic Radiology, Association of University Radiologists, USA*
- ***Samuel Reynolds Pritchard Professor of Engineering****, VT-WFU School of Biomedical Engineering & Sciences, Virginia Polytechnic Institute & State University*
- ***Fellow of the International Society for Optical Engineering*** *(effective 1/1/2007 for specific achievements in bioluminescence tomography and x-ray computed tomography)*
- ***2006 Inverse Problems Highlighted Article*** *(Han WM, Cong WX, Wang G: Mathematical theory and numerical analysis of bioluminescence tomography. Inverse Problems 22:1659-1675, 2006)*
- ***2007 Inverse Problems Highlighted Article*** *(Ye YB, Yu HY, Wang G: Cone-beam pseudo-lambda tomography. Inverse Problems 23:203-215, 2007)*
- *2003-2007 Most Cited Paper (Yu HY, Wang G: Studies on implementation of the Katsevich algorithm for spiral cone-beam CT. Journal of X-ray Science and Technology 12: 97-116, 2004). Journal of X-ray Science and Technology, 2007*
- ***2000-2007 Distinguished Associate Editor Service*** *for Journal of Medical Physics, American Association of Physicists in Medicine, presented on November 26, 2007*
- *2009 Intel Science Talent Search Semifinalist Ms. Lena Ye, "Determination of exact reconstruction regions in composite-circling cone-beam tomography"*
- ***2009 Phys. Med. Biol. Featured & Highlighted Article*** *(Lu Y, Zhao J, Wang G: Exact image reconstruction with triple-source saddle-curve cone-beam scanning. Phys. Med. Biol. 54: 2971-2991, 2009)*
- ***Fellow of the Optical Society of America*** *(effective 10/12/2009 for pioneering contributions to development of bioluminescence tomography)*
- ***2010 Phys. Med. Biol. Featured Article*** *(Shen H, Wang G: A tetrahedron-based inhomogeneous Monte Carlo optical simulator. Phys. Med. Biol. 55 947-962, 2010)*
- ***Dean's Award for Excellence in Research****, College of Engineering, Virginia Tech, 2010*
- ***Distinguished Leading Research Award (DLR Award)****, Virginia Tech – Wake Forest University School of Biomedical Engineering and Sciences, 2010*
- *Prize for New Advances in CT & 3D Imaging (Yang Lv, Katsevich, A, Zhao J, Yu HY, Wang G: Fast exact/quasi-exact FBP algorithms for triple-source helical cone-beam CT), Chinese Society for Stereology, 2010*

I. Research

Publications

Journal papers	*Edited books*	*Chapters*	*Special issues*	*Patents*	*Conference papers (IEEE, SPIE, etc.)*
>280	*3*	*21*	*6*	*20*	*>250*

Journal Publications *(From >280 journal papers and >250 conference papers, of which 39 in IEEE journals, 1 in PRL and 1 in PNAS. According to http://portal.isiknowledge.com, Dr. Ge Wang's h-factor is 30 (doubled over the past 4+ years))*

A. Axiomatic Research

1. ***Wang G****, Li Y: Axiomatic approach for quantification of image resolution. IEEE Signal Processing Letters 6:257-258, 1999*
2. *O'Sullivan JA, Jiang M, Ma XM,* ***Wang G****: Axiomatic quantification of multi-dimensional image resolution. IEEE Signal Processing Letters 9:120-122, 2002*

3. *Meinel Jr. JF, **Wang G**, Jiang M, Frei T, Vannier MW, Hoffman EA: Spatial variation of resolution and noise in multi-slice spiral CT. Academic Radiology 10:607-613, 2003*
4. ***Wang G**, Jiang M: Axiomatic characterization of nonlinear homomorphic means. Journal of Mathematical Analysis and Applications 303:350-363, 2005*
5. *Jiang M, **Wang G**, Ma XM: A general axiomatic system for image resolution quantification. Journal of Mathematical Analysis and Applications 315:462-473, 2006*
6. ***Wang G**, Yang J: Axiomatic quantification of co-authors' relative contributions. arXiv:1003.3362v1, 2010*

B. Bioluminescence/Fluorescence Tomography

1. *Cong WX, Wang LH, **Wang G**: Formulation of photon diffusion from spherical bioluminescent sources in an infinite homogeneous medium. Biomedical Engineering Online 3:12, http://www.biomedical-engineering-online.com/content/3/1/12, 2004*
2. ***Wang G**, Li Y, Jiang M: Uniqueness theorems in bioluminescence tomography. Med. Phys. 31:2289-2299, 2004 (selected for the August 1, 2004 issue of Virtual Journal of Biological Physics Research, published by American Physical Society and American Institute of Physics in cooperation with numerous other societies and publishers, is an edited compilation of links to articles from participating publishers, http://www.vjbio.org) (**Wang G**, Li Y, Jiang M: Erratum to "Uniqueness theorems in bioluminescence tomography" (Medical Physics, Vol. 31, No. 8, pp. 2289 - 2299, 2004). Medical Physics 32:3059, 2005)*
3. *Li H, Tian J, Zhu FP, Cong WX, Wang LV, Hoffman EA, **Wang G**: A mouse optical simulation environment (MOSE) to investigate bioluminescent phenomena with the Monte Carlo method. Academic Radiology 11:1029-1038, 2004*
4. *Li H, Tian J, **Wang G**: A Monte Carlo method based photon transport model for in vivo biological optical imaging. Journal of Software 15:1709-1719, 2004*
5. ***Wang G**, Jaszczak R, Basilion J: Towards molecular imaging. IEEE Trans. Med. Imaging 24:829-831, 2005*
6. *Cong WX, **Wang G**: Kumar D, Liu Y, Jiang M, Wang LH, Hoffman EA, McLennan G, McCray PB, Zabner J, Cong A: A practical reconstruction method for bioluminescence tomography Optics Express 13:6756-6771, 2005*
7. *Li Y, Jiang M, Wang G: Computational optical biopsy. Biomedical Engineering Online 4:36, 2005*
8. *Cong A, **Wang G**: A finite-element-based reconstruction method for 3D fluorescence tomography. Optics Express 13:9847-9857, 2005*
9. *Cong A, **Wang G**: Multi-spectral bioluminescence tomography: Methodology and simulation. International Journal of Biomedical Imaging, ID57614, 2006*
10. *Cong WX, **Wang G**: A boundary integral method for bioluminescence tomography. Journal of Biomedical Optics 11:020503, 2006*
11. *Cong WX, Kumar D, Wang LV, **Wang G**: A Born-type approximation method for bioluminescence tomography. Med. Phys. 33:679-686, 2006*
12. *Han WM, Cong WX, **Wang G**: Mathematical theory and numerical analysis of bioluminescence tomography. Inverse Problems 22:1659-1675, 2006 (highlight from Inverse Problems, selected by the Editorial Board)*
13. ***Wang G**, Cong WX, Kumar D, Qian X, Shen H, Sinn P, Hoffman E, McLennan G, Henry M: In vivo mouse studies with bioluminescence tomography. Optics Express 14:7801-7809, 2006*
14. ***Wang G**, Shen HO, Cong WX, Zhao S, Wei GW: Temperature-modulated bioluminescence tomography. Optics Express 14:7852-7871, 2006*
15. ***Wang G**, Shen H, Kumar D, Qian X, Cong WX: The first bioluminescence tomography system for simultaneous acquisition of multi-view and multi-spectral data. International Journal of Biomedical Imaging, ID58601,2006*
16. *Han WM, Cong WX, **Wang G**: Mathematical study and numerical simulation of multispectral bioluminescence tomography. International Journal of Biomedical Imaging, ID54390, 2006*
17. ***Wang G**, Cong WX, Li Y, Han WM, Durairaj K, Qian X, Shen H, Jiang M, Zhou T, Cheng J, Tian J, Lv Y, Li H, Luo J: Recent development in bioluminescence tomography. Current Medical Imaging Reviews 2:453-457:, 2006*

18. *Lv Y, Tian J, Cong WX, **Wang G**, Luo J, Yang W, Shi J, Li H: A multilevel adaptive finite element algorithm for bioluminescence tomography. Optics Express 14:8211-8223, 2006*
19. *Han WM, **Wang G**: Theoretical and numerical analysis on multispectral bioluminescence tomography. IMA Journal of Applied Mathematics, 1-19, doi:10.1093/imamat/hxl031, 2006*
20. *Kumar D, Cong WX, **Wang G**: A Monte-Carlo method for bioluminescence tomography. Indian Journal of Experimental Biology 45:58-63, 2007*
21. *Shen HO, Cong WX, Qian X, Durairaj K, **Wang G**: A numerical study on validity of the diffusion approximation for computational optical biopsy. Journal of the Optical Society of America A 24:423-429, 2007*
22. *Han, W, Kazmi K, Cong WX, **Wang G**: Bioluminescence tomography with optimized optical parameters. Inverse Problems 23: 1215–1228, 2007*
23. *Li H, Tian J, Luo J, Lu Y, Cong W, **Wang G**: Design and implementation of an optical simulation environment for bioluminescent tomography studies. Progress in Natural Science 17:87-94, 2007*
24. *Lv YJ, Tian J, Cong WX, **Wang G**, Yang W, Qin CH, Xu M: Spectrally resolved bioluminescence tomography with adaptive finite element: Methodology and simulation. Physics in Medicine and Biology 52:4497-4512, 2007*
25. *Cong A, Shen HO, Cong WX, **Wang G**: Improving the accuracy of the diffusion model in highly absorbing media. International Journal of Biomedical Imaging, ID38168, 2007*
26. *M Jiang,* Zhou T, Cheng J, Cong WX, ***Wang G**: Image reconstruction for bioluminescence tomography from partial measurement. Optics Express 15:11095 - 11116, 2007*
27. *Cong W, Liu Y, Cong A, Liu Y, **Wang G**: Flux vector based formulation for photo propagation in the biological tissue. Optics Letters 32:2837-2839, 2007 (selected for inclusion in Virtual Journal for Biomedical Optics (VJBO) 2(11), November 26, 2007)*
28. *Cong W, Shen H, Cong A, Wang Y, **Wang G**: Modeling photon propagation in biological tissues using a generalized Delta-Eddington phase function. Physical Review E 76:051913, 2007*
29. ***Wang G**, Cong WX, Shen H, Qian X, Henry M, Wang Y: Overview of bioluminescence tomography - A new molecular imaging modality. Frontiers in Bioscience 13:1281-1293, 2008*
30. ***Wang G**, Shen H, Liu Y, Cong A, Cong W, Wang Y, Dubey P: Digital spectral separation methods and systems for bioluminescence imaging. Optics Express 16:1719-1732, 2008*
31. *Han WM, **Wang G:** Bioluminescence tomography: Biomedical background, mathematical theory, and numerical approximation. Journal of Computational Mathematics, 26:324-335, 2008 (A special issue dedicated to the 70th birthday of Prof. Cui Junzhi)*
32. *Cong W, Shen H, Cong A, **Wang G**: Integral equation of the photon fluence rate and flux based on a generalized Delta-Eddington phase function. Journal of Biomedical Optics 13, ID024016, 2008*
33. *Chen D, Wei GW, Cong W, **Wang G**: Computational methods for optical molecular imaging. Communications in Numerical Methods in Engineering, DOI: 10.1002/cnm.1164, 25 pages, 2008*
34. *Lv Y, Tian J, Cong W, **Wang G:** Experimental bioluminescence tomography with multi-modality imaging fusion. International Journal of Biomedical Imaging, ID86741, 2007*
35. *Wang ZG, Sun LZ, Fajardo LL, **Wang G**: Modeling and reconstruction of diffuse optical tomography using adjoin method. Communications in Numerical Methods in Engineering 25:657-665, 2009*
36. *Han WM, Cong W, Kazmi K, **Wang G**: An integrated solution and analysis of bioluminescence tomography and diffuse optical tomography. Communications in Numerical Methods in Engineering 25:639-656, DOI: 10.1002/cnm.1163, 2009*
37. *Li YB, Shen HO, Zhu H, Trush M, Jiang M, **Wang G**: In situ real-time chemiluminescence imaging of reactive oxygen species formation in cultured cardiomyocytes. International Journal of Biomedical Imaging, ID941729, 2008*
38. *Han W, Shen H, Kazmi K, Cong WX, **Wang G**: Studies of a mathematical model for temperature-modulated bioluminescence tomography. Applicable Analysis 88:193-213, 2009*
39. *Cong A, Cong WX, Lu Y, Santago P, Chatziioannou A, **Wang G**: Differential evolution approach for regularized bioluminescence tomography. IEEE Trans. Biomedical Engineering 57:2229-2238, 2010*
40. *Cong W, **Wang G**: Bioluminescence tomography based on the phase approximation model. JOSA-A **27**: 174-179, 2010*
41. *Shen H, **Wang G**: A tetrahedron-based inhomogeneous Monte Carlo optical simulator. Phys. Med. Biol. 55 947-962, 2010*

42. *Vogt WC, Shen H, **Wang G**, Rylander CG: Parametric study of tissue optical clearing by localized mechanical compression using combined finite element and Monte Carlo simulation. Journal of Innovative Optical Health Sciences 3:203-211, 2010*
43. *Lu YJ, Zhu BH, Shen H, Rasmussen JC, **Wang G**, Sevick-Muraca EM: Parallel adaptive finite element simplified spherical harmonics approximation solver for frequency domain fluorescence molecular imaging. Phys. Med. Biology 55:4625-4645, 2010*
44. *Gong R, **Wang G**, Cheng X, Han W: A novel approach for studies of multispectral bioluminescence tomography. Numerische Mathematik 115:553-583, DOI 10.1007/s00211-010-0293-8, 2010*
45. *Gao H, Zhao HK, Cong WX, **Wang G**: Recovering bioluminescent source in Gaussians. To appear in Biomedical Optics Express, 2010*
46. *Gao H, Shen HO, **Wang G**, Zhao HK: A cross validation of an RTE solver and a Monte Carlo simulator in biophotonics. To appear in Opt. Express, 2010*
47. *Shen H, **Wang G**: A study on tetrahedron-based inhomogeneous Monte-Carlo optical simulation. To appear in Opt. Express, 2010*

C. Computed Tomography

1. ***Wang G**, Lin TH, Cheng PC, Shinozaki DM: Point spread function of the general cone-beam X-ray reconstruction formula. Journal of Scanning Microscopy 14:187-193, 1992*
2. ***Wang G**, Lin TH, Cheng PC, Shinozaki DM: Cone-beam reconstruction of plate-like specimens. Journal of Scanning Microscopy 14:350-354, 1992*
3. ***Wang G**, Lin TH, Cheng PC, Shinozaki DM: A general cone-beam reconstruction algorithm. IEEE Trans. on Med. Imaging 12:486-496, 1993*
4. ***Wang G**, Lin TH, Cheng PC: A derivative-free non-circular fan-beam reconstruction formula. IEEE Trans. on Image Processing 2:543-547, 1993*
5. ***Wang G**, Lin TH: Comments on "A cone-beam filtered backprojection reconstruction algorithm for cardiac single photon emission computed tomography". IEEE Trans. on Med. Imaging 12:383-384, 1993*
6. ***Wang G**, Vannier MW: Helical CT image noise - Analytical results. Med. Phys. 20:1635-1640, 1993*
7. *Vannier MW, **Wang G**: Spiral CT refines imaging of temporal bone disorders. Diagnostic Imaging 15:116-121, 1993*
8. ***Wang G**, Vannier MW: Longitudinal resolution in volumetric X-ray CT - Analytical comparison between conventional and helical CT. Med. Phys. 21:429-433, 1994*
9. ***Wang G**, Brink JA, Vannier MW: Theoretical FWTM values in helical CT. Med. Phys. 21:753-754, 1994*
10. ***Wang G**, Vannier MW: Stair-step artifacts in three-dimensional helical CT - An experimental study. Radiology 191:79-83, 1994*
11. ***Wang G**, Liu Y, Lin TH, Cheng PC, Shinozaki DM: Half-scan cone-beam X-ray microtomography formula. Journal of Scanning Microscopy 16:216-220, 1994*
12. *Brink JA, Heiken JP, **Wang G**, McEnery KW, Schlueter FJ, Vannier MW: Spiral (helical) CT: Principles and technical considerations. RadioGraphics 14:887-893, 1994*
13. *Vannier MW, **Wang G**: Book Review of Kimura, K. and Koga S., eds. Basic Principles and Clinical Applications of Helical Scan. Applications of Continuous-Rotation CT, AJR 163:322, 1994*
14. ***Wang G**, Vannier MW: Spatial variation of section sensitivity profile in helical CT. Med. Phys. 21:1491-1497, 1994*
15. *Vannier MW, **Wang G**: Spiral CT refines imaging of temporal bone disorders. Diagnostic Imaging International 10:34-38, 1994*
16. *Schlueter FJ, **Wang G**, Hsieh P, Brink JA, Vannier MW: Longitudinal image deblurring in spiral CT. Radiology 193:413-418, 1994*
17. *Brink JA, Lim JT, **Wang G**, Heiken JP, Deyoe LA, Vannier MW: Technical optimization of spiral CT for depiction of renal artery stenosis: in vitro analysis. Radiology 194:157-163, 1995*
18. ***Wang G**, Vannier MW: Preliminary Study on helical CT algorithms for patient motion estimation and compensation. IEEE Trans. on Med. Imaging 14:205-211, 1995*
19. *Vannier MW, **Wang G**, Skinner MW, Esselman GH: Imaging the temporal bone by spiral CT. MEDIZIN IM BILD 1:23-29, 1995*

20. **Wang G**, Skinner MW, Vannier MW: Temporal bone volumetric image deblurring in spiral CT. Academic Radiology 2:888-895, 1995
21. **Wang G**, Lin TH, Cheng PC: Error analysis on the generalized Feldkamp cone-beam algorithm. Journal of Scanning Microscopy 17:361-370, 1995
22. **Wang G**, Cheng PC: Feldkamp-type cone-beam reconstruction: Revisited. Zoological Studies 34(S):159-161, 1995
23. **Wang G**, Vannier MW: Maximum volume coverage in spiral CT. Academic Radiology 3:423-428, 1996
24. **Wang G**, Zhao SY, Cheng PC: Cone-beam X-ray tomographic and stereo-imaging. Biomedical Engineering 8:261-271, 1996
25. **Wang G**, Snyder DL, Vannier MW: Local CT via iterative deblurring. Journal of Scanning Microscopy 18:582-588, 1996
26. Luker GD, Bae KT, Siegel MJ, Don S, Brink JA, **Wang G**, Herman TE: Ghosting of pulmonary nodules with respiratory motion: Comparison of helical and conventional CT using an in vitro pediatric model. AJR 167:1189-1193, 1996
27. **Wang G**, Snyder DL, O'Sullivan JA, Vannier MW: Iterative deblurring for metal artifact reduction. IEEE Trans. on Med. Imaging 15:657-664, 1996
28. Robertson DD, Yuan J, **Wang G**, Vannier MW: Total hip prosthesis metal-artifact suppression using iterative deblurring reconstruction. J. Comput. Assist Tomogr. 21:293-298, 1997 (Won the Giovanni DiChiro Award; the method and software were reported in the paper [27] (Wang et al., IEEE Trans. on Med. Imaging 15:657-664, 1996)
29. **Wang G**, Vannier MW: Low-contrast resolution in volumetric X-ray CT - Analytical comparison between conventional and spiral CT. Med. Phys. 24:373-376, 1997
30. **Wang G**, Vannier MW: Optimal pitch in spiral computed tomography. Med. Phys. 24:1635-1639, 1997
31. Vannier MW, Hildebolt CF, Conover G, Knapp RH, Grothers NY, **Wang G**: Three-dimensional dental imaging by spiral CT. Oral Surgery, Oral Medicine, and Oral Pathology 84:561-570, 1997
32. Brink JA, Woodard PK, Horesh L, Heiken JP, Glazer HS, Anderson CD, **Wang G**, Schwartz DM: Depiction of pulmonary emboli with helical CT: Optimization of display window settings in a porcine model. Radiology 204:703-708, 1997
33. Zhao SY, Welland G, **Wang G**: Wavelet sampling and localization schemes for the Radon transform in two dimensions. SIAM Journal on Applied Mathematics 57:1749-1762, 1997
34. Pan SJ, Liou WS, Shih A, Park MS, **Wang G**, Newberry SP, Kim HG, Shinozaki DM, Cheng PC: Experimental system for X-ray cone-beam microtomography. Microscopy and Microanalysis 4:56-62, 1998
35. **Wang G**, Vannier MW, Skinner MW, Cavalcanti MGP, Harding G: Spiral CT image deblurring for cochlear implantation. IEEE Transactions on Med. Imaging 17:251-262, 1998
36. **Wang G**, Schweiger GD, Vannier MW: An iterative algorithm for X-ray CT fluoroscopy. IEEE Transactions on Med. Imaging 17:853-856, 1998
37. Zhao SY, **Wang G**, Hsieh J: Wavelet filtering algorithm for fan-beam CT. IEE Electronics Letters 34:2395-2396, 1998
38. Vannier MW, **Wang G**, Skinner MW, Rubinstein JT: New x-ray imaging strategies - Implications for cochlear implantation. Review of Progress in Qualitative Nondestructive Evaluation 18(B):1569-1574, 1999
39. **Wang G**, Vannier MW, Cheng PC: Iterative x-ray cone-beam tomography for metal artifact reduction and local region reconstruction. Microscopy and Microanalysis 5:58-65, 1999
40. Redford K, **Wang G**, Vannier MW: Equiangular fan-beam CT reconstruction for a non-circular scanning locus. Optical Engineering 38:1335-1339, 1999
41. **Wang G**, Vannier MW: The effect of pitch in multi-slice spiral/helical CT. Med. Phys. 26: 2648-2653, 1999
42. Brink JA, **Wang G**, McFarland EG: Optimal slice spacing in single-detector helical CT. Radiology 214:575-578, 2000
43. Schweiger GD, Brown BP, Pelsang RE, Dhadha RS, Barloon TJ, **Wang G**: CT fluoroscopy: Technique and utility in guiding biopsies of transiently enhancing hepatic masses. Abdominal Imaging 25:81-85, 2000
44. **Wang G**, Frei T, Vannier MW: A fast algorithm for metal artifact reduction in X-ray CT. Academic Radiology 7:607-614, 2000

45. *Zhao SY, **Wang G**: Feldkamp-type cone-beam tomography in the wavelet framework. IEEE Trans. Med. Imaging 19:922-929, 2000*
46. ***Wang G**, Crawford CR, Kalender WA: Multi-row-detector and cone-beam spiral/helical CT. IEEE Trans. Med. Imaging 19:817-821, 2000*
47. *Shih A, **Wang G**, Cheng PC: A fast algorithm for x-ray cone-beam microtomography. Microscopy and Microanalysis 7:13-23, 2001*
48. *Zhao SY, Robertson DD, **Wang G**, Whiting B, Bae KT: X-ray CT metal artifact reduction using wavelets: an application for imaging total hip prostheses. IEEE Trans. Med. Imaging 19:1238-1247, 2001*
49. *Liu Y, Liu H, Wang Y, **Wang G**: Half-scan cone-beam CT fluoroscopy with multiple X-ray sources. Med. Phys. 28:1466-1471, 2001*
50. ***Wang G**, Vannier MW: Overview on micro-CT scanners for biomedical applications. Advanced Imaging 16:22-27, 2001*
51. *Wang B, **Wang G**: Image reconstruction algorithms for cone-beam CT. Journal of CT Theory and Applications 10:1-8, 2001*
52. *Wang B, Liu H, Zhao S, **Wang G**: Feldkamp-type image reconstruction from equiangular data. Journal of X-Ray Science and Technology 9:113-120, 2001*
53. *Ye YB, **Wang G**, Zhu JH: Linear Diophantine equations for discrete tomography. Journal of X-Ray Science and Technology 10:59-66, 2002*
54. *Zhao SY, Bae KT, Whiting B, **Wang G**: A wavelet method for metal artifact reduction with multiple metallic objects in the field of view. Journal of X-ray Science and Technology 10:67-76, 2002*
55. *Jiang M, **Wang G**: Development of iterative algorithms for image reconstruction. Journal of X-Ray Science and Technology 10:77-86, 2002*
56. ***Wang G**, Book Review - Reprinted classics on computed tomography. Med. Phys. 29:107-108, 2002*
57. *Jiang M, **Wang G**, Skinner MS, Rubinstein J, Vannier MW: Blind deblurring for spiral CT images - Comparative studies on edge-to-noise ratios. Med. Phys. 29:821-829, 2002*
58. ***Wang G**: X-ray micro-CT with a displaced detector array. Med. Phys. 29:1634-1636, 2002*
59. ***Wang G**, Zhao SY, Heuscher D: A knowledge-based cone-beam x-ray CT algorithm for dynamic volumetric cardiac imaging. Med. Phys. 29:1807-1822, 2002*
60. *Lee SW, Cho G, **Wang G**: Artifacts associated with implementation of the Grangeat formula. Med. Phys. 29:2871-2880, 2002*
61. ***Wang G**, Jiang M, Liu H, Lee SW, Hoffman EA: Cone-beam reconstruction for micro-CT. Journal of CT Theory and Applications 11:7-11, 2002*
62. *Lee SW, **Wang G**: A Grangeat-type half-scan algorithm for cone-beam CT. Med. Phys. 30:689-700, 2003*
63. *Ye YB, Zhu JH, **Wang G**: A point-wise limit theorem for filtered backprojection in computed tomography. Med. Phys. 30:816-822, 2003*
64. *Jiang M, **Wang G**: Development of blind image deconvolution and its applications. Journal of X-Ray Science and Technology 11:13-19, 2003*
65. ***Wang G**, Madsen M, Redford K, Zhao S, Vannier MW: A study on the section sensitivity profile in multi-row-detector spiral CT. Journal of X-ray Science and Technology 11:1-11, 2003*
66. *Jiang M, **Wang G**: Convergence of the simultaneous algebraic reconstruction technique (SART). IEEE Trans. Image Processing 12:957-961, 2003*
67. *Jiang M, **Wang G**: Convergence studies on iterative algorithms for image reconstruction. IEEE Trans. Med. Imaging 22:569-579, 2003*
68. *Jiang M, **Wang G**, Skinner MS, Rubinstein J, Vannier MW: Blind deblurring for spiral CT images. IEEE Trans. Med. Imaging 22:837-845, 2003*
69. *Liu V, Lariviere N, **Wang G**: X-ray micro-CT with a displaced detector array: An application for helical cone-beam reconstruction. Medical Physics 30:2758-2761, 2003*
70. ***Wang G**: Revisit to derivative-free noncircular fan-beam reconstruction - Responses to "Discussions on a noncircular fan-beam reconstruction formula" by Huang et al. Computed Tomography Theory and Application 12:39-44, 2003*
71. ***Wang G**, Lee SW: Grangeat-type and Katsevich-type algorithms for cone-beam CT. Journal of CT Theory and Applications 12:45-55, 2003*

72. *Li X, Jiang M, **Wang G**: A numerical simulator in VC++ on PC for iterative image reconstruction. Journal of X-Ray Science and Technology 11:61-70, 2003*
73. *Bennett JR, Bai EW, Halloran JI, **Wang G**: A preliminary study on adaptive field-of-view tracking in peripheral digital subtraction angiography. Journal of X-Ray Science and Technology 11:149-159, 2003*
74. *Lee SW, **Wang G**: A helical half-scan cone-beam CT algorithm for short object geometry in the Grangeat framework. Medical Physics 31:4-16, 2004*
75. *Hsieh J, Wei YC, **Wang G**: Fractional scan algorithms for low-dose CT perfusion. Med. Phys. 31:1254-1257, 2004*
76. *Ye YB, Zhu JH, **Wang G**: Minimum detection windows, PI-line existence and uniqueness for helical cone-beam scanning of variable pitch. Med. Phys. 31:566-572, 2004*
77. *Ye Y, Zhu JH, **Wang G**: Geometric studies on variable radius spiral cone-beam scanning. Medical Physics 31:1473-1480, 2004*
78. *Yu HY, **Wang G**: Studies on implementation of the Katsevich algorithm for spiral cone-beam CT. Journal of X-ray Sci. and Tech. 12:97-116, 2004*
79. *Yu HY, **Wang G**: Feldkamp-type VOI reconstruction from super-short-scan cone-beam data. Med. Phys. 31:1357-1362, 2004*
80. ***Wang G**, Jiang M: Ordered-subset simultaneous algebraic reconstruction techniques (OS-SART). Journal of X-Ray Science and Technology 12:169-177, 2004*
81. *Zeng K, Chen ZQ, Zhang, L, **Wang G**: A half-scan error reduction based algorithm for cone-beam CT. Journal of X-Ray Science and Technology 12:73-82, 2004*
82. *Zeng K, Chen ZQ, Zhang L, **Wang G**: An error-reduction-based algorithm for cone-beam CT. Med. Phys. 31:3206-3212, 2004*
83. ***Wang G**, Liu Y, Ye Y, Zhao S, Hsieh J, Ge S: Top-level design and preliminary physical analysis for the first electron-beam micro-CT scanner. Journal of X-Ray Sci. and Tech. 12:251-260, 2004*
84. *Zhu J, Lee SW, Ye Y, Zhao S, **Wang G**: X-ray transform and 3D Radon transform for ellipsoids and tetrahedra. Journal of X-Ray Sci. and Tech. 12:215-229, 2004*
85. *Wang J, **Wang G**, Jiang M: Blind deblurring of spiral CT images based on ENR and Wiener filter. Journal of X-ray Sci. and Tech.13:49-60, 2005*
86. *Kim KD, Ruprecht A, **Wang G**, Lee JB, Dawson DV, Vannier MW: Accuracy of facial soft tissue thickness measurements in personal computer-based multiplanar reconstructed computed tomographic images: Effect of variable scanning protocols. Forensic Science International 155:28-34, 2005*
87. *Zhao S, Yu H, **Wang G**: A unified framework for exact cone-beam image reconstruction formulas. Med. Phys. 32:1712-1721, 2005 (Zhao SY, Yu HY, **Wang G**: Erratum: "A unified framework for exact cone-beam reconstruction formulas" [Med. Phys. 31, 1712-1721 (2005)]. Med. Phys., 34:4979-4980, 2007)*
88. *Li X, Ni J, **Wang G**: Parallel iterative cone-beam CT image reconstruction on a PC cluster. Journal of X-Ray Sci. and Tech. 13:63-72, 2005*
89. *Ye Y, **Wang G**: A filtered backprojection formula for exact image reconstruction from cone-beam data along a general scanning curve. Med. Phys. 32:42-48, 2005*
90. *Wei Y, **Wang G**, Hsieh J: An intuitive discussion on the ideal ramp filter in computed tomography. International Journal of Computers and Mathematics 49:731-740, 2005*
91. ***Wang G**, Zhao S, Yu HY, Miller CM, Abbas PJ, Gantz B, Rubinstein J: Design, analysis and simulation for development of the first clinical micro-CT scanner. Academic Radiology 12:511-522, 2005*
92. *Yu HY, Ye YB, Zhao SY, **Wang G**: A backprojected filtration algorithm for nonstandard spiral cone-beam CT with an N-PI window. Phys. Med. Biol. 50:2099-2111, 2005*
93. *Ye Y, Zhao S, Yu H, **Wang G**: A general exact reconstruction for cone-beam CT via backprojection-filtration. IEEE Transactions on Medical Imaging 24:1190-1198, 2005*
94. *Zeng K, Zhao S, Fajardo L, **Wang G**: Global low-resolution CT scan regulated tomosynthesis. Journal of CT Theory and Applications 14:63-69, 2005*
95. *Wei Y, **Wang G**, Jiang H: Relation between filtered backprojection and backprojection for X-ray CT. IEEE Signal Processing Letters 12:633-636, 2005*

96. *Zhu JH, Zhao SY, Ye YB, **Wang G**: Computed tomography simulation with superquadrics. Medical Physics 32:3136-3143, 2005*
97. *Zou Y, Pan X, Xia D, **Wang G**: PI-line-based image reconstruction in helical cone-beam computed tomography with a variable pitch. Med. Phys. 32:2639-2648, 2005*
98. *Yu H, Zhao S, Ye Y, **Wang G**: A differentiable Shepp-Logan phantom and its applications in exact cone-beam CT. Phys. Med. Biol. 50:5583-5595, 2005*
99. *Yu H, Zhao S, Ye Y, **Wang G**: Exact BPF and FBP algorithms for nonstandard saddle curves. Med. Phys. 32:3305-3312, 2005*
100. *Wei YC, Hsieh J, **Wang G**: General formula for fan-beam computed tomography. Phys. Rev. Lett. 95:258102, 2005*
101. *Meinel JA, Hoffman EA, Clough A, **Wang G**: Reduction of half-scan shading artifact based on full-scan Correction. Academic Radiology 13:55-62, 2006*
102. *Yu HY, **Wang G**: A general formula for fan-beam Lambda tomography. International Journal of Biomedical Imaging, ID10427, 2006 (Yu HY, **Wang G**: Erratum to "A general formula for fan-beam lambda tomography". International Journal of Biomedical Imaging, ID95295, 2007)*
103. *Yu HY, Ye YB, Zhao S, **Wang G**: Local ROI reconstruction via generalized FBP and BPF algorithms along more flexible curves. International Journal of Biomedical Imaging, ID14989, 2006*
104. *Bai EW, Wang CL, Liu Y, **Wang G**: Controlled cardiac computed tomography. International Journal of Biomedical Imaging, ID14989, 2006*
105. *Deng J, Yu H, Ni J, He T, Zhao SY, Wang L, **Wang G**: A parallel Katsevich algorithm for 3-D CT image reconstruction. Journal of Supercomputing 38:35-47, 2006*
106. *Bai EW, Bennett JR, McCabe R, Sharafuddin MJ, Bai H, Halloran J, Vannier MW, Liu Y, Wang CL, **Wang G**: Study of an adaptive bolus chasing CT angiography. Journal of X-Ray Science and Technology 14: 27-38, 2006*
107. *Wei YC, Yu HY, **Wang G**: Integral Invariants for Computed Tomography. IEEE Signal Processing Letters 13:549- 552, 2006*
108. *Yu HY, Wei YC, Hsieh J, **Wang G**: Data consistency based translational motion artifact reduction in fan-beam CT. IEEE Trans. Medical Imaging 25:792-803, 2006*
109. *Lu DH, Bai EW, Liu J, Yu HY, Wei YC, Cai ZJ, Sharafuddin MJ, Golzarian J, Stolpen A, Saba O, Vannier MW, **Wang G**: Projection-based bolus detection for CT angiography. Journal of Computer Aided Tomography 30:846-849, 2006*
110. *Yu HY, Ye YB, Zhao SY, **Wang G**: Studies on Palamodov's algorithm for reconstruction from data collected along general loci. Inverse Problems 22:447-460, 2006*
111. *Yu HY, Ye YB, Zhao SY, **Wang G**: Reply to the comments by Palamodov on "Studies on Palamodov's algorithm for reconstruction from data collected along general loci". Inverse Problems 22:1505-1506, 2006*
112. *Zeng K, Yu HY, Fajardo LL, **Wang G**: Cone-beam mammo-computed tomography from data along two tilting arcs. Med. Phys. 33:3621-3633, 2006*
113. *Zhao J, Jiang M, Zhuang TG, **Wang G**: Minimum detection window and inter-helix PI-line with triple-source helical cone-beam scanning. Journal of X-Ray Science and Technology, 2006*
114. *Zhao J, Jiang M, Zhuang TG, **Wang G**: An exact reconstruction algorithm for triple-source helical cone-beam CT. Journal of X-ray Science and Technology 14:191-206, 2006*
115. *Ni J, Li X, He T, **Wang G**: Review of parallel computing techniques for computed tomography image reconstruction. Current Medical Imaging Reviews 2:1-10:, 2006*
116. *Yu HY, Ye YB, **Wang G**: Practical cone-beam lambda tomography. Med. Phys. 33:3640-3646, 2006*
117. *Li L, Kang KJ, Chen ZQ, Zhang L, Xin YX, **Wang G**: The FDK algorithm with an expanded definition domain for cone-beam reconstruction preserving oblique line integrals. Journal of X-ray Sci. and Tech.14:217-233, 2006*
118. *Li L, Chen ZQ, Xing YX, Zhang L, Kang KJ, **Wang G**: A general and exact synthetic algorithm for computing parallel projections from cone-beam projections via filtered backprojection. Phys. Med. Biol. 51:5643-5654, 2006*
119. *Cai ZJ, Stolpen A, Sharafuddin MJ, McCabe R, Bai H, Potts T, Vannier M, Li DB, Bi XM, Bennett J, Golzarian J, Sun SL, **Wang G**, Bai EW: Bolus characteristics based on magnetic resonance angiography. Biomedical Engineering Online 5:53 doi:10.1186/1475-925X-5-53, 2006*
120. *Ye Y, Yu HY, **Wang G**: Cone-beam pseudo-lambda tomography. Inverse Problems 23:203–215, 2007*

121. ***Wang G**, Ye Y, Yu HY: Approximate and exact cone-beam reconstruction with standard and non-standard spiral scanning. Phys. Bio. & Med. 52:R1-R13, 2007*
122. *Cai Z, McCabe R, **Wang G**, Bai EW: Bolus chasing computed tomography angiography using local maximum tracking method. Internal Journal of Modeling, Identification and Control 2:305-312, 2007*
123. *Yu HY, Zeng K, Bharkhada D, **Wang G**, Madsen MT, Saba O, Policeni B, Howard MA, Smoker WRK: A segmentation based interpolation method for metal artifact reduction. Academic Radiology 14:495-504, 2007*
124. *Zeng K, Yu HY, Zhao SY, Fajardo L, Ruth C, Jing Z, **Wang G**: Digital tomosynthesis aided by low resolution exact CT. Journal of Computer Assisted Tomography 31:967-983, 2007*
125. *Liu J, Wang C, Liu Y, Bai E, **Wang G**: Selectable source rotational velocity for cardiac CT. Journal of Computer Assisted Tomography 31:16-21, 2007*
126. *Yu HY, **Wang G**: Data consistency based rigid motion artifact reduction in fan-beam CT. IEEE Trans. Medical Imaging 26(2):249-260, 2007*
127. *Bai EW, Cai ZJ, McCabe R, **Wang G**: An adaptive optimal control design for bolus chasing computed tomography angiography. IEEE Transactions on Control Systems Technology 16(1):60-69, 2007*
128. *Zeng K, Bai EW, **Wang G**: A fast CT reconstruction scheme for a general multi-core PC. International Journal of Biomedical Imaging, ID29610, 2007*
129. *Zeng K, Yu HY, Bai EW, **Wang G**: Numerical studies on Palamodov and Generalized Feldkamp algorithm for general cone-beam scanning. Journal of X-ray Science and Technology 52:4331-4344, 2007*
130. *Yu H, Ye Y, Wei YC, **Wang G**: Lambda tomography with discontinuous scanning trajectories. Phys. Med. Biol. 52(14):4331-4344, 2007*
131. *Bharkhada D, Yu HY, Zeng K, Bai EW, **Wang G**: A comparative study on interpolation method for CT from random projections, International Journal of Imaging Systems and Technology 17:91-98, 2007*
132. *Ye YB, Yu HY, Wei YC, **Wang G**: General local reconstruction approach based on truncated Hilbert transform; International Journal of Biomedical Imaging, ID63634, 2007*
133. *Bharkhada D, Yu HY, **Wang G**: Knowledge-based dynamic volumetric cardiac CT with saddle curve trajectory. Journal of Computer Assisted Tomography, 32:942-950, 2007*
134. *Zhao J, Lu Y, Jin YN, Bai EW, **Wang G**: Feldkamp-type reconstruction algorithms for spiral cone-beam CT with variable pitch. Journal of X-ray Science and Technology 15:177-198, 2007*
135. *Wei Y, Yu HY, Hsieh J, **Wang G**: Scheme for computed tomography. Journal of X-ray Science and Technology 15:235-270, 2007 (Wei Y, Yu HY, Hsieh J, **Wang G**: Erratum: Scheme for computed tomography. Journal of X-ray Science and Technology, 16: 65, 2008)*
136. *Yu HY, **Wang G**: Cone-beam composite-circling scan and exact image reconstruction of a quasi-short object. International Journal of Biomedical Imaging, ID87319, 2008*
137. *Ye YB, Yu HY, **Wang G**: Exact interior reconstruction with cone-beam CT. International Journal of Biomedical Imaging, ID10693, 2008*
138. *Jiang M, Wyatt CL, **Wang G**: X-ray phase-contrast imaging with three 2D gratings. International Journal of Biomedical Imaging, ID827152, 2008*
139. *Zhu JH, Li X, Ye YB, **Wang G**: Analysis on the strip-based projection model for discrete tomography. Discrete Applied Mathematics, 156:2356-2367, 2008*
140. *Bai H, Zeng K, Bai EW, **Wang G**: Manual control of the patient table for bolus-chasing CT angiography. Journal of X-ray Science and Technology 16:23-31, 2008*
141. *Yu HY, **Wang G**: A general scheme for velocity tomography. Signal Processing, 88:1165-1175, 2008*
142. ***Wang G**, Yu HY, DeMan B: An outlook on x-ray CT research and development. Med. Phys. 35:1051-1064, 2008 (The Chinese version in Chinese Journal of Medical Instrumentation 32, 13 pages, translated by Tiange Zhuang and Jun Zhao, June 2008)*
143. *Li L, Kang K, Chen Z, Zhang L, Xing Y, Yu HY, **Wang G**: An alternative derivation and description of Smith's data sufficiency condition for exact cone-beam reconstruction. Journal of X-ray Science and Technology,16: 43-49, 2008*
144. *Cai ZJ, Erdahl C, Zeng K, Potts T, Sharafuddin M, Saba O, **Wang G**, Bai EW: Adaptive bolus chasing computed tomography angiography: Control scheme and experimental result. Biomedical Signal Processing and Control, Vol. 3, No. 4, pp. 319-326, 2008*
145. *Zeng K, Laurie LL, Kao S, Franken EA, Park JM, Jiang ZX, Bai EW, **Wang G**: An in vitro evaluation of cone-beam breast CT methods. Journal of X-ray Sciences and Technology, 16: 171-187, 2008*

146. *Zhao, J, Jin YN, Yang L, **Wang G**: A filtered backprojection algorithm for triple-source helical cone-beam CT. IEEE Trans. Medical Imaging,28:384-393, 2008*
147. *Yu HY, Yang JS, Jiang M, **Wang G**: Interior SPECT- Exact and stable ROI reconstruction from uniformly attenuated local projections. Communications in Numerical Methods in Engineering DOI:10/1002/cnm.1206, 18 pages, 2008*
148. *Bharkhada D, Yu H, Shuping, Carr J, **Wang G**: Cardiac CT dose reduction using interior reconstruction algorithm with the aorta and vertebra as known information. Journal of Computer Assisted Tomography 33:338-347, 2009*
149. *Bai EW, Cai ZJ, **Wang G**: Adaptive bolus-chasing computed tomography angiography: A whole body scan considering asymmetric arterial flow in peripheral arteries. Biomedical Signal Processing and Control, doie: 10.1016/j.bspc.2009.01.008, 2009*
150. *Deng J, Yu H, Ni J, Wang L, **Wang G:** Parallelism of iterative CT reconstruction based on local reconstruction algorithm. Journal of Supercomputing, 48:1-14, 2009*
151. *Yu HY, Zhao SY, Hoffman EA, **Wang G**: Ultra-low dose lung CT perfusion regularized by a previous scan. Academic Radiology, 16:363-373, 2009*
152. *Bharkhada D, Yu H, Dixon R, Wei YC, Carr JJ, Bourland D, Hogan R, **Wang G**: Demonstration of dose and scatter reduction for interior tomography. Journal of Computer Assisted Tomography 33:967-972, 2009*
153. *Lv Y, Zhao J, **Wang G**: Exact image reconstruction with triple-source saddle-curve cone-beam scanning. Phys. Med. Biol. 54 2971-2991, 2009*
154. *Bharkhada D, Yu HY, Liu H, Plemmons R, **Wang G**: Line-source-based x-ray tomography. International Journal of Biomedical Imaging, ID534516, 2009*
155. *Yu H, **Wang G**: Compressive sensing based interior tomography. Physics in Medicine and Biology, 54:2791-2805, 2009 (Corrigendum, Hengyong Yu and Ge Wang 2009* Phys. Med. Biol. *54 4341 doi:10.1088/0031-9155/54/13/C01)*
156. *Yu H, Cao G, Burk L, Lee Y, Lu J, Santago P, Zhou O and **Wang G;** Compressive sampling based interior tomography for dynamic carbon nanotube Micro-CT. Journal of X-ray Science and Technology 17(4): 295-303, 2009*
157. *Yu H, Ye Y, **Wang G.**, Interior reconstruction using the truncated Hilbert transform via singular value decomposition., Journal of X-Ray Science and Technology. 2009 16(4):243-251*
158. ***Wang G**, Yu H, Ye Y: A scheme for multi-source interior tomography. Medical Physics 36:3575-3581, 2009*
159. *Ye L, Yu H, **Wang G**: Determination of exact reconstruction Regions in Composite-circling cone-beam tomography. Medical Physics, .36(8):3448-3454, 2009*
160. *Lu Y, Cai ZJ, **Wang G**, Zhao J, Bai EW: Preliminary experimental results on controlled cardiac computed tomography: A phantom study. JXST, 17(2).175-187, 2009*
161. *Yu H, Yang JS, Jiang M, **Wang G**: Supplemental analysis on compressed sensing based interior tomography. PMB 54:N425-N432, 2009*
162. ***Wang G**, Cong WX, Shen HO, Zou Yu: Varying collimation for dark-field extraction. International Journal of Biomedical Imaging, ID847537, 2009*
163. *Han WM, Yu HY, **Wang G**: A general total variation minimization theorem for compressed sensing based interior tomography. Internal Journal of Biomedical Imaging, ID125871, 2009*
164. *Lv Y, Katsevich A, Zhao J, Yu H, **Wang G**: Fast exact/quasi-exact FBP algorithms for triple-source helical cone-beam CT. IEEE Trans. Medical Imaging 29:756-770, 2010*
165. *Lin Y, Lu Y, **Wang G**: Compressed sensing based image reconstruction from overlapped projections. Internal Journal of Biomedical Imaging, ID284073, 2010*
166. *Yang JS, Yu HY, Jiang M, **Wang G**: High-order total variation minimization for interior tomography. Inverse Problems 26:1-29, 2010*
167. *Yu H, **Wang G**: SART-type image reconstruction from a limited number of projections with the sparsity constraint; International Journal of Biomedical Imaging, ID934847, 2010*
168. ***Wang G**, Yu H: Can interior tomography outperform lambda tomography? PNAS 2010 107 (22) E92-E93; published ahead of print May 12, 2010, doi:10.1073/pnas.1002473107*
169. *Lu Y, Yu H, Cao GH, Zhao J, **Wang G**, Zhou O: Multi-beam field emission x-ray system and its reconstruction algorithm. Medical Physics 37:3773-3781, 2010*

170. Yu H, Ji CG, **Wang G**: SART-type image reconstruction from overlapped projections. International Journal of Biomedical Imaging, ID594537, 2010
171. Wei YC, Yu H, **Wang G**: Inverse Fourier transform in the Gamma coordinate system. International Journal of Biomedical Imaging, ID285130, 2010
172. Yu H, **Wang G**: Soft-threshold filtering approach for reconstruction from a limited number of projections. Physics in Medicine and Biology 55):3905-3916, 2010
173. Cong WX, **Wang G**: Higher-order phase shift reconstruction approach. Med. Phys. 37:5238-5242, 2010
174. Wei YC, **Wang G**: New relationship between the divergent beam projection and the Radon transform. To appear Journal of X-ray Science and Technology, 2010
175. **Wang G**, Wei Y: Analysis on derivative-free noncircular fan-beam reconstruction formula. To appear in IEEE Trans. of Image Processing, 2010
176. Ye YB, Yu HY, **Wang G**: Gel'fand-Graev's reconstruction formula in the 3D real space. To appear in Med. Phys., 2010
177. Bharkhada D, Yu H, Zou Y, **Wang G**: Comparative studies on the constraints for interior tomography in a POCS framework. To appear in PMB, 2010
178. Ni J, Deng JJ, He T, Yu H, **Wang G**: Speedup performance analysis of parallel Katsevich algorithm for 3D CT image reconstruction. To appear in International Journal of Computational Science and Engineering, 2010
179. Xu Q, Mou X, **Wang G**, Sieren J, Hoffman EA, Yu H: Statistical interior tomography. To appear in IEEE Trans. Medical Imaging, 2011
180. Cong WX, **Wang G**: X-ray scattering tomography for biological applications. To appear in Journal of X-ray Science and Technology, 2011
181. Wei YC, **Wang G**: New relationship between the divergent beam projection and the Radon transform. To appear in Journal of X-ray Science and Technology, 2011

D. Diversified Work

1. Li WH, **Wang G**: An ALU architecture improving multiplication operation. Journal of Beijing Microcomputers 4:76-82, 1987
2. **Wang G**, Wei YR: Exploration on the graduate course objective examination. Journal of Graduate School of Academia Sinica 5:93-95, 1988
3. Li WH, Wang B, **Wang G**: A preliminary study on linear transform of slowly changing data. Journal of Xidian University of China 2:62-70, 1988
4. **Wang G**, Ding Y: English multiple-choice test modeling and analysis. Journal of Mathematics in Practice and Theory 2:17-21, 1989
5. **Wang G**, Nunez M: A new method of estimating path radiance for band ratio application. International Journal of Remote Sensing 13:527-539, 1992
6. **Wang G**, Vannier MW, Skinner MW, Kalender WA, Polacin A, Ketten DR: Unwrapping cochlear implants by spiral CT. IEEE Trans. on Biomedical Engineering 43:891-900, 1996
7. Vannier MW, Marsh JL, **Wang G**, Christensen GE, Kane AA: Surgical imaging systems. Surgical Technology International 5:35-42, 1996
8. McFarland EG, Brink JA, Loh J, **Wang G**, Balfe DM, Heiken JP, Vannier MW: Visualization of colorectal polyps with spiral CT colonography: Evaluation of processing parameters with perspective volume rendering. Radiology 205: 701-707, 1997
9. McFarland EG, **Wang G**, Brink JA, Balfe DM, Heiken JP, Vannier MW: Central axis determination and digital unraveling of the colon for spiral CT colography. Academic Radiology 4:367-373, 1997
10. Kao SC, **Wang G**: Radiologic volumetry on a personal computer using a stereological method. Academic Radiology 5:665-669, 1998
11. Ketten DR, Skinner MW, Wang G, Vannier MW, Gates GA, Neely JG: In vivo measures of cochlear length and Nucleus Cochlear Implant Array insertion depth. Annals of Otology, Rhinology, and Laryngology 175:1-16, 1998
12. **Wang G**, McFarland EG, Brown BP, Vannier MW: GI tract unraveling with curved cross-sections. IEEE Transactions on Med. Imaging 17:318-322, 1998

13. Liu H, **Wang G**, Xue F, Fajardo LL: Adaptive image interpolation for full-field digital X-ray mammography. Applied Optics 38:253-257, 1999
14. Liu H, **Wang G**, Chen JH, Fajardo LL: Interpolation algorithms for digital mammography systems using multiple detectors. Academic Radiology 6:170-175, 1999
15. Valev V, **Wang G**, Vannier MW: Techniques for CT colonography (virtual colonoscopy). Critical Reviews in Biomedical Engineering 27:1-25, 1999
16. Dave SB, **Wang G**, Brown BP, McFarland EG, Zhang Z, Vannier MW: Straightening the colon with curved cross sections - A novel approach to computed tomographic colography. Academic Radiology 6:398-410, 1999
17. **Wang G**, Han W: Minimum error bound of signal reconstruction. IEEE Signal Processing Letters 6:309-311, 1999
18. Jiang H, Liu H, **Wang G**, Chen W, Fajardo LL: A localization algorithm and error analysis for stereo X-ray image guidance. Med. Phys. 27:885-893, 2000
19. Zhang Z, **Wang G**, Brown BP, McFarland EG, Haller J, Vannier MW: A fast algorithm for soft straightening of the colon. Academic Radiology 7:142-148, 2000
20. Yoo SK, **Wang G**, Rubinstein JT, Skinner MW, Vannier MW: Three-dimensional modeling and visualization of the cochlea on the Internet. IEEE trans. on Information Technology in Biomedicine (Special Issue on Multimedia Information Technology in Biomedicine) 4:144-151, 2000
21. Yang SY, **Wang G**, Skinner MW, Rubinstein JT, Vannier MW: Localization of cochlear implant electrodes in radiographs. Med. Phys. 27:775-777, 2000
22. **Wang G**, Skinner MW, Rubinstein JT, Howard MA, Vannier MW: Digital X-ray stereophotogrammetry for cochlear implantation. IEEE Trans. on Biomedical Engineering 47:1120-1130, 2000
23. Xu F, Liu H, **Wang G**, Alford B: Comparison of adaptive and conventional linear interpolation algorithms and their application in digital radiography. Electronic Imaging 9:22-31, 2000
24. Zhang Z, **Wang G**, Brown BP, Vannier MW: Distortion reduction for fast soft straightening of the colon. Academic Radiology 7:506-515, 2000
25. Yoo SK, **Wang G**, Rubinstein JT, Vannier MW: Three-dimensional geometric modeling of the cochlea using helico-spiral approximation. IEEE Trans. Biomedical Engineering 47:1392-1402, 2000
26. Liu H, **Wang G**: Design of a dual CCD configuration to improve the signal-to-noise ratio. Med. Phys. 27:2435-2437, 2000
27. **Wang G**: Book review on "Handbook of medical imaging - processing and analysis" (edited by Isaac N. Bankman et al., Academic Press, 2000). IEEE Trans. Med. Imaging 20:249-250, 2001
28. Vannier MW, **Wang G**: Book reviews, NIBIB, and IOM breast cancer report. IEEE Trans. Med. Imaging 20:145-146, 2001
29. Yoo SK, **Wang G**, Rubinstein J, Vannier MW: Semi-automatic segmentation of the cochlea using real-time volume rendering and regional adaptive snake modeling. Journal of Digital Imaging 4:173-181, 2001
30. Jiang H, Chen WR, **Wang G**, Liu H: Localization error analysis for stereo x-ray image guidance with probability method. Med. Engineering and Physics 23:573-581, 2001
31. Christensen GE, He J, Dill JA, Rubinstein JT, Vannier MW, **Wang G**: Automatic measurement of the labyrinth using image registration and a deformable inner ear atlas. Acad Radiology 10:988-999, 2003
32. Liu H, Sun LZ, **Wang G**, Vannier MW: Analytic modeling of breast elastography. Med. Phys. 30:2340-2349, 2003
33. Yin HM, Sun LZ, **Wang G**, Vannier MW: Modeling of elastic modulus evolution of cirrhotic human liver. IEEE Trans. Biomedical Engineering 51:1854-1856, 2004
34. Yoo SK, **Wang G**, Collison F, Rubinstein JT, Vannier MW, Kim HJ, Kim NH: Three-dimensional localization of cochlear implant electrodes using epipolar stereophotogrammetry. IEEE Trans. Biomedical Engineering 51:838-846, 2004
35. Hoffman EA, Clough AV, Christensen GE, Lin C, McLennan G, Reinhardt JM, Simon BA, Sonka M, Tawhai MH, van Beek EJ, **Wang G**: Forum for team science targeted towards a comprehensive imaging-based analysis of the lung. Academic Radiology 11:1370-80, 2004
36. Yin HM, Sun LZ, **Wang G**, Yamada T, Wang J, Vannier MW: ImageParser: a tool for finite element generation from three-dimensional medical images. Biomedical Engineering Online 2004 3:31 (http://www.biomedical-engineering-online.com/content/3/1/31)

37. ***Wang G**: Review of the book "Mathematical Techniques in Multisensor Data Fusion" by David L. Hall and Sonya A. H. McMullen. Biomedical Engineering Online 4:23, 2005 (http://www.biomedical-engineering-online.com/content/4/1/23)*
38. ***Wang G**: Review of the book "Electrical impedance tomography" edited by David S. Holder. Biomedical Engineering Online 4:27, 2005 (http://www.biomedical-engineering-online.com/content/4/1/27)*
39. *Liu Y, Sun LZ, **Wang G**: Tomography-based 3-D anisotropic elastography using boundary measurements. IEEE Trans. Medical Imaging 24:1323-1333, 2005*
40. ***Wang G**: Editorial for the inaugural issue: Features and perspectives. International Journal of Biomedical Imaging, ID81409, 2006*
41. *Wang ZG, Sun LZ, **Wang G**, Fajardo LL: Elasto-mammography: Theory, algorithm, and phantom study. International Journal of Biomedical Imaging, ID53050, 2006*
42. *Sun YH, Wu PR, Wei GW, **Wang G**: Evolution operator based single-step method for image processing. International Journal of Biomedical Imaging, ID83847, 2006*
43. *Liu Y, **Wang G**, Sun LZ: Anisotropic elastography for local passive properties and active contractility of myocardium from dynamic heart imaging sequence. International Journal of Biomedical Imaging, ID45957, 2006*
44. *Zhao J, Cao LJ, Zhuang TG, **Wang G**: Digital eversion of a hollow structure - An application in virtual colonography. International Journal of Biomedical Imaging, ID763028, 2008*
45. *Wang ZG, Liu Y, **Wang G**, Sun LZ: Elastography method for reconstruction of nonlinear breast tissue properties. Internal Journal of Biomedical Imaging, ID406854, 2009*
46. *Wei GW, **Wang G**: Editorial: Special issue on recent advances in computational techniques for biomedical imaging, Communications in Numerical Methods in Engineering 25: 581-582, 2009*
47. *Cai ZJ, Bai EW, McCabe R, Zerhouni M, **Wang G**, Raghavan ML, Kratzberg J: A dynamic arterial tree phantom for studies of bolus chasing CT angiography. International Journal of Biomedical Engineering and Technology 4:88-100, 2010*
48. *Li L, Chen ZQ, Xin J, Yu H, **Wang G**: Experimental studies of head motion effect for high resolution CT imaging. Optical Engineering 49:063201-1-6, 2010*
49. *Yang J, Yu H, Jiang M, **Wang G**: High order total variation minimization for interior SPECT. To appear in Inverse Problems, 2010*

Books

1. *Cheng PC, Huang PP, Wu JL, **Wang G**, Kim HG (Editors): Focus on multidimensional microscopy (I) - Instrumentation and image processing, World Scientific, Singapore, 1999 (ISBN 981-02-3991-2)*
2. *Cheng PC, Huang PP, Wu JL, **Wang G**, Kim HG (Editors): Focus on multidimensional microscopy (II) - Biological and material applications, World Scientific, Singapore, 1999 (ISBN 981-02-3992-0)*
3. *Censor Y, Jiang M, **Wang G**: Biomedical mathematics: Promising directions in imaging, therapy planning and inverse problems. Medical Physics Publishing, Madison, Wisconsin, USA, 2009*

Special Issues

1. ***Wang G**, Crawford CR, Kalender WA (Guest Editors): Multi-row-detector spiral/helical CT. Special issue of IEEE Trans. Medical Imaging, September, 2000*
2. ***Wang G**, Jaszczak R, Basilion J (Guest Editors): Molecular imaging. Special issue of IEEE Trans. Medical Imaging, July, 2005*
3. ***Wang G**, Bresler Y, Ntziachristos V (Guest Editors): Compressive sensing for biomedical imaging. Special issue of IEEE Trans. Medical Imaging, 2010*
4. *Liu H, **Wang G**, Brill A, Flowers C: Medical applications of modern imaging technologies. Special issue of Journal of X-ray Science & Technology 10(1), 2002*
5. *Ni J, Yu HY, **Wang G**: Computations & biomedical engineering: Medical imaging and medical data processing. Special issue of International Journal of Computational Science and Engineering, 2007*
6. *Wei GW, **Wang G**: Recent advances in computational techniques for biomedical imaging, Communication in Numerical Methods in Engineering, 2008*

Chapters

1. *Cheng PC, Acharya R, Lin TH, Samarabandu JK, **Wang G**, Shinozaki DM, Berezney R, Meng CL, Tarng WH, Liou WS, Tan TC, Summers RG, Kuang H, Musial C: 3-D image analysis and visualization in light microscopy and X-ray microtomography (Chap. 13). Visualization in biomedical microscopies (Editor: Kriete A), VCH Publisher, Weinheim, 361-398, 1992*
2. ***Wang G**, Lin TH, Shinozaki DM, Kim HG, Cheng PC: Cone-beam x-ray microtomography (Chap. 9). In Multidimensional Microscopy (Editors: Cheng PC, Lin TH, Wu WL, Wu JL), Springer-Verlag, New York, 151-169, 1993*
3. ***Wang G**, Liou WS, Lin TH, Cheng PC: Image restoration in light microscopy (Chap. 11). Multidimensional Microscopy (Editors: Cheng PC, Lin TH, Wu WL, Wu JL), Springer-Verlag, New York, 191-208, 1994*
4. *Cheng PC, Pareddy DR, Lin TH, Samarabandu JK, Acharya R, **Wang G**, Liou WS: Confocal microscopy of botanical specimens (Chap. 19). Multidimensional Microscopy (Editors: Cheng PC, Lin TH, Wu WL, Wu JL), Springer-Verlag, New York, 339-380, 1993*
5. *Vannier MW, **Wang G**: Principles of spiral CT (Chap. 1). Spiral CT of the chest (Editors: Remy-Jardin M, Remy J), Springer-Verlag, New York, 1-32, 1996*
6. ***Wang G**, Zhao SY, Cheng PC: Exact and approximate cone-beam X-ray microtomography (Chap. 1). Focus on multidimensional microscopy (I) (Editors: Cheng PC, Huang PP, Wu JL, **Wang G**, Kim HG), World Scientific, Singapore, 233-261, 1999*
7. ***Wang G**, Vannier MW: Computerized tomography. Encyclopedia of Electrical and Electronics Engineering (Editor: Webster JG), John Wiley & Sons, vol. 4, 8-24, 1999*
8. *Rockett P, **Wang G**: The principles of x-ray computed tomography. Standard Handbook of Biomedical Engineering and Design (Editor-in-Chief: Kutz M), McGraw-Hill, ISBN 0-07-135637-1,1-26, 2003*
9. *Lv DH, Bai EW, **Wang G**: Computed tomography. Wiley Encyclopedia of Biomedical Engineering (Editor: Akay M), John Wiley & Sons, 2005*
10. *Tang XY, **Wang G**: Computed tomography simulators. Encyclopedia of Medical Devices and Instrumentation (Editor: Dr. John Webster), John Wiley & Sons, 2005*
11. *Jiang M, **Wang G**, Li Y: Inverse problems in bioluminescence tomography. Frontier and Prospect of Contemporary Applied Mathematics – Series in Contemporary Applied Mathematics (Editors: Ciarlet PG, Li T), Higher Education Press (Beijing) & World Scientific, 2005*
12. *Jiang M, **Wang G**: Uniqueness results for multi-spectral bioluminescence tomography. Mathematical Methods in Biomedical Imaging and Intensity-Modulated Radiation Therapy (IMRT)' (Editors: Censor Y, Jiang M, Louis AK), Edizioni della Normale, Pisa, Italy, 153-184, 2008*
13. ***Wang G**, Cong WX, Yu HY: Development of x-ray computed tomography and bioluminescence tomography. Mathematical Methods in Biomedical Imaging and Intensity-Modulated Radiation Therapy (IMRT)" (Editors: Censor Y, Jiang M, Louis AK), Edizioni della Normale, Pisa, Italy, 425-446, 2008*
14. *Amin AR, **Wang G**: Identification and characterization of transcriptome-based biomarkers in arthritis and cancer for personalized medicine by translational genomics. Biomedical Mathematics: Promising Directions in Imaging, Therapy Planning and Inverse Problems (Editors: Censor Y, Jiang M, Wang G), Medical Physics Publishing, Madison, WI, USA, 19-32, 2010*
15. *Jiang M, **Wang G**: Mathematical theory for x-ray phase-contrast imaging with 2D grating interferometry. Biomedical Mathematics: Promising Directions in Imaging, Therapy Planning and Inverse Problems (Editors: Censor Y, Jiang M, Wang G), Medical Physics Publishing, Madison, WI, USA, 201-220, 2010*
16. ***Wang G**, Yu HY, Ye YB: Interior tomography: Practical applications. Biomedical Mathematics: Promising Directions in Imaging, Therapy Planning and Inverse Problems (Editors: Censor Y, Jiang M, Wang G), Medical Physics Publishing, Madison, WI, USA, 495-508, 2010*
17. *Ye YB, Yu HY, **Wang G**: Interior tomography: Mathematical analysis. Biomedical Mathematics: Promising Directions in Imaging, Therapy Planning and Inverse Problems (Editors: Censor Y, Jiang M, Wang G), Medical Physics Publishing, Madison, WI, USA, 543-561, 2010*
18. *Shen H, Goldstein AS, **Wang G**: Biomedical imaging and image processing in tissue engineering. The Tissue Engineering Book: State of the Art, Visions, and Limitations. Springer Science + Business Media, 2010*

19. *Shen H, Cong W, Xu Y, Rylander C, Rylander MN, Furth M, Christ GJ, Lee SJ, Geary RL, Yoo JJ, Soker S, **Wang G**: Optical molecular tomography for regenerative medicine. The Handbook of Enabling Technologies for Regenerative Medicine, Artect House, 2010*
20. *Li L, Chen ZQ, **Wang G**: Reconstruction algorithms. Cone Beam Computed Tomography (Editor: C. C. Shaw). Series: Imaging in Medical Diagnosis and Therapy (WR Hendee, Series Editor), Taylor & Francis, 2011*
21. *Lv YJ, **Wang G**: Preclinical optical molecular imaging. Multimodality Molecular Imaging of Small Animals: Instrumentation and Applications (Editor: Habib Zaidi), Springer-Verlag, 2011*

***Patents** (http://www.uspto.gov/patft; http://www.freepatentsonline.com/index.html)*

1. *Wang G, Snyder DL, O'Sullivan JA, Cheng PC, Vannier MW: Iterative algorithms for cone-beam tomography from incomplete data. US patent 5,909,476, 1999*
2. *Wang G, Schweiger GD, Vannier MW: An iterative algorithm for x-ray CT fluoroscopy. US patent 6,101,236, 2000*
3. *Wang G, McFarland EG, Brown BP, Zhang Z, Vannier MW: GI tract unraveling with curved cross-sections. US patent 6,212,420, 2001*
4. *Wang G, Vannier MW: Bolus-chasing angiography with adaptive real-time computed tomography. US patent 6,535,821, 2003*
5. *Bai EW, Wang G, Vannier MW: System and method for adaptive bolus chasing computed tomography (CT) angiography. US patent 7,522,744, 2009*
6. *Hsieh J, Wang G: A progressive updating approach for volumetric CT image reconstruction and its clinical applications. US patent 6,850,585, 2005*
7. *Wang G, Hsieh J, Wei YC: Methods, apparatus, and computer readable mediums for performing perfusion studies. US patent 6,934,353, 2005*
8. *Heuscher DJ, Zhao S, Matthews D, Wang G: Knowledge-based dynamic computed tomography imaging. US patent 7,058,440, 2006*
9. *Wang G, Lee SW: Methods and devices for CT reconstruction using a Grangeat approach. US patent 6,983,034, 2006*
10. *Wang G, Ye Y: Systems and methods of non-standard spiral cone-beam computed tomography (CT). US patent 7,373,937, 2008*
11. *Wei Y, Hsieh J, Wang G: CT image reconstruction through employment of function that describes interpreted movement of source around particular point of object. US patent 7,376,213, B1, 2008*
12. *赵俊，姜明，庄天戈，**Wang G**:*

    2N+1源螺旋CT的精确重建方法，中国发明专利（申请号：200610030332.X，申请日：2006.8.24，公开号：CN1907226A, 公开日：2007.2.7，专利号：ZL 200610030332.X，授权公告日：2009.4.22）
13. *Hsieh J, Wei Y, **Wang G**: Correlation-based motion estimation of object to be imaged. US 7,587,022 B1, 2009*
14. ***Wang G**, Ye Y, Yu HY: Interior tomography and instant tomography reconstruction from truncated limited angle projection data. US patent 7,697,658 B2, issued on April 13, 2010*
15. ***Wang G**, Zhao SY: Clinical micro-CT (CMCT) methods, techniques and apparatus. US patent 7,840,249, 2010*
16. *Rylander C, Campbell TA, **Wang G**, Xu Y, Kosoglu MA: Fiber array for optical imaging and therapeutics. PCT International Application No: PCT/US2010/025809, March 1, 2010*
17. *Wang G, Cong A, Han WM, Jiang M, Shen HO, Cong WX: Systems and methods for multi-spectral bioluminescence tomography. Patent disclosure filed with Univ. of Iowa Research Foundation in April 2004; provisional application 60/756,036, Feb. 28, 2006*
18. *Wang G, Li Y, Jiang M, Qian X, Cong WX: Computational optical biopsy methods, techniques and apparatus. Patent disclosure filed with Univ. of Iowa Research Foundation in Dec. 2003; provisional patent filed in 2005; formal US patent application filed in 2006*
19. *Wang G, Yu H: Systems and methods for exact or approximate cardiac CT. Virginia Tech Patent Disclosure (July 17, 2007), VTIP Ref: 07-099; US patent Application: 60/960,389, July 17, 2007*
20. *Sun LZ, Liu Y, Wang ZG, Wang G: Method and apparatus for elastomammography. UC patent case no. 2006-605-1, US 2007/0238966 A1, October 11, 2007*

21. *Wang G, Hoffman EA, McLennan G: Bioluminescent CT method and apparatus. Patent disclosure filled in July 2002; US provisional application filled in March 2003; US patent application (US No. 60/453,177), filed in March 2004*
22. *Wang G, Cong WX: Multi-parameter x-ray computed tomography methods and systems. May 22, 2008*
23. *Wang G, Liu Y, Zhang J, Sun LZ: Tomography-based dynamic cardiac elastography. July 20, 2008*
24. ***Wang G**, Zhao J, Lu Y, Yu HY, Katsevich A: Cardiac computed tomography methods and systems using fast exact/quasi-exact filtered back projection algorithms. US patent application 12/914,790, Oct. 28, 2010*
25. ***Wang G**, et al.: Tomography-based and MRI-based imaging systems. US patent application # 12/916,458, Oct. 29, 2010*
26. ***Wang G**, et al.: Extended interior methods and systems for spectral, optical, and photoacoustic imaging. US patent application filed on 11/12/10*
27. ***Wang G**, Ritman E, Yu HY: BIG DIPPER (Biomedical Imaging Group – Dynamic Interior Pulsed Plural-sourcE Rotating-gantry (BIG DIPPER) system). Disclosure filed on 11/22/10, US provisional application filed.*

***IP Disclosures at Virginia Tech**: http://vtip.livewebdev.com/availableTech/search.php?widget=205*

***Conference Publications**: Numerous*

News Articles and On-line Presentation

1. *Lavery A: First bioluminescent CT prototype is "a new imaging modality". Clinica World Medical Device & Diagnostic News, page 2, PJB Publications Ltd., Richmond, Surrey, UK, December 17th, 2003 (www.clinica.co.uk)*
2. *Butkus, B: Instrument enables bioluminescence computed tomography. International Biophotonics, pages 17-18, Laurin Publishing, Pittsfield, MA, USA, February, 2004 (http://www.photonics.com/bio)*
3. *Wang G: Bioluminescence tomography. Stanford University 2005 MIPS/Philips Medical Molecular Imaging Seminar Series, January 3, 2005 (http://mips.stanford.edu/public/mi_seminar05.adp)*
4. *Hoff LT: Molecular imaging advance watches tumors grow, shrink. RSNA News, November issue, pages 10-11, 2007*
5. *Bem S: Bioluminescence tomography development in Virginia Tech. Video clip, MedstarAdvances® Producer, Medstar Television, www.medstar.com, October 2007*
6. *Newswise (http://www.newswise.com/articles/view/530437): New molecular imaging approach identifies tumors. Released May 31, 2007*
7. *Bioluminescence tomography (http://www.photonics.com/content/bio/2008/March/journals/92144.aspx), March 2008*
8. *Savage N: Medical imagers lower dose. IEEE Spectrum Magazine, pp. 14-15, March 2010*

II. Service

Journal Editorship

- ***Editor-in-Chief for International Journal of Biomedical Imaging (2005-)***
- *Editorial board member, Recent Patents on Medical Imaging (2009-)*
- *Guest editor for the special issue on "Recent Advances in Computational Techniques for Biomedical Imaging'", Communications in Numerical Methods in Engineering, 2008*
- *Editorial board member (2008-), Contemporary Engineering Sciences, Hikari, Bulgaria*
- *Editorial board members (2007-) for Open Applied Informatics Journal, Open Electrical and Electronic Engineering Journal, Open Medical Imaging Journal, Open Medical Imaging Reviews, Open Medical Imaging Letters*
- *Editorial Board (2007-) for Journal of X-ray Science and Technology*
- *Editorial Board (2010-) for Journal of Computer Assisted Tomography*
- *Guest Editor for the special issue on molecular imaging of IEEE Transactions on Medical Imaging (5/05)*
- *Editor for Current Medical Imaging Reviews (1/2005-)*
- *Editor (Biomedical Imaging) for Biomedical Engineering Online (2003-2005)*
- *Associate Editor for IEEE Transactions on Medical Imaging (1/2001-)*
- *Associate Editor for Medical Physics (1/2000-)*
- *Associate Editor for Computed Tomography Theory and Applications (2001-2005)*
- *Guest Editor for the special issue on X-ray imaging of Journal of X-Ray Science and Technology (2002)*
- *Guest Editor for the special issue on multi-slice/cone-beam CT of IEEE Transactions on Medical Imaging (10/2000)*
- *Guest Associate Editor for Medical Physics (1998, 1999)*
- *Member for selection of the best Medical Physics paper for the Sylvia Sorkin Greenfield Award (1999-2006)*

Grant Reviewership

- ***NIH**: ICMICs ZCA1 SRLB-9 (M1), 2010, 2011; ZDC1 SRB R-33, 2011; MEDI, 2010; ZRG1 SBIB-P (02), BMIT/MEDI member conflict grants, 2008–2009; SSS-7, 2004-2006; SEP, 2003; NCRR, 2002; NIDCD, 2001;*
- ***NSF**: 2001 (DBES), 2003 (DMS)*
- ***DOD**: 1999 (USAMRMC), 2010 (Era of Hope)*

National and University Committees

1. *Diagnostic X-Ray Imaging Committee Member, AAPM, 1999-Now*
2. *Member of the Medical Physics Group for CT quality control and dose monitoring at Washington University Medical Center, 1993-1996*
3. *Organizer of the 4th International Conference for Young Computer Scientists (ICYCS 1995), Beijing, China, Jul. 1995*
4. *Session chairs of "Image Processing and Reconstruction I" and "Near-field and Other Microscopy II", the 8th International Conference on 3D Image Processing in Microscopy and the 7th International Conference on Confocal Microscopy, Taipei, Apr. 1995*
5. *Plenary session chair of "Image modeling in confocal reflection and transmission microscopes", Session Chair of "Image resolution and reconstruction", the 10th International Conference on 3D Image Processing in Microscopy and the 9th International Conference on Confocal Microscopy, Buffalo, NY, April 1997*
6. *Technical committee member, the 13th IEEE Symposium on Computer-Based Medical Systems, Houston, TX, June 23-24, 2000*
7. *Program committee member, the SPIE International Symposium on Biomedical Photonics and Optoelectronic Imaging, November 8-10, 2000*
8. *Research committee member, University of Iowa College of Medicine, October 2000-Now*

9. *Scientific committee member, the 2nd Beijing International Conference on Physics and Engineering of Medical Imaging, October 24-28, 2001*
10. *CT session chair, RSNA, 2003, 2004*
11. *Program committee member, Special Technical Session/workshop: Grid Computing Technologies and Applications in the 2004 International Conference on Parallel and Distributed Processing and Applications, Las Vegas, Nevada, June 21-24, 2004*
12. *Session Chair, Computational methods for medical science, 17th IMACS World Congress - Scientific Computation, Applied Mathematics and Simulation, Paris, France, July 11 - 15, 2005*
13. *University of Iowa Animal Imaging Facility Advisory Committee, 2004-2005*
14. *University of Iowa CT Scanner Advisory Committee, University of Iowa Research Committee, 7/2004-8/2005*
15. *Program committee, the International Multi-Symposiums on Computer and Computational Sciences (IMSCCS|06), June 20-24, Zhejiang University, Hangzhou, China*
16. *Scientific Committee, Fully Three-Dimensional Image Reconstruction in Radiology and Nuclear Medicine, Lindau, Germany, July 9-13, 2007*
17. *Session Chair, An Interdisciplinary Workshop on Mathematical Methods in Biomedical Imaging and Intensity-Modulated Radiation Therapy (IMRT), Pisa, Italy, October 15-19, 2007*
18. *Conference Co-chair, International Conference on Biomedical Inverse Problems – Imaging, Therapy Planning and Other Promising Directions, Huangguoshu, China, Nov. 3-9, 2008*
19. *Faculty Advisory Board, ICTAS, Virginia Tech, 2008-Now*
20. *Program committee, SPIE Conference on Developments in X-Ray Tomography, 2002-2010*
21. *Scientific Committee and Session Chair, Fully Three-Dimensional Image Reconstruction in Radiology and Nuclear Medicine, Beijing, China, September 5-10, 2009*
22. *"Biological and Drug Discovery Imaging" Committee for OSA Biomed 2010, Miami, Florida, USA, April 11-14, 2010*
23. *Scientific Committee and Session Chair, the First International Meeting on Image Formation in X-Ray Computed Tomography, Salt Lake City, Utah, USA, June 6-9,2010*
24. *Program Committee and Session Chair, SPIE Conference on Developments in X-ray Tomography, San Diego, California, USA, Aug. 2-5, 2010*
25. *Scientific Committee, Fully Three-Dimensional Image Reconstruction in Radiology and Nuclear Medicine, Potsdam, Germany, July 11-15, 2011*
26. *General Chair, 2014 IEEE International Symposium on Biomedical Imaging, Beijing, China*
27. *Chair of the Search Committee for a VT-WFU SBES assistant professor position, 222 applicants, 2011*
28. *Program Committee, the First IEEE Conference in Medical Imaging Informatics. China, Sept. 26-29, 2011*

III. Teaching

Courses at Graduate School of Academia Sinica, University of Iowa, and Virginia Tech

Title: ***Digital Picture Processing***
Semester: *Fall 1986*
Length: *80 hours*
Institution: *Graduate School of Academia Sinica*
Prerequisite: *Advanced linear algebra, stochastic processes, linear system theory, digital signal processing*
Textbook: *Rosenfeld A, Kak AC: Digital picture processing. 2nd edition, Academic Press, New York, 1982*

Title: ***Computer Vision***
Semester: *Fall 1987*
Length: *80 hours*
Institution: *Graduate School of Academia Sinica*
Prerequisite: *Digital picture processing, artificial intelligence*
Textbook: *Ballard DH, Brown CM: Computer Vision. Prentice-Hall, Englewood Cliffs, New Jersey, 1982*

BME188: ***Imaging Practicum***
Semester: *Spring 2001*
Credit Hours: *4*
Institution: *University of Iowa*
Prerequisite: *BME185 Physics and Analysis of Biomedical Images I,*
BME186 Physics and Analysis of Biomedical Images II
Textbook: *Lecture Notes by Ge Wang*

BMES_6514_16995_200901: ***Medical Imaging II***
Semester: *Spring 2009*
Credit Hours: *4*
Institution: *Virginia Tech & Wake Forest University*
Instructors: *Craig Hamilton, Katherine Holzbaur, Robert Kraft, Pete Santago, Ge Wang*

Teaching Seminars, Lectures, and Training Sessions:

Numerous at Washington University in St. Louis, University of Iowa, Virginia Tech, Wake Forest University, and many other intuitions and companies nationally and internationally

Online Resources: *Seminars, Training, Courses, Related Research (click the links for further details)*

Guest Professorship

- *Northeastern University (Computer Science, 02-05)*
- *Beijing Union University (Electrical & Computer Engineering, 02-05)*
- *Beijing Jiaotong University (Information Science, 06-09)*
- *China Medical University (Guest Professor, from 09)*
- *Shanghai Jiaotong University (Biomedical Engineering (03-07); Advisory Professor (from 07, life time))*
- *Tsinghua University (Engineering Physics, from 03)*
- *Peking University (Mathematics, from 03)*
- *Xidian University (Honorable Professor, from 08, life time)*
- *UCSD (Visiting Professor of Radiation Oncology, August, 10)*

Dr. Ge Wang's PhD Students in Biomedical Imaging

#	Name (Co-advisor/Advisor)	Topic	Period	Employment	Email
1	Deepak Bharkhada	Cardiac CT methods	05-10	Harvard U Postdoctoral	dkbharkhada@yahoo.com
2	Junjun Deng (Lihe Wang)	Fast CT reconstruction	05-10	Siemens Preclinical Engineer	junjundeng@hotmail.com
3	Seung Wook Lee (Gyuseong Cho)	Approximate CBCT	01-03	Atomic Energy Inst Scientist	swlee@kaist.ac.kr
4	Liang Li (Zhiqiang Chen)	Exact CBCT	04-07	Tsinghua U Faculty	liliang02@mails.tsinghua.edu.cn
5	Xiang Li	Iterative CT	01-05	GE Engineer / Consultant	seanlix@gmail.com
6	Haiou Shen (Hantao Zhang)	BLT	01-06	Virginia Tech Scientist	hhshen@vt.edu
7	Jeremy Wang (Lizhi Sun)	CT elastography	04-10	Sun Life Financial Engineer	wzg219@hotmail.com
8	Jun Zhao (Tiange Zhuang)	Multi-source CBCT	03-06	Shanghai Jiaotong U Faculty	junzhao@sjtu.edu.cn
9	Kai Zeng	Tomosynthesis	04-08	GE GRC Engineer	zengkai@ge.com
10	Jiehua Zhu (YB Ye, SY Zhao)	Spiral CBCT	01-05	Georgia Southern U Faculty	jzhu@GeorgiaSouthern.edu
11	James Bennett	Cardiac CT systems	10-		jrbennet@gmail.com
12	Alex Cong	Optical Tomography	06-		alexcong@gmail.com
13	Peng He (Biao Wei)	True-color CT	10-		hepeng_vvv@hotmail.com
14	Xin Jin (Zhiqiang Chen)	Interior CT	10-		jinxincn@gmail.com
15	Spencer Lee (Ed Fox)	SecondLife	09-		zamfir@vt.edu
16	Yang Lu (Jun Zhao)	Triple-source CBCT	08-		lvyang1917@gmail.com
17	Sourav Mishra	Grating-based Imaging	10-		sourav@vt.edu
18	Kriti Sen Sharma	Nano-CT deblurring	09-		kritisen@vt.edu

Lab Alumni

Postdoctoral Fellows, Visiting, Research or Regular Faculty

#	Name	Topic	Period	Employment	Email
1	Bruce Brown	CT colonoscopy	06-08	U of Iowa Faculty	Bruce-brown@uiowa.edu
2	Kumar Durai	Optical imaging	03-06	Periyar Maniammai College Faculty	kumar_durai@yahoo.com
3	Laurie Fajardo	Breast imaging	02-06	U of Iowa Faculty	l-fajardo@uiowa.edu
4	Changguo Ji	True-color CT	09-10	GE Healthcare Engineer	cgji@yahoo.com
5	Ming Jiang	Inverse problems	00-05	Peking U Faculty	ming-jiang@pku.edu.cn
6	Jie Liu	Cardiac CT	04-05	Beijing Jiaotong U Faculty	lj@computer.njyu.edu.cn
7	Yi Liu	CT elastography	03-05	Indiana-Purdue U Research Faculty	liu5@iupui.edu
8	Zhanping Liu	Lung CT	2000	UPenn Research Fellow	zhanpingliu@hotmail.com
9	Donghui Lv	CT angiography	04-05	Shanghai U Faculty	dhlu@staff.shu.edu.cn
10	Jun Ni	Parallel computing	00-06	U of Iowa Faculty	Jun-ni@uiowa.edu
11	Xin Qian	Optical biopsy	05-07	UNC Research Faculty	xqian@physics.unc.edu
12	Venny Valev	CT colonoscopy	97-98	Wroclaw U of Tech Faculty	valev@math.bas.bg
13	Michael Vannier	Spiral CT	96-03	U of Chicago Faculty	mvannier@radiology.bsd.uchicago.edu
14	Yuchuan Wei	CT theory	04-08	Wake Forest U Research Fellow	ywei@wfubmc.edu
15	Sun Kuo Yoo	Cochlear modeling	98-00	Yonsei U Faculty	sunkyoo@yumc.yonsei.ac.kr
16	Zhan Zhang	CT colonoscopy	98-00	NIH Research Fellow	zhan.zhang@hotmail.com
17	Jun Zhao	CT angiography	04-05	Shanghai Jiaotong U Faculty	junzhao@sjtu.edu.cn
18	Shiying Zhao	CT theory	04-05	UMSL Faculty	zhao@arch.cs.umsl.edu

MS, Undergraduate and High-school Interns

#	Name	Topic	Period
1	Henri Bai	CT angiography	05-06
2	Bret Bulery	Bioluminescence imaging	05-06
3	Frederick Collison	Stereophotogrammetry	01-05
4	Sanjay Dave	CT colonoscopy	97-97
5	Cody Edgell	Multi-scale CT	2010
6	Ken Eng	Interior tomography	2008
7	Mark Fleckenstein	CT imaging	2006
8	Javier Gomez	Thermal tomography	2008
9	Pilsung Kang	Cloud computing	2010
10	Ray Lee	Weak light detection	09-10
11	Peng Lu	Bibliometrics	2010
12	Mandy Halling	CT colonoscopy	99-01
13	Tao He	Parallel computing	04-06
14	Ying Hou	CT angiography	04-05
15	Lily Huang	Java programming	99-01
16	Nicholas Lariviere	Cone-beam CT	04-05
17	David Li	Visualization	2005
18	Vinson Liu	Cone-beam CT	02-02
19	Mark Luo	Image analysis	04-05
20	David McCracken	Optical imaging	2010
21	John Meinel	Lung CT	01-04
22	Kathy Redford	Fan-beam CT	97-99
23	Matthew Ruder	Second Life	2009
24	Siying Yang	Image processing	99-10
25	Lena Ye	Cone-beam CT	06-08
26	Ivan Ye	Bibliometrics	10-10
27	Roy Zhang	Optical imaging	2006

nature biotechnology

PERSPECTIVE

Looking and listening to light: the evolution of whole-body photonic imaging

Vasilis Ntziachristos[1], Jorge Ripoll[1,2], Lihong V Wang[3] & Ralph Weissleder[1]

Optical imaging of live animals has grown into an important tool in biomedical research as advances in photonic technology and reporter strategies have led to widespread exploration of biological processes *in vivo*. Although much attention has been paid to microscopy, macroscopic imaging has allowed small-animal imaging with larger fields of view (from several millimeters to several centimeters depending on implementation). Photographic methods have been the mainstay for fluorescence and bioluminescence macroscopy in whole animals, but emphasis is shifting to photonic methods that use tomographic principles to noninvasively image optical contrast at depths of several millimeters to centimeters with high sensitivity and sub-millimeter to millimeter resolution. Recent theoretical and instrumentation advances allow the use of large data sets and multiple projections and offer practical systems for quantitative, three-dimensional whole-body images. For photonic imaging to fully realize its potential, however, further progress will be needed in refining optical inversion methods and data acquisition techniques.

Small-animal imaging is rapidly becoming a cornerstone in biomedical investigation, serving as an important translation tool between *in vitro* research and clinical application. Recently, key advances in the *in vivo* reporting of genomics and proteomics have intensified the development of dedicated small-animal imaging systems and strategies[1–6]. Linked to these developments is an emerging shift from traditional *in vitro* assay–based research to *in vivo* imaging–based research. *In vivo* imaging can improve our ability to probe complex biologic interactions dynamically and to study disease and treatment responses over time in the same animal, thus offering the potential to accelerate basic research and drug discovery using fewer animals.

Two major approaches have been adopted in the development of *in vivo* small-animal imaging. The first is an elegant adaptation of proven clinical imaging technologies to the smaller animal dimensions. It includes all of the major radiological modalities; that is, positron emission tomography (PET), single photon emission computed tomography (SPECT), magnetic resonance imaging (MRI), ultrasound, X-ray computed tomography (CT) and multi-modality approaches[1,5,6]. The resulting imaging systems attain higher resolution and detection sensitivity compared with their clinical counterparts because of the smaller field of view used and the corresponding modification of the operating characteristics (for example, higher field strengths for MRI or higher frequencies for ultrasound).

The second approach focuses on new imaging technologies, primarily macroscopic imaging based on photonics. These novel methods extend beyond three-dimensional *in vivo* microscopy (such as multi-photon or confocal microscopy), which is not well suited for whole-body imaging because of its limited penetration depth (<1 mm) and the restricted field of view typically achieved. Here, progress in instrumentation and methodology is combined with ingenious advances in fluorescence or bioluminescence reporter gene/reporter probe[1,4,7] strategies, activatable fluorescent probes and targeted fluorescent probes[8,9] for *in vivo* molecular sensing. Whole-body fluorescence and bioluminescence imaging have transformed the ways gene expression and protein functions are visualized *in vivo*[10,11]. In most cases, optical detection has been accomplished using photographic methods, using low-light cameras and appropriate filters. Photon attenuation, however, is strongly nonlinear as a function of depth and of the optical heterogeneity of tissue, which obscures signal quantification. Planar imaging is further complicated by the inability to resolve depth and by tissue scattering, which limits spatial resolution. For these reasons, although planar methods are useful, they do not harness the true potential of the optical imaging technologies.

The emergence of mathematical models that describe photon propagation in tissues, combined with advanced illumination and detection schemes, and appropriate tomographic principles, can significantly improve visualization capacity in tissue. Tomography enables quantitative three-dimensional volumetric imaging of opaque media and can overcome planar imaging limitations. The combination of these advances with adept contrast mechanisms using highly specific fluorescent probes or the photoacoustic phenomenon has facilitated a new generation of photonic imaging systems that is rapidly maturing and can greatly facilitate small-animal research by complementing the laboratory microscope, spectrophotometer and flow cytometer with whole-body *in vivo* molecular imaging capacity.

This review focuses on novel macroscopic photonic imaging technologies that, in combination with emerging reporter strategies, promise to provide researchers with unprecedented power to visualize biological processes. We compare photographic and tomographic optical imaging and describe the three major optical domains of optical tomography

[1]Center for Molecular Imaging Research (CMIR), Massachusetts General Hospital & Harvard Medical School CNY149, 13th street 5406, Charlestown, Massachusetts 02129, USA. [2]Institute for Electronic Structure and Laser, Foundation of Research and Technology-Hellas, P.O. Box 1527, 71110 Heraklion, Greece. [3]Optical Imaging Laboratory, Department of Biomedical Engineering, Texas A&M University, 3120 TAMU, College Station, Texas 77843-3120, USA. Correspondence should be addressed to V.N. (vasilis@helix.mgh.harvard.edu).

Published online 4 March 2005; doi:10.1038/nbt1074

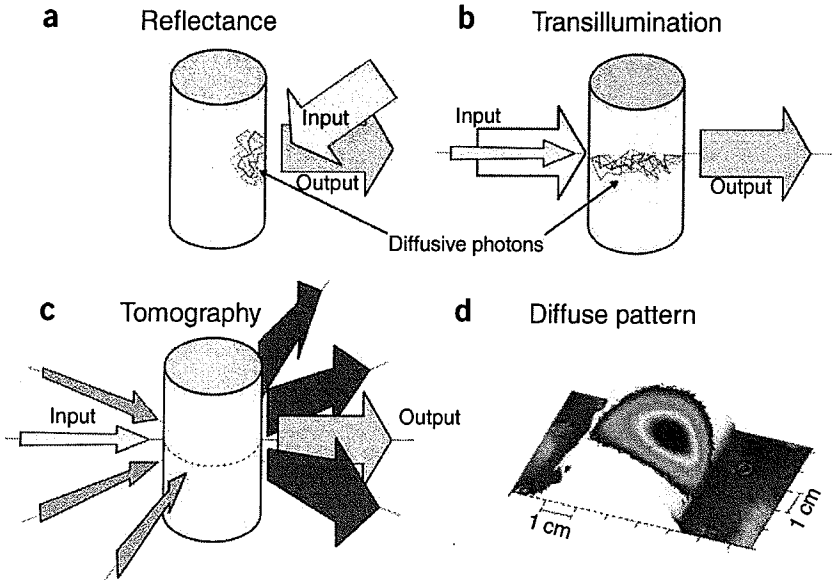

Figure 1 Modes of data collection. **(a,b)** Planar imaging. Fluorescence reflectance imaging. Excitation light (input) is expanded on the object surface and fluorescence light (output) collected from the same side of the object. Scattered photon trajectories are simplistically demonstrated with a few lines to demonstrate the typical volume sampling. **(b)** Transillumination illuminates the object from the opposite side from the data collection so that light propagates through the object. Photon scattering is also indicated with a few lines and indicates the volume sampling differences in relation to **a**. Transillumination can be obtained with a single point source (green), a summation of multiple point sources or with an expanded planar beam (light gray). **(c)** Tomography. Illustration of data collection where multiple point-source transillumination data are time-shared around a cylindrical geometry. Different geometries and the use of reflected data can also be used for tomographic purposes. The direction indicated by the arrows shows the general photon trajectory established. The pattern of data collected is, in fact, diffusive as is evident from the experimental measurements shown in **(d)** obtained from a transilluminated homogeneous diffusive cylinder.

(that is, time, frequency and constant intensity). Particular weight is given to recent noncontact imaging approaches and tomographic specifics that significantly improve imaging performance and enable the development of practical and accurate systems. State-of-the-art *in vivo* imaging examples are illustrated. Bioluminescence and photoacoustic tomography are also reviewed, together with the expected impact of these technologies in biomedical research.

Planar imaging

Planar imaging, the simplest technique for detecting optical reporter molecules *in vivo*, uses photographic principles to capture light emitted from the animals[12–14] and has broadly affected biomedical research[7,11,15]. For fluorescence imaging, the animal is typically illuminated with a broad light beam tuned to the excitation wavelength of the fluorochrome of interest and is photographed at the emission wavelengths by a highly sensitive and low noise charged-coupled device (CCD) camera using appropriate filters and large aperture lenses for high photon collection efficiency (**Fig. 1a**). These low-light images are superimposed on mouse photographs obtained at the excitation wavelength or with white light illumination. This is the most common whole-body fluorescence imaging approach today and is termed fluorescence reflectance imaging (FRI). Advanced forms of FRI use spectral information to differentiate between different fluorochromes. Yang *et al.*[14], for example, demonstrated that the use of a highly sensitive color CCD camera can detect green fluorescent proteins expressed by tumors implanted superficially in living animals. More recently, to improve detection contrast (see **Fig. 2**), Gao *et al.*[16] have used spectral un-mixing, a technique that can differentiate multiple fluorochromes from nonspecific background fluorescence on the basis of their spectral characteristics (for details, see ref. 17). Bioluminescence signals can be similarly detected, but in the absence of external illumination light. In contrast, fluorescence transillumination imaging illuminates the animal with a broad light beam or a raster scan of focused beam and images are collected from the opposite side of the illumination source (**Fig. 1b**).

Planar imaging offers an attractive tool for high-throughput imaging and it is technically easy to implement. However, it also has important limitations, such as the single projection viewing, the restricted penetration depth of a few millimeters and the nonlinear relationship between the signal strength and the depth and the tissue optical properties. These features limit the applicability of the method primarily to superficial observations and may lead to erroneous interpretation of the data collected if the nonlinear effects are not explicitly corrected or accounted for. **Box 1** outlines some examples of planar imaging limitations in relation to depth and tissue optical properties and contrasts them with tomography.

Fluorescence tomography

Tomographic reconstruction of fluorescence biodistribution has its roots in the early 1990s when the first theoretical frameworks for tomography of diffuse media were proposed to spatially resolve intrinsic tissue contrast (primarily absorption and scattering) in the

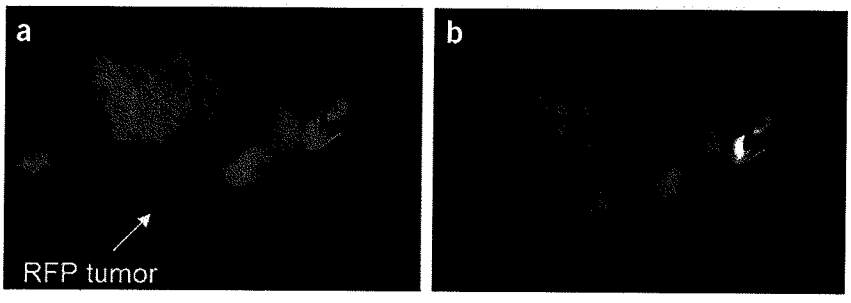

Figure 2 Spectral imaging applied to *in vivo* fluorescence detection. **(a)** Standard color image obtained from a green fluorescence protein (GFP)-expressing mouse implanted with a red fluorescent protein (RFP)-expressing tumor. **(b)** Spectral imaging and processing improves visualization of the RFP signal, which can be separated from the mouse intrinsic autofluorescence and GFP fluorescence. Images and analysis were provided by Cambridge Research & Instrumentation (CRI); samples were provided by Anticancer.

context of studying hemodynamics or organelle concentration[18–21]. This work followed original observations that near-infrared light (NIR: 650 nm–900 nm) can penetrate several centimeters into tissues because of the low photon absorption in this spectral window[22,23]. In contrast to high-energy rays, however, NIR photons are highly scattered in tissue and they become diffuse within approximately a millimeter of propagation[24]. For tomography, multiple points on the tissue boundary are illuminated in a time-sharing fashion (**Fig. 1c**) and diffuse light patterns are collected around the boundary (**Fig. 1d**) using photodetector sets or a CCD camera. Each source-detector pair effectively implements a different projection through the tissue, albeit following diffusive propagation patterns . Fluorescence measurements can be obtained using appropriate filters in front of the detectors, although the same generic tomographic principles are used for reconstruction of intrinsic tissue contrast, that is, absorption or scattering. These measurements are then combined in a tomographic scheme, which can be written as a system of equations that are solved for the unknown, spatially dependent fluorochrome concentration. This generic mainframe, combined with appropriate fluorescent molecules with specificity to cellular and sub-cellular processes, has led to the development of fluorescence molecular tomography (FMT), a technology directed towards noninvasive quantitative

Box 1 Performance characteristics of planar and tomographic imaging

A side-by-side comparison of the performance of planar and tomographic imaging in visualizing tissue-mimicking phantoms reveals some of the likely drawbacks of the former approach in imaging small animals. **Figure 6a** shows planar and tomographic imaging of two ~1.5-mm diameter fluorescent tubes containing cyanine 5.5, which are immersed in a diffusive fluid with the average optical properties of small animals and imaged through a glass window. Both planar and FMT resolve the tubes when they are placed in contact with the glass window, although FMT offers better resolution. However, planar imaging detection becomes highly challenging as the tubes move deeper in the diffuse medium, away from the glass window, even at the 3 mm depth. Depth sensitivity depends strongly on the light strength used and the size and concentration of the fluorochrome used, but the images demonstrate the superior ability of tomography to look deeper into diffuse media with higher resolution, using in this case identical hardware to that used with the planar imaging. The color images are reconstructed slices obtained at different depths and superimposed on gray scale photographs of the tubes for visualization purposes[52].

Similarly, imaging fluorochromes with varying background optical properties is shown in **Figure 6b**. Both planar and FMT accurately resolve the 2:1 relation in fluorochrome concentration between the left and right tubes when the background absorption is the same in both tubes (top row). However, when India ink is added in the left tube to simulate a threefold increase in vascularization (absorption), the planar image erroneously reports a ~1:1 cyanine 5.5 concentration in the two tubes (bottom row). This is because the added ink absorbs more fluorescent photons. In contrast, FMT can correct for the added absorption and demonstrates more robust performance, reporting 1.8:1 relation in this case[52].

Finally, **Figure 6c** demonstrates the capacity of FMT to image fluorochromes in a highly diffusive medium that simulates tissue optical heterogeneity. The image labeled nBorn shows that the use of normalization methods (in this case, as described in ref. 41) can accurately resolve the fluorescence distribution, despite the highly heterogeneous background. The absence of data normalization, however, yields images that are affected by the background heterogeneity, as shown in the image labeled hBorn. The planar imaging could not detect the presence of the fluorochrome in this case.

Overall, these findings indicate that planar imaging should be used with caution. Signal intensity relates linearly to fluorochrome concentration but nonlinearly to depth, size and optical properties, and its measurement is further complicated by the highly scattering nature of tissue. FMT has the potential to circumvent some of these limitations and offers more robust and accurate imaging.

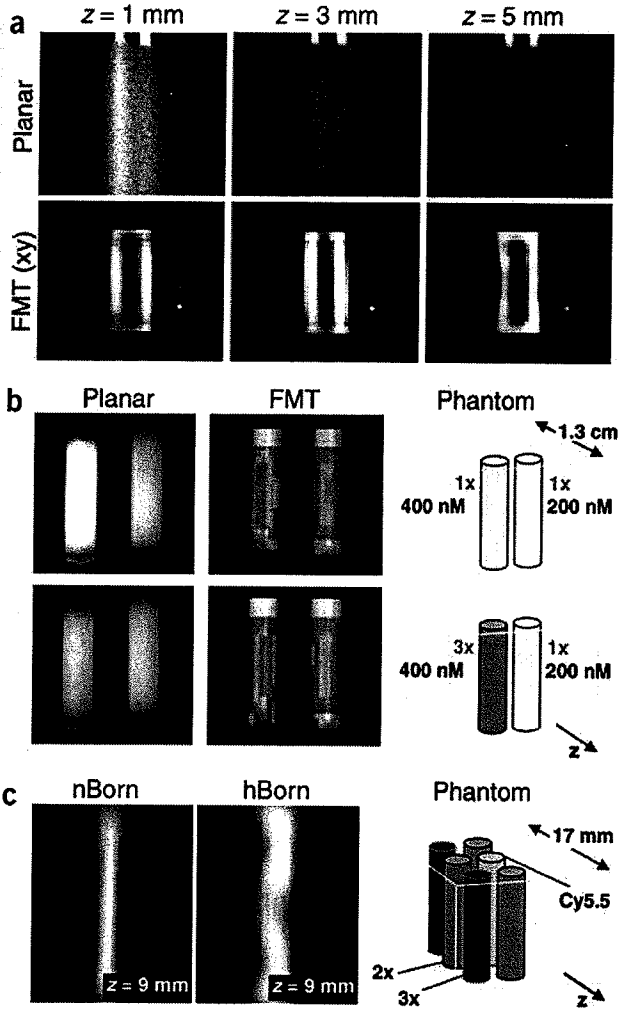

Figure 6 Performance of planar and tomographic imaging. (**a**) Two ~1.5mm diameter fluorescent tubes (500 nM cyanine 5.5, 3 mm apart) immersed at different depths in an intralipid and India ink solution, simulating the optical properties of small animals. (**b**) Planar and reconstructed images of two fluorescent tubes, the left containing twice as much cyanine 5.5 as the right tube (400 nM versus 200 nM). The tubes are immersed in the same diffuse fluid as in **a**. (**c**) A single fluorescing tube is asymmetrically surrounded by five absorbers at twofold and threefold the background absorption. The tube is reconstructed using a normalized (nBorn) and not normalized method (hBorn).

Table 1 Optical domains

Domain	Time	Frequency	Continuous wave
Resolution[a]	0.5–1 mm	0.5–1 mm	1 mm
Sensitivity[a]	Picomoles	Picomoles	Picomoles-femtomoles
Depth[b]	<30 mm	<30 mm	<50 mm
Contrast	T, A/S, F/L	T, A/S, F/L	T, F, B
Fluorochrome quantification	Yes	Yes	Yes
Signal-to-Noise Ratio	Medium	Medium	High
Cost	High	Medium/high	Low/medium

[a]Reported for fluorochromes at the center of 15 mm thick tissues. [b]Assuming ~10 picomoles of an organic fluorochrome. A, absorption; S, scattering; F, fluorescence concentration; L, fluorescence lifetime; T, attenuation, B, bioluminescence.

molecular imaging of whole animals and tissues. Tomography can overcome several of the limitations of planar imaging, as summarized in **Box 1.**

Optical domains. There are three distinct illumination-detection technology domains for optical tomography; that is, the time-domain (TD), the frequency domain (FD) and the continuous wave (CW) domain. Each has distinct advantages and disadvantages, and the selection of the appropriate technology largely depends on the specific application (**Table 1**).

For molecular investigations where the goal is to localize and quantify fluorescent probes, CW imaging offers excellent detection characteristics. CW domain methods use light of constant intensity and require simple and low-cost optical components[25]. They further offer optimum signal-to-noise performance because CW light sources and detectors are typically more stable and have low noise characteristics compared with those sources and detectors used in TD and FD methods. The major disadvantages of CW domain methods include the difficulty of resolving the tissue absorption from scattering and the inability to image fluorescence lifetime. Another caveat is that, unlike TD or FD methods, resolution is entirely dependent on a tissue's optical properties and geometry; it can not otherwise be optimized.

When independent measurements of tissue absorption, scattering or fluorochrome lifetime are required, the use of TD or FD technology becomes essential[22,26,27]. TD methods illuminate tissue with ultrafast (femtosecond to picosecond) photon pulses and resolve the arrival of the photons as a function of time at different locations around the tissue boundary. In contrast to CW methods, they can use early arriving photons to improve resolution because highly diffusive photons are rejected[28–30]. On the downside, TD methods are less sensitive than CW methods because of the lower duty cycles achieved (that is, the length of time the laser beam and detector is on), resulting in dimmer average light intensity available for imaging. In addition, TD instrumentation is noisier than CW systems due to time and intensity fluctuations that are associated with ultrafast switching electronics and pulsing lasers.

The third mode, FD technology, uses light of a modulated intensity at a frequency f, which establishes a photon wave of the same frequency in the diffuse medium[31]. Measurements of the light intensity and the phase shift of the photon wavefront away from the source or the excited fluorochromes reveal information about the tissue optical properties and fluorochrome bio-distribution[32]. FD methods are less affected by ambient light than CW and TD methods. However, they require frequencies of several hundred MHz or higher to achieve improvements in resolution over CW. They are also less robust than CW methods because of the reduced signal-to-noise detection involved in sensing high frequencies. Data obtained at multiple frequencies improve FD imaging performance and can become equivalent to TD data via the inverse Fourier Transform.

Improving spatial sampling. Previous fluorescence tomography investigations focused primarily on feasibility studies with simple tissue-mimicking phantoms and on algorithmic validation. Typical systems used a limited number of sources and detectors arranged around the tissue boundary using light-guiding fibers. In several instances, a matching fluid was used to surround the tissue and achieve optimal photon coupling and a simplified experimental arrangement; otherwise, fibers were brought in contact with the tissue. This technology typically yielded coarse spatial photon-sampling on the boundary, resulting in 10^2–10^3 total measurements, which is generally insufficient for high-fidelity volumetric imaging. In addition, the fiber-based technology complicated experimental procedures because either the tissue had to be surrounded by fluids or meticulous engineering had to be exercised to ensure the optimal contact of each individual fiber with the tissue[33]. This set of approaches compromised imaging performance and reduced overall enthusiasm for optical tomography.

More recently, it has been shown that sub-millimeter spaced arrays of sources and detectors (that is, data sets on the order of 10^4–10^6 measurements or more) are necessary for high-fidelity, small-animal imaging[25]. To achieve such large data sets, researchers have

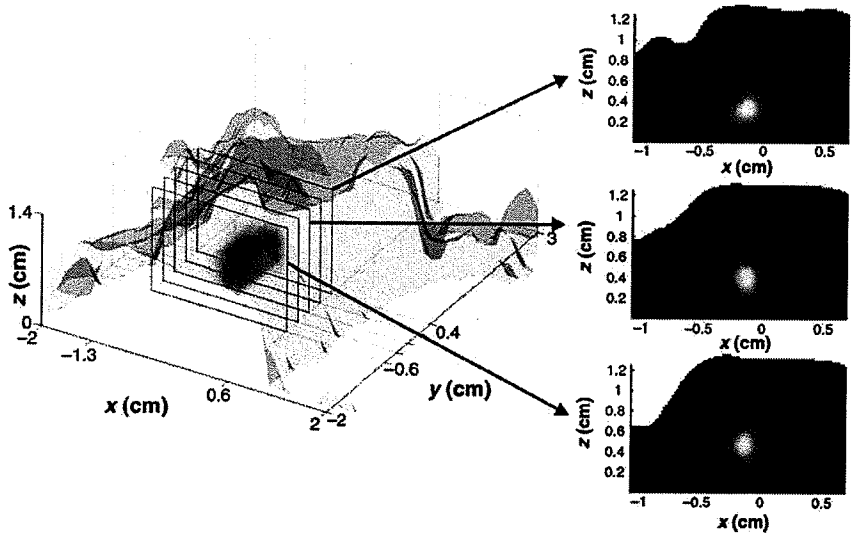

Figure 3 Fluorescence reconstruction of a fluorescent tube inserted in a euthanized animal obtained in the absence of contact detection. Image reconstruction is based on mathematical models that describe the composite photon propagation in tissue and in air (for details see ref. 36). The animal surface was captured using photo-grammetry, that is, the mathematical combination of photographs obtained under different angles to deduce the physical dimension of the animal.

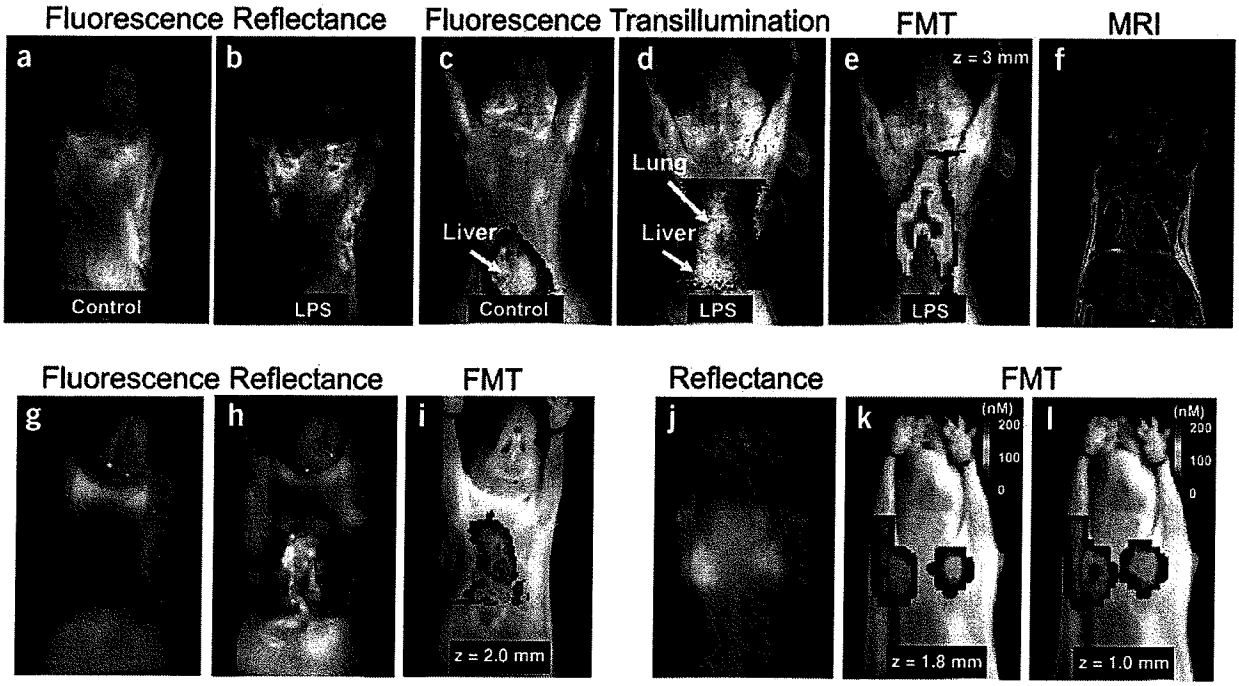

Figure 4 *In vivo* fluorescence imaging. (**a–e**) Imaging of proteolytic activity in LPS-induced pulmonary inflammation. Fluorescence reflectance images of the LPS-challenged and nonchallenged mouse (control) injected with a cathepsin-sensitive fluorescent probe (**a,b**). Fluorescence transillumination images of control and LPS-challenged mouse, respectively (**c,d**). Fluorescence Molecular Tomography slice (**e**) and corresponding T1-weighted MR image (**f**). (**g–i**) Imaging of lung tumors. *In vivo* fluorescence reflectance image (**g**). *Post mortem* fluorescence reflectance image after skin and rib-cage removal (**h**). (**i**) FMT slice at 2 mm depth under the surface. (**a–i**) Images are courtesy of investigators at the Laboratory for Bio-optics and Molecular Imaging/CMIR. (**j–l**) Differential imaging of treatment effects using an annexin V-Cy5.5 probe. *In vivo* planar reflectance image (**j**), two consecutive FMT slices obtained at 1 mm and 1.8 mm under the animal surface (**k,l**) (see text for details).

introduced free-space and noncontact imaging approaches. Free-space tomography is based on appropriate forward models that predict the composite propagation of photons in diffuse media and in air[34] and is enabled by noncontact collection methods, such as direct lens coupling of CCD cameras onto nonbounded tissue[35]. Free-space imaging is further combined with surface capture optical methods to yield an accurate description of the arbitrary tissue boundaries. These collection schemes offer high-quality data sets, high-spatial photon sampling and experimental simplicity because they both avoid the use of matching fluids/complex fiber interfaces and eliminate the associated fiber-tissue coupling issues. The feasibility of this approach has been recently showcased with phantoms[35] and animals[36]. **Figure 3** depicts reconstructed images of a 1.5-mm diameter fluorescent tube (500 nM of cyanine 5.5) inserted through the esophagus of a euthanized animal. With these advances, it is now possible to obtain practical, complete projection (360°), noncontact systems that, similar to other tomographic modalities (e.g., X-ray CT), can offer optimum imaging performance.

Forward problem and inversion. Two factors have a significant influence on tomographic performance: first, the selection of appropriate mathematical models that describe photon propagation in tissues (that is, the forward problem); and second, the selection of image reconstruction algorithms (that is, the inverse problem). Typical forward problems used for fluorescence tomography of tissues are based on numerical or analytical solutions of the diffusion equation[37–41] solved for the excitation and fluorescence fields. Forward models based on approximate solutions to the radiative transport equation[42] or on diffusion equation solutions merged with radiosity principles[43] have been proposed for regimes where solutions of the diffusion equation become less accurate (such as, situations using early photons, millimeter-sized, source-detector separations or in void, nondiffusive regions).

A particular scheme that recently enabled *in vivo* application[44] has been the inversion of normalized data (that is, by solving for the ratio of fluorescence measurements over excitation measurements to minimize the sensitivity to tissue heterogeneity and to theoretical inaccuracies[41] (see **Box 1**). Such methods are computationally fast, robust and simple to implement and can be used with analytical and numerical solvers. More integrated approaches are based on iterative numerical solutions, and they handle heterogeneity explicitly by solving first for the background absorption and scattering and then implementing this information for fluorescence solutions[40]. Overall, the need for fast forward and inversion algorithms is becoming ever more important as data sets increase in size as a result of the application of newer generation noncontact instruments. The use of fast analytical solvers[45] or the acceleration of numerical solutions using, for example, multi-grid methods[46,47] are important contributions to achieving practical inversion schemes.

***In vivo* applications. Figure 4** summarizes FMT studies from our group using noncontact approaches for fluorescence tomography of small animals. The results are contrasted with planar imaging methods to illuminate differences. **Figure 4a–f** depicts findings from an *in vivo* imaging study of inflammatory lung disease. In this study, pulmonary inflammation was induced by intratracheal lipopolysaccharide (LPS) instillation in a BALB/c mouse using a previously described procedure[48] (LPS administration has previously been shown to upregulate cathepsins in macrophages as well as other pro-inflammatory pathways[49,50]). The

animal was imaged 24 h after challenge following administration of a fluorescence-activatable probe sensitive to major cathepsins (B > S, K, L) associated with inflammation[51]. Although the fluorescence reflectance images, shown in **Figure 4a,b**, are unable to resolve protease activity from the lung, transillumination images (**Fig. 4c,d**) do depict a marked difference in fluorescence distribution between the control and the LPS-treated animal. Correspondingly, a tomographic slice (**Fig. 4e**), obtained 3 mm under the surface, better demarcates the lung inflammation and demonstrates good congruence with the anatomical magnetic resonance image shown in **Fig. 4f**, which was obtained under identical placement conditions. **Fig. 4e** does not depict signal from the liver because the reconstruction algorithm automatically rejects fluorescence signals corresponding to excitation patterns that have been highly absorbed.

In a related example from our laboratory, a Lewis Lung carcinoma tumor (LLC), was grown in the lung of a nu/nu female after direct injection of 10^6 LLC cells mixed with MatrigelHC and targeted with the same fluorescent activatable probe used in **Fig. 4a–e**. The tumor was not visible on fluorescence reflectance images (**Fig. 4g**) *in vivo* but could be seen by FRI when the skin and the front rib cage were removed after the mouse was killed (**Fig. 4h**). Conversely, FMT (**Fig. 4i**) could detect contrast congruent with the appearance of the tumor. Tomographic feasibility to resolve molecular activity in animal brain tumors has also been shown based on fiber-based systems[44].

Finally, in **Figure 4j–l**, we illustrate the ability of tomography to image treatment effects *in vivo*. In this study[52], a mouse bearing LLC tumors sensitive and resistant to cyclophosphamide was treated with the drug and injected with a phosphatidylserine (PS)-sensing annexin V–based probe conjugated to the cyanine 5.5 fluorochrome to probe apoptosis. In **Figure 4j–l**, the drug-sensitive and drug-resistant tumors are in the left and right mammary area, respectively. Because of the superficial nature of the tumors, both the planar (**Fig. 4j**) and the two tomographic slices obtained from two adjacent depths (**Fig. 4k,l**) resolve the tumors. The tomography, however, allows more accurate quantification, tumor-to-tissue contrast, depth and size estimation. Planar imaging did not correctly indicate levels of apoptosis in some instances because of unequal absorption between the two tumors[52].

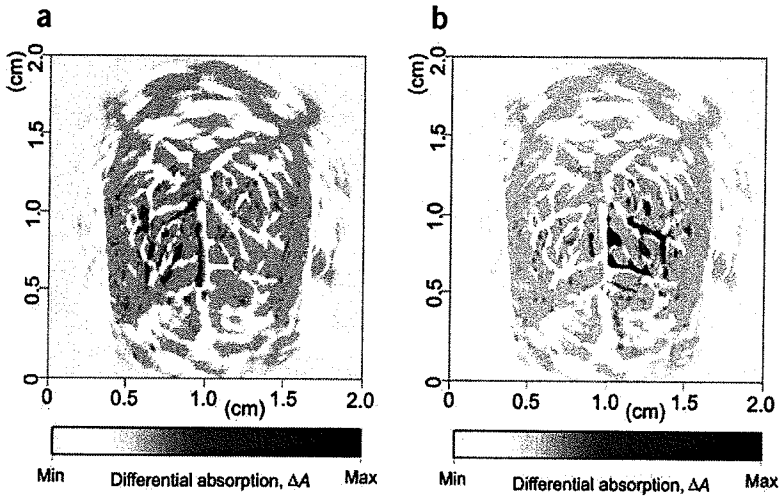

Figure 5 Visualization of brain structure and function using photoacoustic tomography (modified from ref. 57. **(a,b)** Functional maps of brain activities corresponding to the left-side **(a)** and right-side **(b)** whisker stimulations, respectively, acquired with the skin and skull intact.

Bioluminescence tomography

Bioluminescence imaging uses enzymes, which convert unique substrates into light in the presence of oxygen and other factors (e.g., ATP, Mg)[4]. The propagation of emitted photons can be modeled, similarly to fluorescence photon propagation, as a diffusion process. Bioluminescence tomography can therefore be based on the same framework used for fluorescence tomography but light is collected from the subject in the absence of external illumination sources. Because internal bioluminescent light is continuously on during the measurement, bioluminescence tomography operates only in CW mode. One of the major advantages of the technique is that there is no inherent background bioluminescence in most tissues, which yields high imaging contrast. Methods for bioluminescence tomography have recently been reported[53,54], and there is a great impetus for *in vivo* tomographic applications for improving localization and quantification beyond what has been achieved by planar methods.

However, the unavailability of external illumination sources complicates the tomographic problem, compared to fluorescence tomography, because it becomes mathematically more difficult and possibly less accurate, to resolve problems of internal sources (bioluminescence) compared with problems using external sources (fluorescence) because of the fewer source-detector pairs (projections) available. This problem is also common in other tomography methods (e.g., SPECT versus CT), although the experimental and image formation characteristics are different for high-energy and near-infrared photons. A combination of multi-view angle (360°) imaging with a priori information on tissue heterogeneity could improve the performance of the bioluminescence inverse problem[58]. *In vivo* applications of bioluminescence tomography have not yet been reported; however this technology is being actively researched and may become available in the future.

Photoacoustic tomography

When a short laser pulse, typically in the nanosecond range, is spatially broadened and then used to irradiate biological tissue, it produces a temperature rise on the order of milli-Kelvin in a short time frame. Consequently, thermoelastic expansion causes emission of acoustic waves, referred to as photoacoustic waves, that can be measured by wideband ultrasonic transducers around the sample. This phenomenon, discovered by Alexander Graham Bell, has been recently exploited for small-animal imaging, because the acquired photoacoustic waves can be combined mathematically to reconstruct the distribution of optical energy absorption[55,56]. The technique, termed photoacoustic tomography (PAT), also referred to as optoacoustic or thermoacoustic tomography, attains the advantage of combining ultrasonic-scale spatial resolution with high sensitivity to tissue light absorption[57,58] and can yield information on physiology or on exogenously administered light absorbers.

This technique has been used recently for visualization of the brain structure and lesions, of cerebral hemodynamic responses to hyperoxia and hypoxia and of cerebral cortical responses to neuroactivities induced by whisker stimulations in rats[57]. **Figure 5** depicts two images of the superficial cerebral cortex of the rat after stimulation of the left-side and the right-side rat whiskers, respectively. These

images were obtained after subtraction of the image without whisker stimulations from the two PAT images with whisker stimulations. This differential contrast is attributed to the altered blood volume and oxygenation associated with the whisker stimulations. Similarly, noninvasive *in vivo* imaging of exogenous contrast agents in the rat brain using indocyanine green stabilized with polyethylene glycol has been also demonstrated[56].

Outlook

The advancement of new whole-animal imaging technologies presents new opportunities for biomedical research. Tomographic methods can transform macroscopic optical observations of tissues from a crude qualitative tool to an accurate three-dimensional imaging technique. This is important for capitalizing on the advantages of fluorescence and the bioluminescence methods: first, high molecular specificity; second, the use of nonionizing radiation that simplifies the operation and the chemical synthesis of reporter probes; third, the ability to use optical switches (molecular beacons) for achieving high sensitivity and specificity; fourth, optical probe stability because there is no intensity decay over time; and fifth, the potential for simultaneous investigations of multiple targets using spectral differentiation of probes.

These imaging principles can be applied to different biomedical research areas, including cancer, cardiovascular, immunologic/inflammatory and neurodegenerative diseases[5,10,11]. Important to these new developments is the accessibility of a larger number of sites and organs compared to the number that can be assessed using planar imaging. While small animal photonic tomography does not reach the resolution of optical microscopy, molecular activity is detected based on the high specificity of the optical probes employed (similarly to PET and SPECT), even if single cells and molecules are not explicitly resolved.

One other advantage of fluorescence tomography is that it can be combined with microscopy in a straightforward manner. Because it uses the same optical probe as fluorescence microscopy, a sample can first be visualized and quantified volumetrically *in vivo* as a function of time and then observed at high resolution with microscopy using excised samples or surgical intervention in the case of tissues that are not typically accessible by microscopy (that is, when samples are deeper or larger than ~400–700 μm).

The combination of modalities with complementing features offers an attractive future direction for study. Although optical tomography yields high molecular contrast versatility and specificity, photoacoustic imaging offers improved resolution to imaging light absorption. The combination of the two techniques could not only yield a straightforward superposition of optical and photoacoustic images, but also use PAT images as a priori information for constructing more accurate models for photon propagation in tissues, which will further mitigate the optical inversion problem. Other imaging modalities, such as CT, MRI or ultrasound, may also be used to register PAT images or fluorescence images onto high-resolution anatomical images, thereby improving the information content of the combined imaging approach.

Overall, these new technologies will continue to emerge and diversify, and new clinical applications will be identified; for example, in imaging human joints or the breast, in eye healthcare and in endoscopic applications, where appropriate photon models and limited angle projections would improve imaging performance. Currently, only a few sets of approaches and ideas about photonic imaging methodology have been explored. Light offers a plethora of contrast mechanisms and can be manipulated in several ways to further improve the performance and capability of these methods.

ACKNOWLEDGMENTS

V.N. is supported in part by National Institutes of Health (NIH) grants RO1 EB 000750-1, 1-NO1-CO027105 and R33 CA 91807. J. Ripoll acknowledges support from EU Integrated Project "Molecular Imaging" LSHG-CT-2003-503259. R.W. is supported in part by NIH grants P50 CA86355, R24 CA92782, R33 CA091807, PO1 AI054904, PO1 CA69246 and grants from the Donald W. Reynolds Foundation and Siemens Medical Systems.

COMPETING INTERESTS STATEMENT

The authors declare competing financial interests (see the *Nature Biotechnology* website for details).

Published online at http://www.nature.com/naturebiotechnology/

1. Massoud, T.F. & Gambhir, S.S. Molecular imaging in living subjects: seeing fundamental biological processes in a new light. *Genes Dev.* **17**, 545–580 (2003).
2. Blasberg, R.G. *In vivo* molecular-genetic imaging: multi-modality nuclear and optical combinations. *Nucl. Med. Biol.* **30**, 879–888 (2003).
3. Budinger, T.F., Benaron, D.A. & Koretsky, A.P. Imaging transgenic animals. *Annu. Rev. Biomed. Eng.* **1**, 611–648 (1999).
4. Contag, C.H. & Bachmann, M.H. Advances in *in vivo* bioluminescence imaging of gene expression. *Annu. Rev. Biomed. Eng.* **4**, 235–260 (2002).
5. Piwnica-Worms, D., Schuster, D.P. & Garbow, J.R. Molecular imaging of host-pathogen interactions in intact small animals. *Cell. Microbiol.* **6**, 319–331 (2004).
6. Weissleder, R. Scaling down imaging: molecular mapping of cancer in mice. *Nat. Rev. Cancer* **2**, 11–18 (2002).
7. Hoffman, R. Green fluorescent protein imaging of tumour growth, metastasis, and angiogenesis in mouse models. *Lancet Oncol.* **3**, 546–556 (2002).
8. Bornhop, D.J., Contag, C.H., Licha, K. & Murphy, C.J. Advance in contrast agents, reporters, and detection. *J. Biomed. Opt.* **6**, 106–110 (2001).
9. Tung, C., Mahmood, U., Bredow, S. & Weissleder, R. *In vivo* imaging of proteolytic enzyme activity using a novel molecular reporter. *Cancer Res.* **60**, 4953–4958 (2000).
10. Herschman, H.R. Molecular imaging: looking at problems, seeing solutions. *Science* **302**, 605–608 (2003).
11. Weissleder, R. & Ntziachristos, V. Shedding light onto live molecular targets. *Nat. Med.* **9**, 123–128 (2003).
12. Reynolds, J.S. *et al.* Imaging of spontaneous canine mammary tumors using fluorescent contrast agents. *Photochem. Photobiol.* **70**, 87–94 (1999).
13. Mahmood, U., Tung, C., Bogdanov, A. & Weissleder, R. Near infrared optical imaging system to detect tumor protease activity. *Radiology* **213**, 866–870 (1999).
14. Yang, M. *et al.* Whole-body optical imaging of green fluorescent protein-expressing tumors and metastases. Proc. *Natl. Acad. Sci. USA* **97**, 1206–1211 (2000).
15. Contag, C.H. & Ross, B.D. It's not just about anatomy: *in vivo* bioluminescence imaging as an eyepiece into biology. *J. Magn. Reson. Imaging* **16**, 378–387 (2002).
16. Farkas, D.L. *et al.* Non-invasive image acquisition and advanced processing in optical bioimaging. *Comput. Med. Imaging Graph.* **22**, 89–102 (1998).
17. Gao, X., Cui, Y., Levenson, R.M., Chung, L.W.K. & Nie, S. *In vivo* cancer targeting and imaging with semiconductor quantum dots. *Nat. Biotechnol.* **22**, 969–976 (2004).
18. Arridge, S.R., Schweiger, M., Hiraoka, M. & Delpy, D.T.A. *Finite-Element Approach For Modeling Photon Transport In Tissue. Med. Phys.* **20**, 299–309 (1993).
19. Graber, H.L. & Barbour, R.L. High-resolution near-infrared (nir) imaging of dense scattering media by diffusion tomography. *FASEB J.* **7**, A720–A720 (1993).
20. Schotland, J.C. & Leigh, J.S. Photon diffusion imaging. *FASEB J.* **6**, A446–A446 (1992).
21. Yodh, A.G. & Chance, B. Spectroscopy and imaging with diffusing light. *Phys. Today* **48**, 34–40 (1995).
22. Chance, B. Optical Method. *Annu. Rev. Biophys. Biophys. Chem.* **20**, 1–28 (1991).
23. Jobsis, F.F. Noninvasive, infrared monitoring of cerebral and myocardial oxygen sufficiency and circulatory parameters. *Science* **198**, 1264–1267 (1977).
24. Patterson, M.S., Chance, B. & Wilson, B.C. Time resolved reflectance and transmittance for the noninvasive measurement of tissue optical-properties. *Appl. Opt.* **28**, 2331–2336 (1989).
25. Graves, E., Ripoll, J., Weissleder, R. & Ntziachristos, V.A. Sub-millimeter resolution fluorescence molecular imaging system for small animal imaging. *Med. Phys.* **30**, 901–911 (2003).
26. Alfano, R.R. *et al.* Time-resolved and nonlinear optical imaging for medical applications. *Ann. NY Acad. Sci.* **838**, 14–28 (1998).
27. Sevick, E.M., Chance, B., Leigh, J., Nioka, S. & Maris, M. Quantitation of time-resolved and frequency-resolved optical-spectra for the determination of tissue oxygenation. *Anal. Biochem.* **195**, 330–351 (1991).
28. Cai, W. *et al.* Optical tomographic image reconstruction from ultrafast time-sliced transmission measurements. *Appl. Opt.* **38**, 4237–4246 (1999).
29. Chen, K., Perelman, L.T., Zhang, Q.G., Dasari, R.R. & Feld, M.S. Optical computed tomography in a turbid medium using early arriving photons. *J. Biomed. Opt.* **5**, 144–154 (2000).
30. Turner, G., Zacharakis, I., Soubret, A. & Ntziachristos, V. Complete angle projection diffuse optical tomography using early photons. *Optics Letters* **30**, 409–411 (2005).
31. Boas, D.A., Oleary, M.A., Chance, B. & Yodh, A.G. Scattering of diffuse photon density waves by spherical inhomogeneities within turbid media - analytic solution and applications. *Proc. Natl. Acad. Sci. USA* **91**, 4887–4891 (1994).
32. Godavarty, A. *et al.* Fluorescence-enhanced optical imaging in large tissue volumes using a gain-modulated ICCD camera. *Phys. Med. Biol.* **48**, 1701–1720 (2003).

33. Boas, D.A. *et al.* Imaging the body with diffuse optical tomography. *IEEE Signal Process. Mag.* **18**, 57–75 (2001).
34. Ripoll, J., Schultz, R. & Ntziachristos, V. Free-space propagation of diffuse light: Theory and Experiments. *Phys. Rev. Lett.* **91**, 103901–103904 (2003).
35. Schultz, R., Ripoll, J. & Ntziachristos, V. Experimental fluorescence tomography of arbitrarily shaped diffuse objects using non-contact measurements. *Opt. Lett.* **28**, 1701–1703 (2003).
36. Schultz, R., Ripoll, J. & Ntziachristos, V. Fluorescence tomography of tissues with non-contact measurements. *IEEE Med. Imag.* **23**, 492–500 (2004).
37. Chang, J., Graber, H.L. & Barbour, R.L. Imaging of fluorescence in highly scattering media. *IEEE Trans. Biomed. Eng.* **44**, 810–822 (1997).
38. Eppstein, M.J., Hawrysz, D.J., Godavarty, A. & Sevick-Muraca, E.M. Three-dimensional, Bayesian image reconstruction from sparse and noisy data sets: near-infrared fluorescence tomography. *Proc. Natl. Acad. Sci. USA* **99**, 9619–9624 (2002).
39. Jiang, H.B. Frequency-domain fluorescent diffusion tomography: a finite- element-based algorithm and simulations. *Appl. Opt.* **37**, 5337–5343 (1998).
40. Milstein, A.B. *et al.* Fluorescence optical diffusion tomography. *Appl. Opt.* **42**, 3081–3094 (2003).
41. Ntziachristos, V. & Weissleder, R. Experimental three-dimensional fluorescence reconstruction of diffuse media using a normalized Born approximation. *Opt. Lett.* **26**, 893–895 (2001).
42. Klose, A.D. & Hielscher, A.H. Fluorescence tomography with simulated data based on the equation of radiative transfer. *Opt. Lett.* **28**, 1019–1021 (2003).
43. Dehghani, H., Arridge, S.R., Schweiger, M. & Delpy, D.T. Optical tomography in the presence of void regions. *J. Opt. Soc. Am. A Opt. Image Sci. Vis.* **17**, 1659–1670 (2000).
44. Ntziachristos, V., Tung, C., Bremer, C. & Weissleder, R. Fluorescence-mediated tomography resolves protease activity *in vivo*. *Nat. Med.* **8**, 757–760 (2002).
45. Ripoll, J., Nieto-Vesperinas, M., Weissleder, R. & Ntziachristos, V. Fast analytical approximation for arbitrary geometries in diffuse optical tomography. *Opt. Lett.* **27**, 527–529 (2002).
46. Gu, X., Xu, Y. & Jiang, H. Mesh-based enhancement schemes in diffuse optical tomography. *Med. Phys.* **30**, 861–869 (2003).
47. Ye, J.C., Bouman, C.A., Webb, K.J. & Millane, R.P. Nonlinear multigrid algorithms for Bayesian optical diffusion tomography. *IEEE Trans. Image Process.* **10**, 909–922 (2001).
48. Vernooy, J., Dentener, M., van Suylen, R., Buurman, W. & Wouters, E. Long-term intratracheal lipopolysaccharide exposure in mice results in chronic lung inflammation and persistent pathology. *Am. J. Respir. Cell Mol. Biol.* **26**, 152–159 (2002).
49. Lautwein, A. *et al.* Inflammatory stimuli recruit cathepsin activity to late endosomal compartments in human dendritic cells. *Eur. J. Immunol.* **32**, 3348–3357 (2002).
50. Prin-Mathieu, C. *et al.* Enzymatic activities of bovine peripheral blood leukocytes and milk polymorphonuclear neutrophils during intramammary inflammation caused by lipopolysaccharide. Clin. Diagn. *Lab. Immunol.* **9**, 812–817 (2002).
51. Weissleder, R., Tung, C.H., Mahmood, U. & Bogdanov, A. *In vivo* imaging of tumors with protease-activated near-infrared fluorescent probes. *Nat. Biotechnol.* **17**, 375–378 (1999).
52. Ntziachristos, V. *et al.* Visualization of anti-tumor treatment by means of fluorescence molecular tomography using an annexin V - Cy5.5 conjugate. *Proc. Natl. Acad. Sci. USA* **101**, 12294–12299 (2004).
53. Wang, G., Li, Y. & Jiang, M. Uniqueness theorems in bioluminescence tomography. *Med. Phys.* **31**, 2289–2299 (2004).
54. Gu, X., Zhang, Q., Larcom, L. & Jiang, H.B. Three-dimensional bioluminescence tomography with model-based reconstruction. *Opt. Express* **12**, 3996–4000 (2004).
55. Hoelen, C.G.A. & de Mul, F.F.M. Image reconstruction for photoacoustic scanning of tissue structures. *Appl. Opt.* **39**, 5872–5883 (2000).
56. Wang, X. *et al.* Noninvasive photoacoustic angiography of animal brains *in vivo* with near-infrared light and an optical contrast agent. *Opt. Lett.* **29**, 730–732 (2004).
57. Wang, X. *et al.* Noninvasive laser-induced photoacoustic tomography for structural and functional *in vivo* imaging of the brain. *Nat. Biotechnol.* **21**, 803–806 (2003).
58. Karabutov, A.A., Savateeva, E.V. & Oraevsky, A.A. Optoacoustic tomography: new modality of laser diagnostic systems. *Laser Phys.* **13**, 711–723 (2003).

RESEARCH REPORT

Comparison of noninvasive fluorescent and bioluminescent small animal optical imaging

Garry Choy[1], Sarah O'Connor[1], Felix E. Diehn[2], Nick Costouros[1], H. Richard Alexander[1], Peter Choyke[2], and Steven K. Libutti[1]

BioTechniques 35:1022-1030 (November 2003)

Optical imaging is a modality that is cost-effective, rapid, easy to use, and can be readily applied to studying disease processes and biology in vivo. For this study, we used a green fluorescent protein (GFP)- and luciferase-expressing mouse tumor model to compare and contrast the quantitative and qualitative capabilities of a fluorescent reporter gene (GFP) and a bioluminescent reporter gene (luciferase). We describe the relationship between tumor volume, tumor mass, and bioluminescent/fluorescent intensity for both GFP and luciferase. Bioluminescent luciferase imaging was shown to be more sensitive than fluorescent GFP imaging. Luciferase-expressing tumors were detected as early as 1 day after tumor cell inoculation, whereas GFP-expressing tumors were not detected until 7 days later. Both bioluminescent and fluorescent intensity correlated significantly and linearly with tumor volume and tumor weight, as measured by caliper. Compared to bioluminescent imaging, fluorescent imaging does not require the injection of a substrate and may be appropriate for applications where sensitivity is not as critical. Knowing the relative strengths of each imaging modality will be important in guiding the decision to use fluorescence or bioluminescence.

INTRODUCTION

Recently, there has been increasing interest and efforts devoted to developing methods for whole-body imaging in mice. The currently available imaging technologies such as magnetic resonance imaging (MRI), computed tomography (CT), positron emission tomography (PET), and single photon emission computed tomographic (SPECT) offer deep tissue penetration and high spatial resolution. However, compared to noninvasive small animal optical imaging, these techniques are very costly and time-consuming to implement. Optical imaging is a modality that is cost-effective, rapid, easy to use, and can be readily applied to studying disease processes and biology in vivo.

Two commonly used reporter genes, green fluorescent protein (GFP) and luciferase, have been extensively used in vivo and in vitro. GFP, originally cloned from the jellyfish *Aequorea victoria*, has also been used extensively to study subcellular processes such as gene expression and protein localization (1–4). Typical of fluorescent imaging, acquisition of GFP signal relies on excitation by an external light source. Bioluminescence imaging, on the other hand, is based on the endogenous production of light by the expression of the enzyme luciferase. This enzyme, found in fireflies and other bioluminescent organisms, produces light upon reacting with the substrate luciferin in the presence of oxygen and ATP. Like GFP, luciferase has been used extensively in vitro to study cellular processes (5,6). In small animal imaging, GFP and luciferase have both been employed to study transgene expression, tumor growth/treatment/metastasis, and infectious disease processes (7–18). Despite these similarities in their applications, bioluminescent imaging differs considerably from fluorescent imaging.

Since bioluminescent imaging does not require an excitation light source, there is extremely low background, which is often caused by autofluorescence. Hence, bioluminescent imaging enables the imaging of processes that produce minimal signal, such as in the case of lymphocyte trafficking in vivo or the detection of a small number of cancer cells in vivo (19–23). Furthermore, GFP fluorescent images can be acquired in real-time in the millisecond range, while bioluminescent images are acquired in the minute timescale.

GFP- and luciferase-based imaging techniques both differ in the type of information obtained and in implementation. As a result, fluorescent and bioluminescent imaging can be applied differently in vivo for specific scientific investigations. Considering the unique abilities and unique applications of either GFP or luciferase, experiments that compare these two imaging techniques qualitatively and quantitatively have not yet been described. In this study, we use a GFP- and luciferase-expressing mouse tumor model to compare the two optical imaging techniques. We compare the sensitivity of both techniques in detecting tumor lesions as well as their ability to quantitatively describe the relationship between tumor volume, tumor mass, and bioluminescent/fluorescent intensity.

[1]National Cancer Institute, NIH, Bethesda and [2]Warren G. Magnuson Clinical Center, NIH, Bethesda, MD, USA

MATERIALS AND METHODS

Retroviral GFP and Luciferase Transduction

Vectors pCLNC-GFP, pMD.G, and cell line 293GP were obtained from P. Robbins, National Cancer Institute (NCI), Bethesda, MD. Vector pCLNC-LUC, containing the (firefly) luciferase gene, was constructed in our laboratory and is based on the pCLNCX retroviral vector system (24). Vector pCLNC-GFP contains the GFP gene and is based on the pCLNCX retroviral vector system (24). Pseudotyped retroviral particles were generated as previously described (25). In brief, 293GP cells were stably transfected with retroviral *gag* and *pol* elements. The pMD.G vector contains the G protein gene from vesicular stomatitis virus. The 293GP cells were then cotransfected with the pMD.G and pCLNC-GFP vectors. MC38 murine colon adenocarcinoma cells (Surgery Branch, NCI) were transduced with retroviral supernatant in the presence of hexadimethrine bromide (8 μg/mL; Sigma, St. Louis, MO, USA) and selected in G418 (400 μg/mL; Invitrogen, Carlsbad, CA, USA). Expression of GFP was assessed by fluorescence microscopy. Expression of luciferase in each clone was assessed by a commercially available Luciferase Assay System (Promega, Madison, WI, USA). The in vitro growth rate of the MC38-GFP cell line was similar to that of the parental line, and the expression of GFP was stable in vitro even in the absence of selection agents (data not shown).

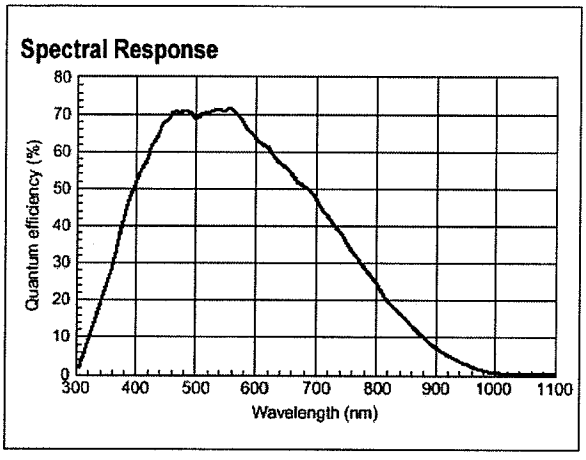

Figure 1. Spectral sensitivity of ORCA 2-ER charge-coupled device (CCD) camera used in this study.

Whole-Body Optical Imaging System

Imaging was conducted using an ORCA 2-ER charge-coupled device (CCD) camera (Hamamatsu Photonics KK, Hamamatsu, Japan) fitted with a c-mount 2/3″ format, 12.5–75 mm, f1.8 lens (Toyo, Irvine, CA, USA) attached to a custom-made light-tight imaging chamber (Microscopic Services, Rockville, MD, USA). The detector uses an ER-150 (Hamamatsu Photonics KK) CCD progressive scan interline chip with microlens and is cooled by Peltier cooling/forced-air cooling with hermetic sealing. The spectral sensitivity of the detector is illustrated in Figure 1. Before all imaging, mice were shaved to remove fur. Mice were then anesthetized with 7 to 8 mg ketamine/xylazine injected intraperitoneally (i.p.). For fluorescent imaging, a 150 W light source (Schott-Fostec, New York, NY, USA) and a GFP filter set [excitation filter (HQ470, 40×), barrier filter (OG515); Chroma, Brattleboro, VT, USA] were used. An integration time of 200–300 ms was used for GFP signal acquisition. For bioluminescent imaging, the GFP barrier filter was removed, and the light source was turned off. Five minutes prior to imaging, the substrate luciferin (Biotium, Hayward, CA, USA) suspended in phosphate-buffered saline (PBS) (20 mg/mL) was injected i.p. at a dose of 100 mg/kg. An integration time of 10 min was used for bioluminescent image acquisition. All images were transferred to a Power Mac® G4 computer and were analyzed by Openlab 3.1 software (Improvision, Lexington, MA, USA).

Tumor Formation and Implantation in Animals

MC38-GFP or MC38-LUC cell lines were cultured in Dulbecco's modified Eagle's medium (DMEM), 10% fetal calf serum, 100 U/mL penicillin, 100 μg/mL streptomycin, 50 μg/mL gentamicin, 0.5 μg/mL fungizone, and 4 mM glutamine (Biofluids, Rockville, MD USA). Seven-week-old female B57BL/6 mice were shaved and injected subcutaneously (s.c.) with 1×10^6 cells suspended in PBS on their flank. At indicated time points, the length and width of tumors were measured by calipers. Tumor volumes were calculated according to the formula:

$$\text{volume} = 0.52 \times \text{length} \times \text{width}^2$$

(0.52 is the constant used to calculate volume for an ellipsoid). All animal experiments were conducted under protocols approved by the National Institutes of Health (NIH) Animal Care and Use Committee (Bethesda, MD, USA).

Western Blot Analysis

To assess expression levels of GFP and luciferase, Western blot analysis was performed on both excised tumors (5 days postinjection) and cell lines. Cultured cells were lysed using radioimmunoprecipitation assay (RIPA) buffer (26). Specifically, approximately 1×10^7 of MC38-GFP and 1×10^7 MC38-LUC were lysed for protein extraction yielding comparable concentrations of protein in lysate. Excised tumors were homogenized using FastPrep® FP120 (Thermo Savant, Holbrook, NY, USA) in RIPA buffer. Extracts of cultured cells and excised tumors were then loaded (30 μg/lane). Lysates were then resolved by sodium dodecyl sulfate polyacrylamide gel electrophoresis (SDS-PAGE) and transferred to nitrocellulose membranes. For MC38-GFP cells and tumors, a primary antibody to GFP was used (AbCam, Cambridge, UK). For MC38-LUC cells and tumors, a primary antibody to firefly luciferase was used (AbCam). Secondary antibodies (Amersham Biosciences, Piscataway, NJ, USA) were horseradish peroxidase-conjugated, and detection was performed using the ECL™ chemiluminescence kit (Amersham Biosciences). To assess expression levels, blots were digitized and analyzed by software (NIH Image, Bethesda, MD, USA).

Animal Sacrifice

MC38-GFP and MC38-Luc tumors were harvested and weighed immediately after the mice were sacrificed at the conclusion of the experiments. No

desiccation of tumor was performed prior to measurements.

Statistical Methods

Microsoft® Excel® was used to perform all statistical analysis. All data represent mean values ± standard errors ($\bar{X} \pm$ SEM).

RESULTS AND DISCUSSION

A murine colon adenocarcinoma line (MC38) was successfully engineered to stably express either GFP or luciferase by retroviral transduction, and the highest expressing clones were selected for in vivo study. MC38-GFP and MC38-LUC murine colon adenocarcinoma xenografts were implanted s.c. into the right flanks of mice. Tumor burden over time was followed with volume measurements by caliper and noninvasive fluorescent and bioluminescent imaging (Figure 2, A–D). Bioluminescent luciferase imaging was shown to be more sensitive than fluorescent GFP imaging. Luciferase-expressing (MC38-LUC) tumors were detected as early as 1 day (Figure 2B) after tumor cell inoculation, whereas GFP-expressing (MC38-GFP) tumors were not detected until 7 days later. For both tumor types, caliper measurements could be performed by day 5 postinjection (Figure 2, A and C).

For both types of imaging, bioluminescent and fluorescent intensity correlated significantly and linearly with tumor volume, as measured by caliper (Figure 3, A and B). For GFP fluorescent imaging, a slightly stronger correlation was found between fluorescent intensity and tumor weight (Figure 3E; $R^2 = 0.83$) than between tumor volume and weight (Figure 3C; $R^2 = 0.80$). A significantly stronger correlation was found between bioluminescent intensity and tumor weight (Figure 3F; $R^2 = 0.93$) than between volume and weight (Figure 3D; $R^2 = 0.82$). Each group initially consisted of ten mice, and seven to eight per group survived through the course of the experiments.

Western blot analysis was also performed to confirm in vitro and in vivo expression of both GFP and luciferase (Figure 4). Results demonstrate that there is stable expression of GFP and luciferase in cell culture as well as in tumors that excised 5 days postinjection. Specifically in the cultured cell lines, expression level of GFP was similar to that of luciferase (relative expression of GFP/luciferase = 1.3). Because the mechanism of light production for both GFP and luciferase are completely different, it is important to note that even equal levels of GFP and luciferase protein do not necessarily guarantee the same level of light production.

Although both whole-mouse fluorescent and bioluminescent imaging has proven useful, the direct comparison of these two techniques has not yet been described. Here, we have attempted to use GFP- and luciferase-expressing murine colon adenocarcinomas to characterize both qualitative and quantitative abilities of these two types of optical imaging techniques.

We have demonstrated that serial tumor volume measurements by caliper closely matched photon count (bioluminescence) and fluorescent intensity (Figure 3). A significant correlation ($R^2 = 0.99$) between tumor volume measurement and fluorescent intensity was found, which supports our previously published data (18). Bioluminescent imaging also correlated well to tumor volume measurements ($R^2 = 0.97$) (Figure 3, A and B). This experiment suggests that both GFP- and luciferase-based imaging techniques can be readily used to assess changes in tumor volume over time.

We also describe the quantitative relationships between tumor mass, tumor volume, and fluorescent intensity or photon count. On the last day of experiments, mice were euthanized and tumors

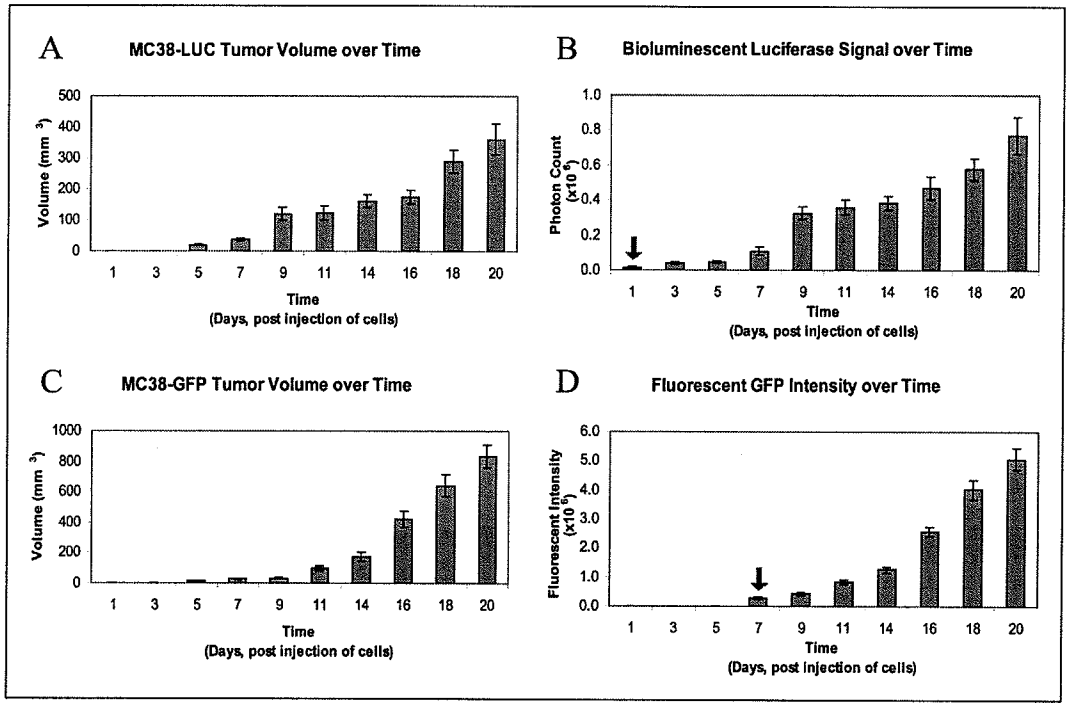

Figure 2. Serial measurements of tumor volume, fluorescence, and bioluminescence. MC38-LUC or MC38-GFP tumor cells were injected subcutaneously (s.c.) into the right flanks of C57/BL6 mice. Both tumor volume measurements by caliper and noninvasive whole-body optical imaging were performed every other day after injection. (A) Serial tumor volume measurements of MC38-LUC xenografts. (B) Bioluminescence over time. Red arrow indicates initial detection of signal. (C) Serial tumor volume measurements of MC38-GFP xenografts. (D) Fluorescence over time. Red arrow indicates initial detection of signal. $n = 7$–10 per group.

were weighed. We found that tumor weight and tumor volume correlated linearly for both GFP ($R^2 = 0.80$) and luciferase ($R^2 = 0.82$) imaging (Figure 3, C and D). However, the correlation between tumor weights and fluorescent intensity or photon count was slightly more robust for GFP and significantly more robust for luciferase than correlations with volume measurements. Interestingly, the correlation between tumor weight and imaging quantification was stronger ($R^2 = 0.92$) for luciferase than for GFP ($R^2 = 0.83$) (Figure 3, E and F). This suggests that bioluminescence may be a more sensitive method for estimating the true volume of viable cells in the tumor (assuming that true

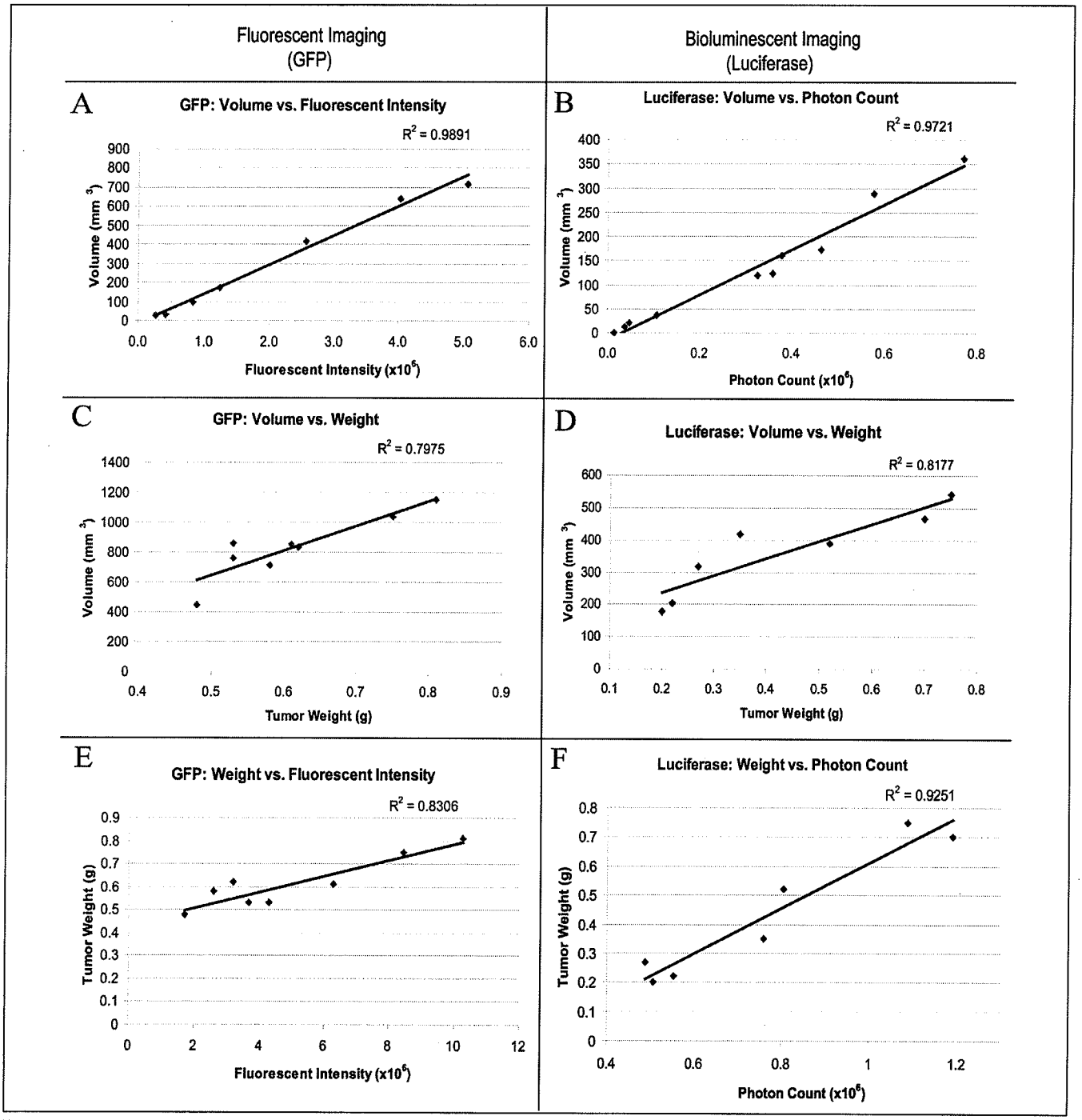

Figure 3. Correlations of tumor volume, tumor weight, fluorescent intensity, and photon counts. (A and B) Tumor volumes of MC38-GFP xenografts (A) and MC38-LUC xenografts (B) were correlated to fluorescent intensities on each experimental time point. (C–F) On day 20, mice were sacrificed and tumors were harvested and weighed. The MC38-GFP tumor weights were then correlated to tumor volume (C) and fluorescent intensity (E). The MC38-LUC tumor weights were correlated to tumor volume (D) and photon counts (F). $n = 7–10$ per group.

Table 1. Summary of Comparative Features of GFP-Based Fluorescent Imaging and Luciferase-Based Bioluminescent Imaging

	GFP	Luciferase
Signal-to-noise ratio	Low	High
Earliest tumor detection in experiment	Day 7	Day 1
No. of mice that can be imaged	Few (one mouse for our system; depends on excitation light source design)	Many (up to 10 mice demonstrated in our system)
Substrate	None	Luciferin
Volume vs. imaging correlation	0.99	0.97
Biomass vs. imaging correlation	0.81	0.93
Image acquisition time	Milliseconds (200–300 ms)	Minutes (10 min)
Special requirements	none	ATP plus oxygen required for sufficient light production

biomass is closely related to weight) than fluorescence.

Furthermore, bioluminescent imaging was able to detect tumors significantly earlier than fluorescent imaging. Luciferase-expressing tumors were detected as early as 1 day after injection of tumor cells, whereas GFP fluorescence was not detected until day 7 postinjection (Figure 3). This result highlights the high sensitivity and minimal background intrinsic to bioluminescent imaging. Background signal noise is minimal because there is virtually no endogenous bioluminescence from mammalian cells. However, GFP fluorescence is hampered by severe autofluorescence due to light reflection and light absorbance and scattering, thereby preventing the detection of low signals. Researchers are currently investigating and developing new technologies to address the problem of autofluorescence. For example, Levenson and colleagues have demonstrated that background in GFP fluorescence imaging can be eliminated using a novel method of spectral imaging (19).

Fluorescent and bioluminescent imaging modalities each offer distinct advantages that can be maximized, depending on the application. Features of both types of imaging are compared in Table 1. Certain types of experiments may deem luciferase-based imaging to be more appropriate. If one needs to detect low signals, luciferase-based imaging may be the better choice. For example, luciferase-based imaging has been used for studying lymphocyte tracking, in which the signal is extremely low (25). Because luciferase allows for the detection of low and high signals, bioluminescent imaging provides a wider dynamic range. Interestingly, longer wavelengths permit deeper tissue penetration in vivo. In contrast to an emission of 510 nm by GFP, the luciferase-luciferin reaction produces light that emits at a longer wavelength of approximately 600 nm, possibly enabling deeper tissue penetration. As a result, luciferase-based imaging may be useful in situations where one needs higher sensitivity, wider dynamic signal bandwidth, and deeper tissue penetration.

In other applications, GFP fluorescent imaging may be worth considering. GFP is extensively used in cell biology and in vitro assays for its strong signal and microscopic-level spatial resolution. If whole-body mouse imaging needs to be combined or followed by in vitro assays, GFP is a very viable option. The acquisition of the fluorescent GFP signal also does not require substrate injection, thereby minimizing the preparative procedures required, and i.p. injections may be prohibitive in certain types of experiments. Since luciferin is a relatively expensive substrate, GFP may also be more cost-effective.

However, if GFP is to be used, the issues of autofluorescence and lower sensitivity must be taken into account. To achieve greater depth of penetration and to minimize the problem of autofluorescence in GFP imaging, Hoffman et al. reported that steps such as skin flaps and endoscopic technology can be used (8). In other studies, CCD cameras have been attached to microscopes, which enable higher magnification to aid in the detection of small GFP-labeled tumors (20,21). Furthermore, the intensity of GFP signals can be very high and can therefore

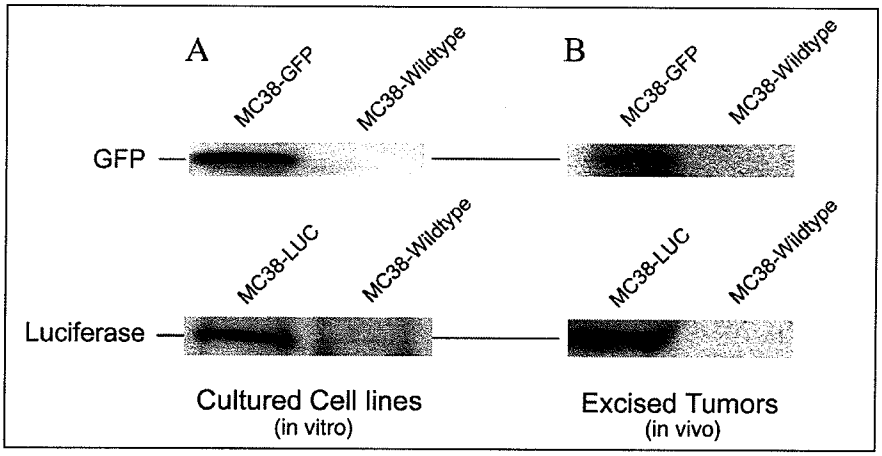

Figure 4. Western blot analysis of in vitro and in vivo green fluorescent protein (GFP) and luciferase expression. (A) Expression levels of GFP and luciferase protein from lysates of cells in culture. (B) Expression levels of GFP and luciferase protein from extracts of excised tumors that were resected 5 days postimplantation.

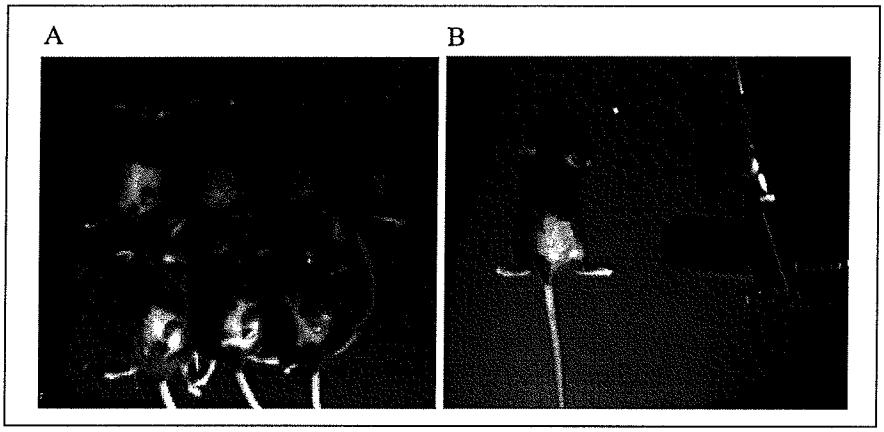

Figure 5. Comparison of the number of mice that can be imaged simultaneously via bioluminescent imaging and fluorescent imaging. (A) Sample image of bioluminescence imaging, in which many mice can be imaged at the same time. All mice need to be injected with the substrate luciferin prior to imaging, and no external light source is required. (B) GFP fluorescent imaging requires an external light source emitting at a specific wavelength of 510 nm. The excitation light source has an optimal center of intensity so only one tumor/mouse can be optimally imaged at any one time.

allow for extremely short image exposure times. As a result, CCD cameras can perform real-time imaging of GFP in nonanesthetized and active animals with implanted tumors (2).

Hardware design is also dependent on the type of imaging performed. Fluorescent imaging requires an external light source, whereas bioluminescent imaging does not. In bioluminescent imaging, light is emitted endogenously from the tissue due to the luciferase-luciferin chemical reaction. However, fluorescent mouse imaging can be limited by the design of the excitation light source. In our imaging system, there is only one excitation fiber-optic light source, which can only allow for imaging of one mouse at a time. As a result, the number of mice that can be imaged by fluorescence imaging depends on the design of the excitation light source. The scalability of both types of imaging is illustrated in Figure 5.

In addition to equipment for fluorescence imaging, the CCD is a key component of any optical imaging system that must be carefully chosen. Our imaging system configuring consists of a CCD camera that is sensitive to emission wavelengths for both GFP and luciferase. These technical specifications can be further optimized, as there are

numerous equipment types available on the market. In addition to high signal-to-noise ratios for the detector, high quantum efficiency over the emission wavelengths needs to be a primary criterion in hardware selection (27).

Cytotoxicity of both GFP and luciferase may also be a possible concern that should be considered by the investigator. Despite the extensive use of luciferase and GFP for in vitro studies, the potential toxicities of these reporters have yet to be fully investigated. For example, where some studies have documented the nontoxic nature of GFP, some studies have demonstrated that GFP may be toxic and that high protein levels may induce apoptosis (20,28). When excited for extended periods of time, GFP may also generate free radicals with potentially cytotoxic properties (29). Luciferase and its substrate, luciferin, have been reported to mainly exhibit low toxicity with no apparent effects on the health of animals (16,17,22,23). Because questions remain regarding the immunogenicity and toxicity of these reporters and also the substrate luciferin, this may be a potential avenue of future study.

Thus far, we have demonstrated the quantitative capabilities of both luciferase-based bioluminescent and GFP-based fluorescent in vivo imaging. Both GFP and luciferase, as reporter constructs, have been shown to harness distinct strengths that can be taken into consideration when choosing fluorescence or bioluminescence as the optical imaging modality for a particular experiment. Each technique has a role, and the two may be complementary.

ACKNOWLEDGMENTS

G.C. is a Howard Hughes Medical Institute-NIH Research Scholar.

REFERENCES

1. **Prasher, D.C. V.K. Eckenrode, W.W. Ward, F.G. Prendergast, and M.J. Cormier.** 1992. Primary structure of the *Aequorea victoria* green-fluorescent protein. Gene *111*:229-333.
2. **Subramanian, S. and F. Srienc.** 1996. Quantitative analysis of transient gene expression in mammalian cells using the green fluorescent protein. J. Biotechnol. *49*:137-151.
3. **Chalfie, M.** 1995. Green fluorescent protein. Photochem. Photobiol. *62*:651-656.
4. **Kain, S.R, M. Adams, A. Kondepudi, T.T. Yang, W.W. Ward, and P. Kitts.** 1995. Green fluorescent protein as a reporter of gene expression and protein localization. BioTechniques *19*:650-655.
5. **Hastings, J.W.** 1996. Chemistries and colors of bioluminescent reactions: a review. Gene *173*:5-11.
6. **Wood, K.V.** 1996. Marker proteins for gene expression. Curr. Opin. Biotech. *6*:50-80.
7. **Contag, C.H., D. Jenkins, P.R. Contag, and R.S. Negrin.** 2000. Use of reporter genes for optical measurements of neoplastic disease in vivo. Neoplasia *2*:41-52.
8. **Hoffman, R.M.** 2001. Visualization of GFP-expressing tumors and metastasis in vivo. BioTechniques *30*:1016-1024.
9. **Bouvet, M., J. Wang, S.R. Nardin, R. Nasirpour, M. Yang, E. Baranov, P. Jiang, A.R. Moossa, and R.M. Hoffman.** 2000. Real-time optical imaging of primary tumor growth and multiple metastatic events in a pancreatic cancer orthotopic model. Cancer Res. *62*:1534-1540.
10. **Hasegawa, S., M. Yang, T. Chishima, Y. Miyagi, H. Shimada, A.R. Moossa, and R.M. Hoffman.** 2001. In vivo tumor delivery of the green fluorescent protein gene to report future occurrence of metastasis. Cancer Gene Ther. *7*:1336-1340.
11. **Hoffman, R.M.** 2001. Visualization of GFP-expressing tumors and metastasis in vivo. BioTechniques *30*:1016-1024.
12. **Yang, M., E. Baranov, J.W. Wang, P. Jiang, X. Wang, F.X. Sun, M. Bouvet, A.R. Moossa, et al.** 2002. Direct external imaging of nascent cancer, tumor progression, angiogenesis, and metastasis on internal organs in the fluorescent orthotopic model. Proc. Natl. Acad. Sci. USA *99*:3824-3829.
13. **Zhao, M., E. Yang, E. Baranov, X. Wang, S. Penman, A.R. Moossa, and R.M. Hoffman.** 2001. Spatial-temporal imaging of bacterial infection and antibiotic response in intact animals. Proc. Natl. Acad. Sci. USA *98*: 9814-9818.
14. **Rehemtulla, A., L.D. Stegman, S.J. Cardozo, S. Gupta, D.E. Hall, C.H. Contag, and B.D. Ross.** 2000. Rapid and quantitative assessment of cancer treatment response using in vivo bioluminescence imaging. Neoplasia *2*:491-495.
15. **Sweeney, T.J., V. Mailaender, A.A. Tucker, A.B. Olomu, W. Zhang, Y. Cao, R.S. Negrin, and C.H. Contag.** 1999. Visualizing the kinetics of tumor-cell clearance in living animals. Proc. Natl. Acad. Sci. USA *96*: 12044-12049.
16. **Contag, C.H., P.R. Contag, J.L. Mullins, S.D. Spilman, D.K. Stevenson, and D.A. Benaron.** 1995. Photonic detection of bacterial pathogens in living hosts. Mol. Microbiol. *18*:593-603.
17. **Contag, C.H., S. Spilman, P.R. Contag, M. Oshiro, B. Eames, P. Dennery, D.K. Stevenson, and D.A. Benaron.** 1997. Visualizing gene expression in living animals using a bioluminescent reporter. Photochem. Photbiol. *66*:523-531.
18. **Diehn, F.E., N.G. Costouros, M.S. Miller, A.L. Feldman, H.R. Alexander, K.C.P. Li, and S.K. Libutti.** 2002. Noninvasive fluorescent imaging reliably estimates biomass in vivo. BioTechniques *33*:1250-1255.
19. **Levenson, R., M. Yang, and R.M. Hoffman.** 2003. Whole-body spectral imaging of fluorescently labeled orthotopic lung tumors in the live mouse. Proc. Am. Assoc. Cancer Res. *44*:776.
20. **Yang, M., E. Baranov, P. Jiang, F.X. Sun, X.M. Li, L. Li, S. Hasegawa, M. Bouvet, et al.** 2000. Whole-body optical imaging of green fluorescent protein-expressing tumors and metastases. Proc. Natl. Acad. Sci. USA *97*:1206-1211.
21. **Chaudhuri, T.R., J.M. Mountz, B.E. Rogers, E.E. Partridge, and K.R. Zinn.** 2001. Light-based imaging of green fluorescent protein-positive ovarian cancer xenografts during therapy. Gynecol. Oncol. *82*:581-589.
22. **Hardy, J., M. Edinger, M.H. Bachmann, R.S. Negrin, C.G. Fathman, and C.H. Contag.** 2001. Bioluminescence imaging of lymphocyte trafficking in vivo. Exp. Hematol. *29*:1353-1360.
23. **Edinger, M., T.J. Sweeney, A.A. Tucker, A.B. Olomu, R.S. Negrin, and C.H. Contag.** 1999. Noninvasive assessment of tumor cell proliferation in animal models. Neoplasia *1*: 303-310.
24. **Naviaux, R.K., E. Costanzi, M. Haas, and I.M. Verma.** 1996. The pCL vector system: rapid production of helper-free, high-titer, recombinant retroviruses. J. Virol. *70*:5701-5705.
25. **Feldman, A.L., H.R. Alexander, S.M. Hewitt, D. Lorang, C.E. Thiruvathukal, E.M. Turner, and S.K. Libutti.** 2001. Effect of retroviral endostatin gene transfer on subcutaneous and intraperitoneal growth of murine tumors. J. Natl. Cancer Inst. *93*: 1014-1020.
26. **Atadja, P., H. Wong, C. Veillette, and K. Riabowol.** 1995. Overexpression of cyclin D1 blocks proliferation of normal diploid fibroblasts. Exp. Cell Res. *217*:205-216.
27. **Rice, B.W., M.D. Cable, and M.B. Nelson.** 2001. In vivo imaging of light-emitting probes. J. Biomed. Optics *6*:432-440.
28. **Liu, H., M. Jan, C. Chou, P. Chen, and N. Ke.** 1999. Is green fluorescent protein toxic to the living cells? Biochem. Biophys. Res. Commun. *260*:712-717.
29. **Clontech.** 1996. Living Color GFP Application Notes. CLONTECH Laboratories, Palo Alto, CA.

Received 4 May 2003; accepted 2 September 2003.

Address correspondence to:

Steven K. Libutti
Surgery Branch, Center for Cancer Research
National Cancer Institute
10 Center Drive, Room 2B07
Bethesda, MD 20892, USA
e-mail: libuttis@mail.nih.gov

Wang, Ge

From: Elizabeth Bowman [Elizabeth.Bowman@caliperls.com]
Sent: Monday, January 10, 2011 3:20 PM
To: Wang, Ge
Subject: Presentation: Low dose μCT / 3-D multimodal co-registration (optical/μCT)
Attachments: Quantum FX uCT Overview 2010.pdf

Hi Dr. Wang,

I'm going to be in your area with our Pre-Clinical Radiology Senior Scientist, Jeff Meganck, Ph.D. on **Thursday, Feb.10th** and was wondering if you'd be interested in scheduling a meeting to discuss applications of our low dose, high speed μCT system (Quantum FX) and 3-D multimodal co-registration?

Dr. Meganck and I would also be accompanied by our Director of Technical Applications, Alexandra De Lille, DVM, PhD. Dr. DeLille has experience with a range of imaging modalities, but she primarily focuses on the biology and applications of optical, optical/X-ray and optical/ μCT imaging.

In case you're not familiar with the technology, the Quantum is the first high speed, low dose μCT system that delivers high quality images and enables the use of μCT at every imaging point throughout longitudinal studies. It provides a 3-D anatomical view of disease activity, tumor development and therapeutic response over the course of a study, without the risk of altering the disease pathology or ablating the mice (terminal end points).

The Quantum FX μCT is a standalone system, but also compliments the IVIS Spectrum and gives you the ability to co-register optical data with high quality μCT scans for quantitative functional and anatomical imaging throughout your study. It's possible to perform a complete 3D CT/Optical in just a couple of minutes by integrating Spectrum/Quantum μCT.

Attached a slide deck on the Quantum FX μCT and multi modal co-registration.

If this is something that may be of interest to you and your colleagues, please let me know if you're available to schedule a meeting/presentation on **Thursday, Feb.10th**.

Thank you,
Elizabeth

The following link is for the QuantumFX brochure.
QuantumFX - http://www.caliperls.com/assets/024/8472.pdf

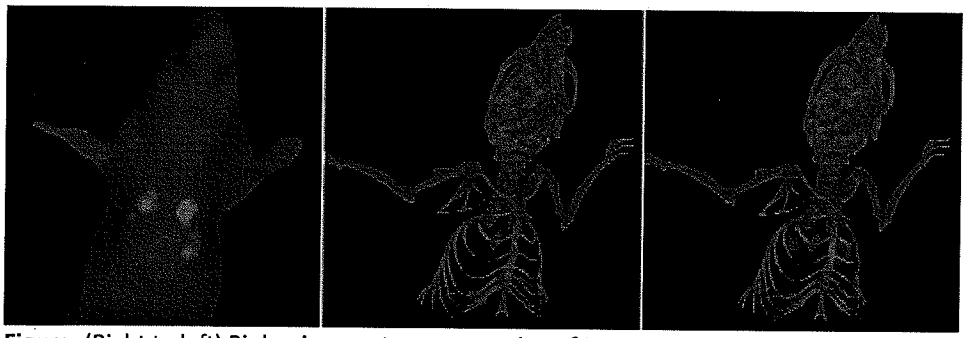

Figure: (Right to left) Bioluminescent reconstruction of MDA-MB-231 D3H2 LN-Luc Metastases within the lung. Quantum FX μCT scan. Co-registration of optical sources and μCT scan.

Elizabeth Bowman
Senior Account Manager, Southeast

Caliper Life Science, formerly Xenogen Corp.
68 Elm Street

Technology Overview

Anna Christensen PhD
Imaging Product Manager

Caliper LifeSciences

Molecular Imaging

Trends in Molecular Imaging

Leading in Enabling Technology

1. Imaging in 3D- Quantitative Approach
Pinpoint localization and quantitative assessment of tumors, metastases, sites of infection and other disease pathologies.

2. Imaging in Multimodality
Maximize the content extracted from preclinical models by integrating diverse imaging modalities in a single longitudinal study

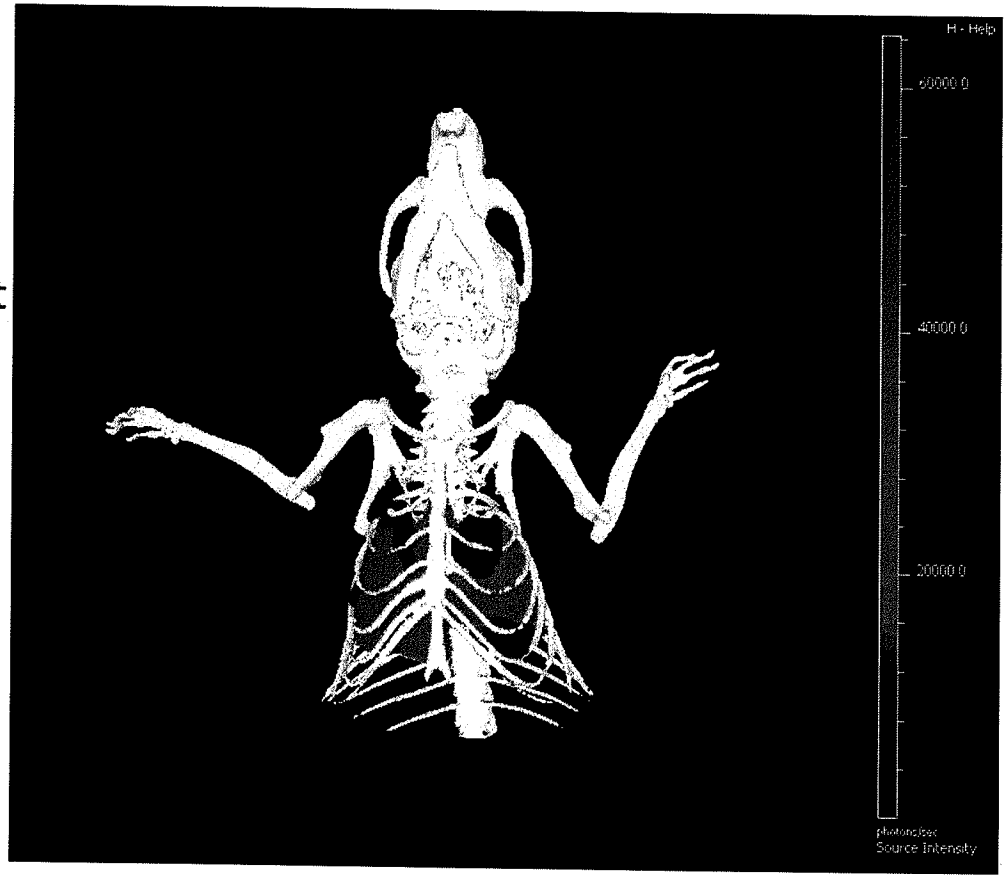

Molecular Imaging

Trends in Molecular Imaging

Addressing the Needs of Our Customers

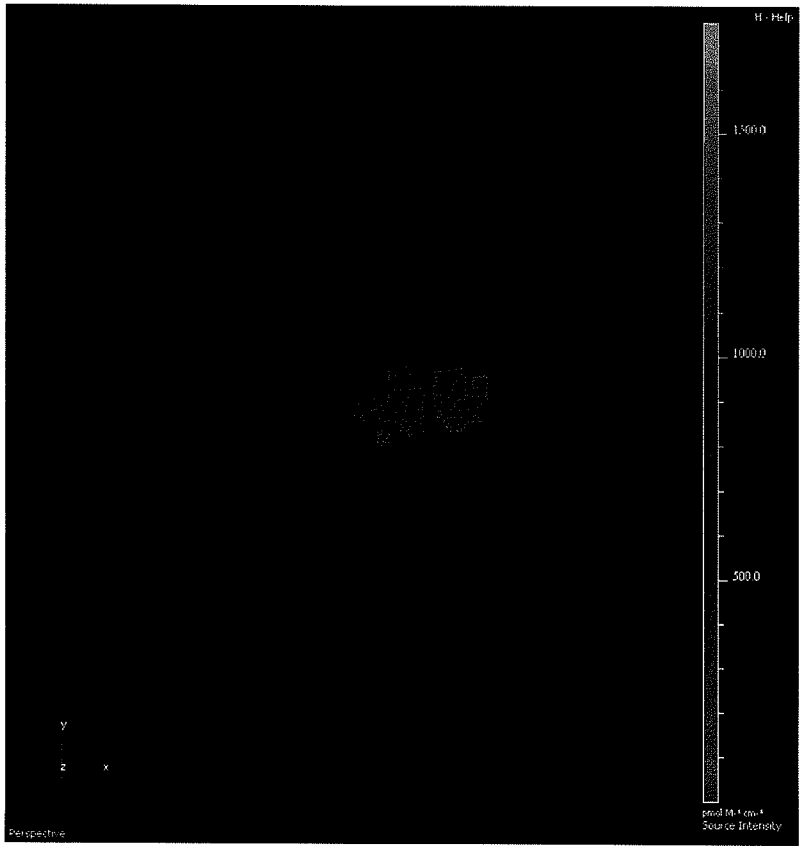

QD805 in lungs, AF750 in liver, co-registered with CT

Quantum FX enables low dose µCT and co-registers with IVIS Optical 3D

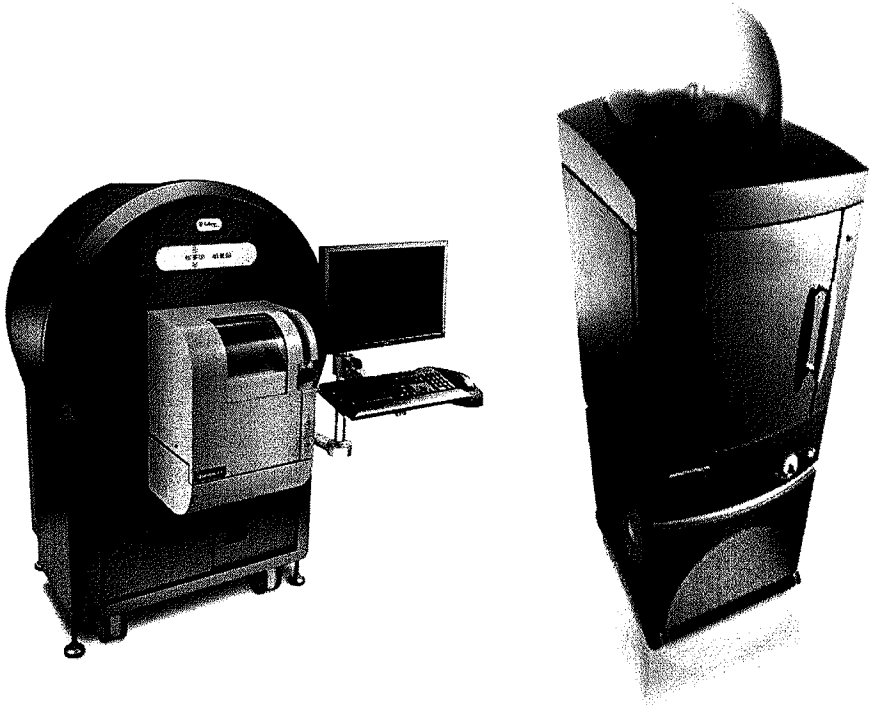

CALIPER | IMAGING PLATFORM

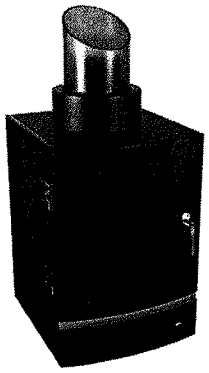

IVIS Lumina II

- Entry-level optical imaging
- Flexible and expandable with options and accessories
- Calibrated for quantitative longitudinal studies

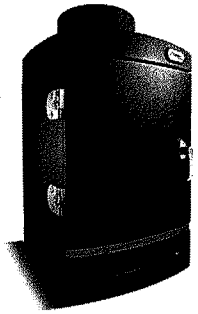

IVIS Kinetic

- Fast and conventional imaging in one system
- Calibrated for quantitative longitudinal studies
- Characterization of real-time event monitoring

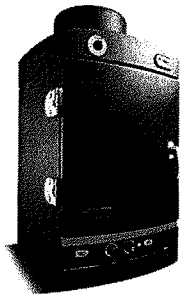

IVIS Lumina XR

- X-ray, Bioluminescence, and fluorescence detection and co-registration
- Anatomical reference for optical signals
- Absolute calibration for longitudinal studies

IVIS Spectrum

- Total optical imaging package in one system
- Absolute quantitation independent of location and size of source
- 3D visualization

Quantum FX

- Purpose-built for longitudinal imaging
- Low dosage per scan
- Fast imaging times
- High resolution images

QuantumFX µCT-Anatomical Resolution

IVIS Co-registration

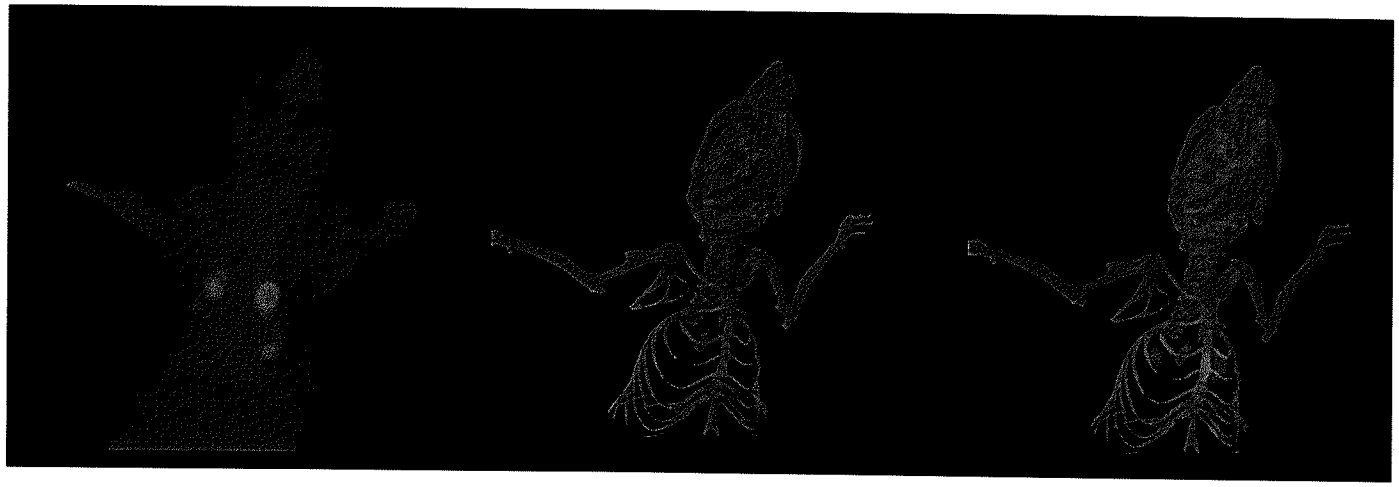

(Left to right) Bioluminescent reconstruction of MDA-MB-231 D3H2 LN-Luc Metastases within the lung. Quantum FX uCT scan. Co-registration of optical sources and uCT scan.

Quantum Micro *CT*

Low Dose CT for longitudinal studies

- **High speed imaging**
  - Intuitive software interface
  - 18 second scan for high throughput
  - 3D processing board for 45 second results
  - Workflow supports ~30 animals per hour
- **Exquisite Image Quality at Low Doses**
  - Excellent image quality and resolution for longitudinal in-vivo studies at the fraction of the dose
- **Purpose-built for small animal imaging**
  - Integrated animal handling
  - Compatible with XGI-8 anesthesia
  - Animal transfer and co-registration tools to IVIS Optical Imaging platforms

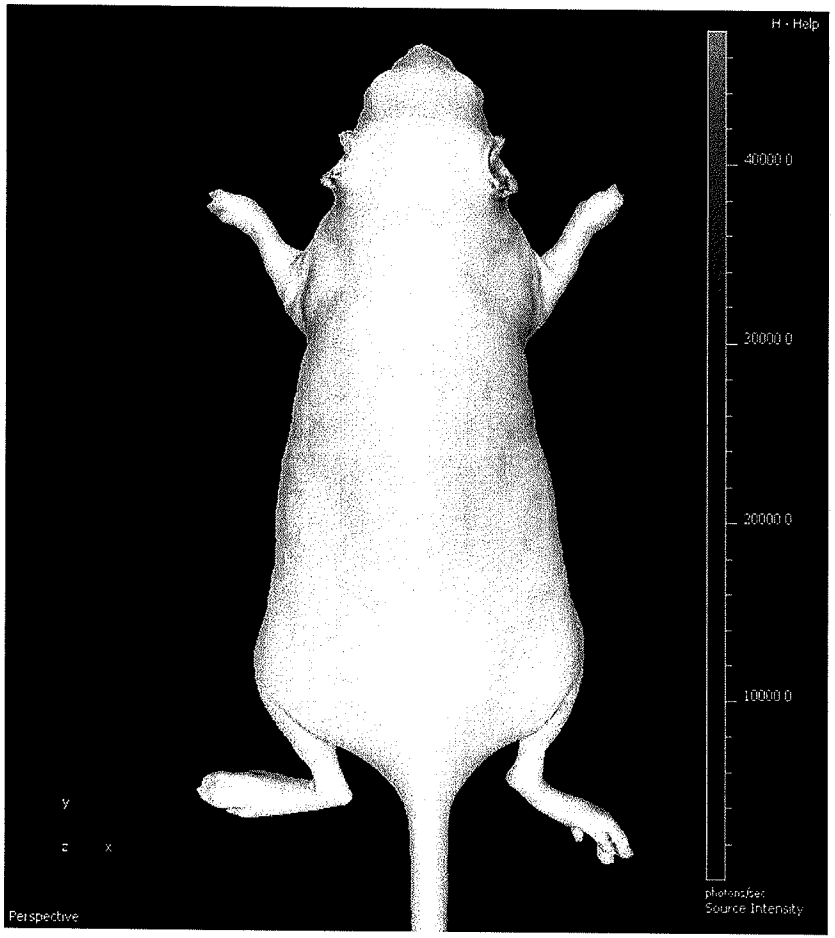

Quantum Micro *CT*

High resolution CT for longitudinal studies

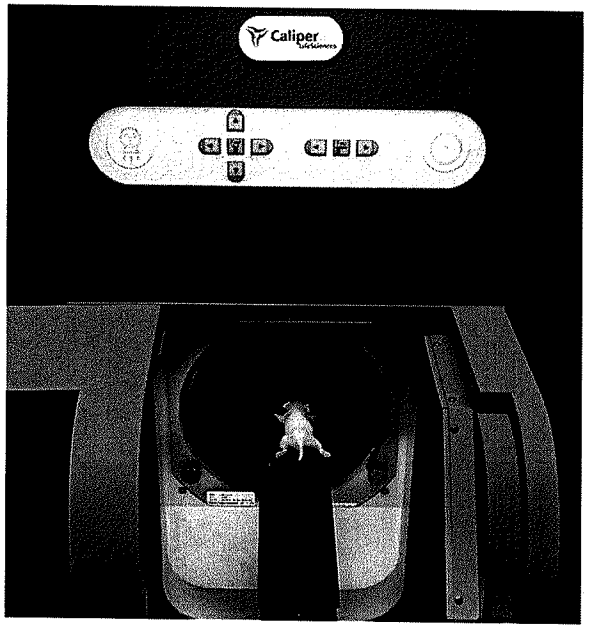

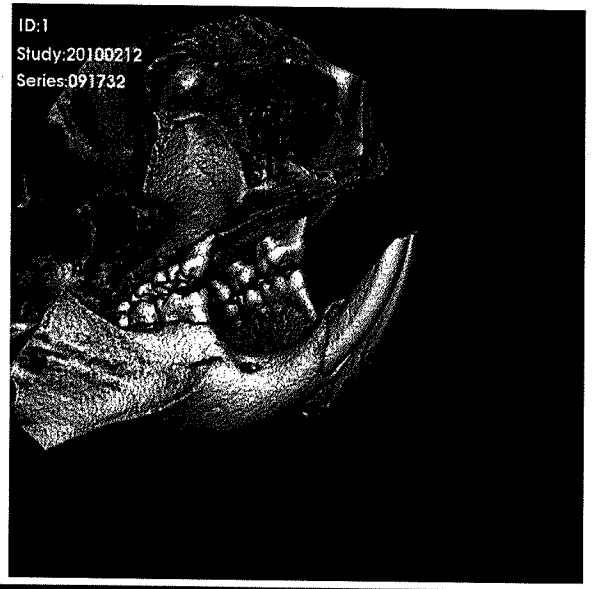

QuantumFX µCT

Understanding your needs

What performance do you need from a microCT system for pre-clinical imaging studies?

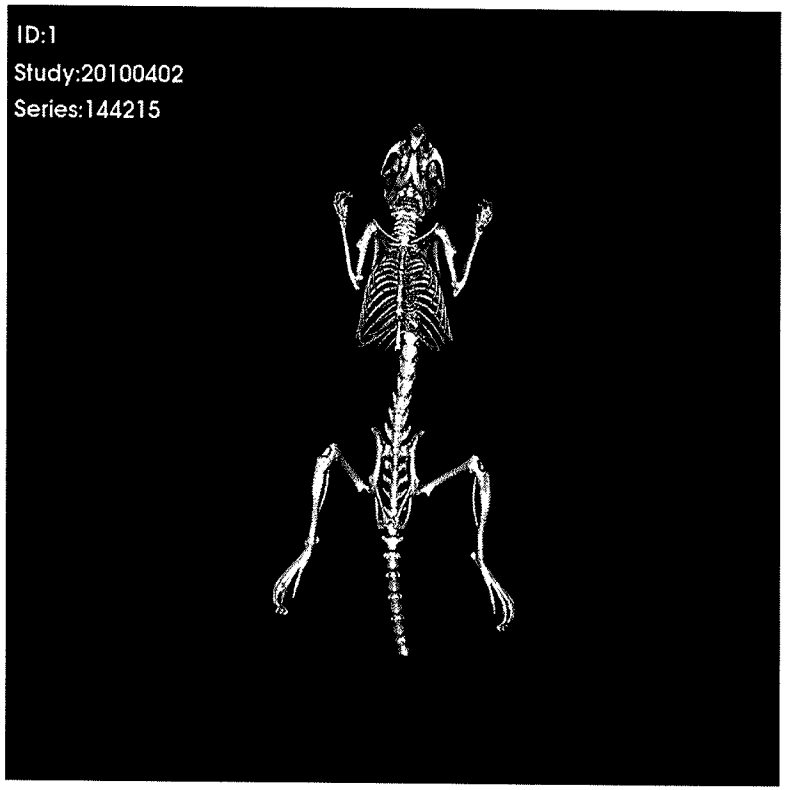

- Low X-ray dose
- Easy to use
- Fast
- Resolution
- Easy co-registration

What would characterize the ideal microCT system for pre-clinical imaging studies?

- Designed for pre-clinical microCT
- Specialized needs of pre-clinical imaging
- Support

QuantumFX µCT

Low Dose CT for longitudinal studies

Traditional micro CT workflow

- 2D X-ray is used for approximate localization with low X-ray dose
- MicroCT is used for a single image at high-dose to co-register with optical data

2D Xray → 2D Xray → Micro CT

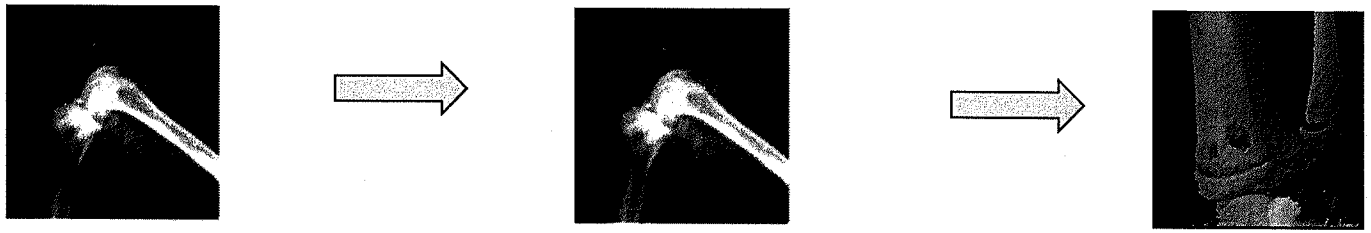

Sacrifice Mouse after high-dose CT imaging

Quantum Micro CT workflow

Multiple CT time points with co-registration capability

Minimal radiation effects, better characterization of pathology

Micro CT → Micro CT → Micro CT → Micro CT → Micro CT → Micro CT

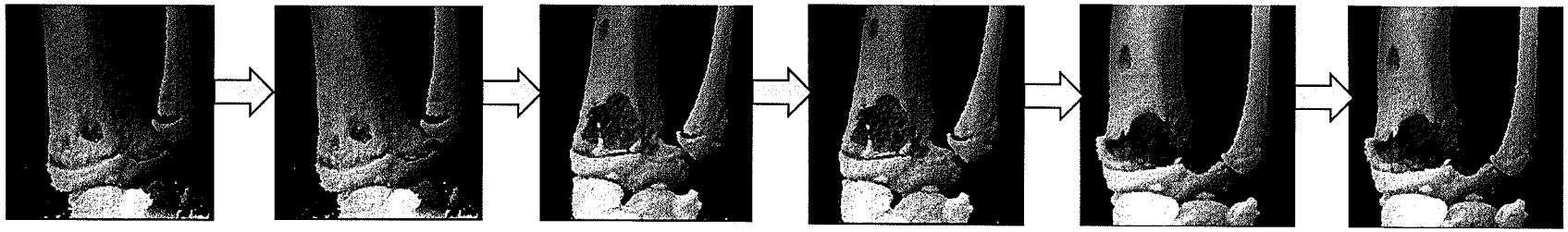

QuantumFX µCT

High resolution CT for longitudinal studies

Planar X-ray

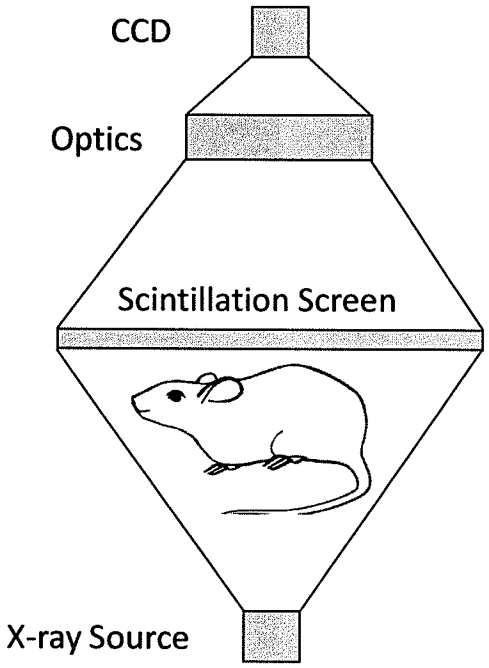

Typical Image Acquisition Time	
10 sec	18 sec
X-ray source characteristics	
40 kV	90 kV
100 µA	80 µA
Typical Mouse Dosage	
3-15 mGy	11 mGy

High resolution Insight Micro CT

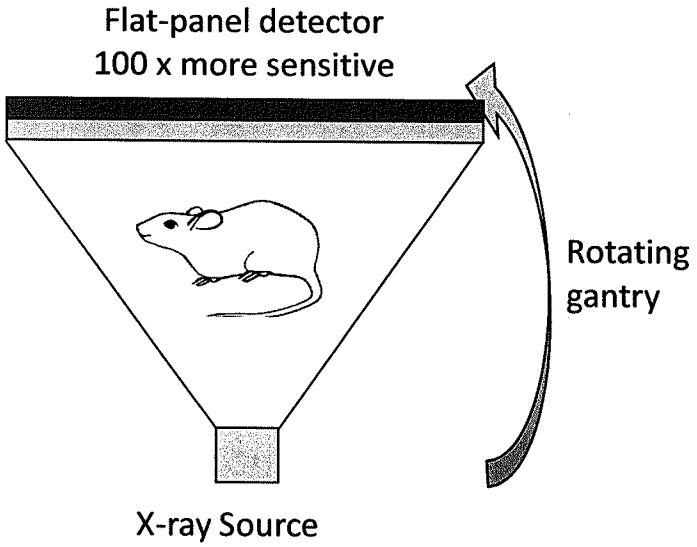

Exposure
CT Imaging

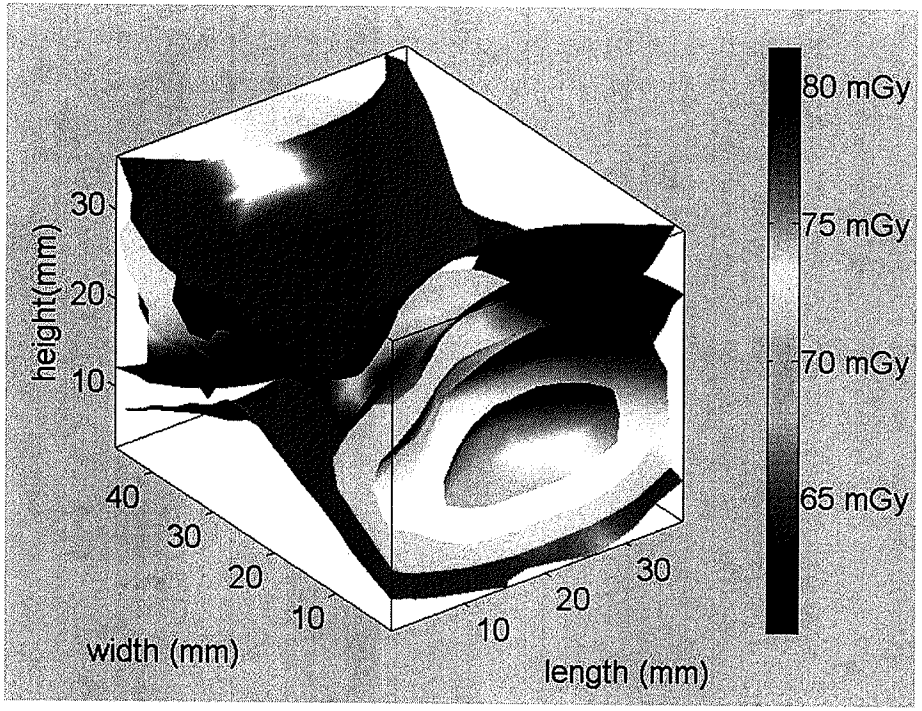

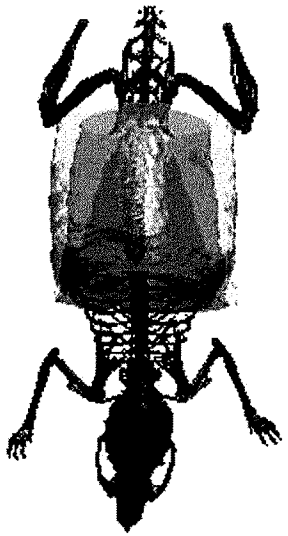

2 minute scan with 90 kV tube voltage with a uCT dose phantom developed at Stanford University. The dose close to the surface is around 80. Non Phantom scans requiring only 17 seconds translates to 11 mGy. The dose in the center of the phantom is 70 mGy (10 mGy for a 17 sec dose scan, 18s complete scan).

- 1 – 2 Gy generally used to ablate the mouse immune system
- 5% of ablation dosage would be 50 to 100 mGy, usually end of experiment dose
- 5 to 10 images with Quantum FX less than 5% of ablation dose

Exposure
CT Imaging

Quantum FX

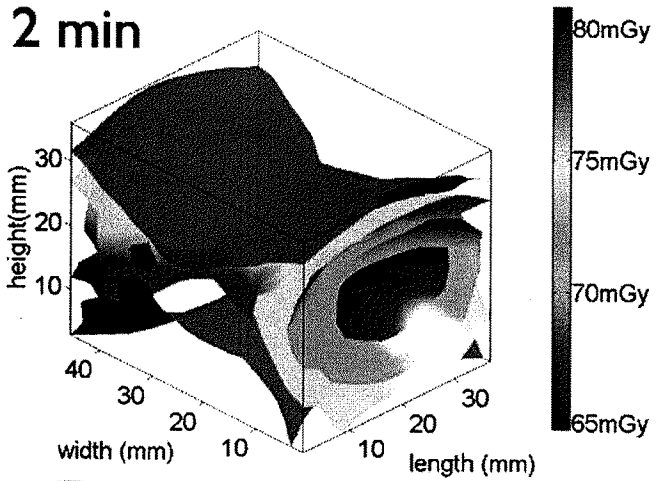

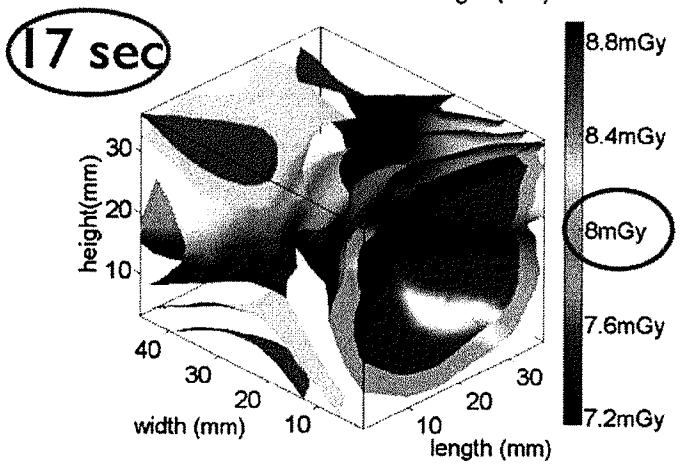

GE Explore Locus

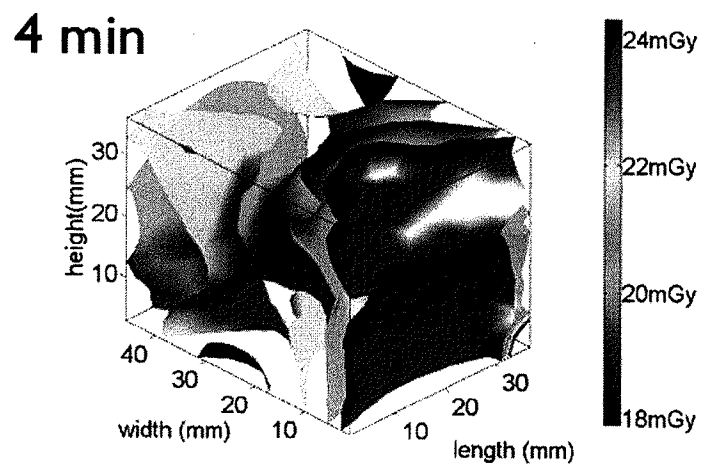

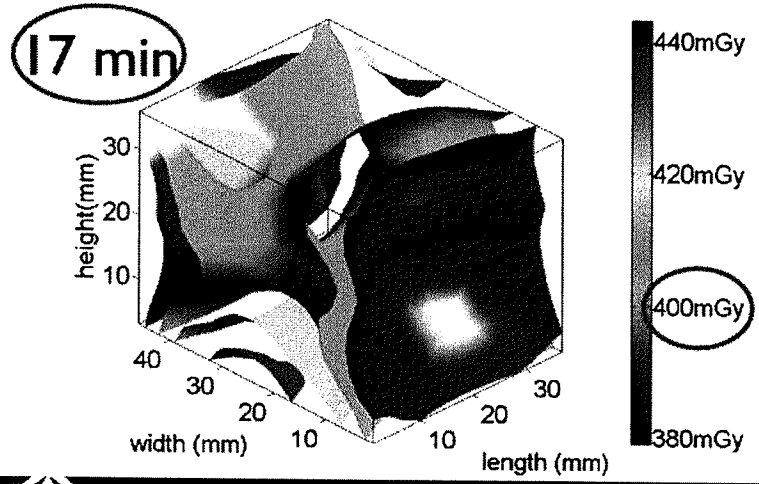

QuantumFX µCT

Signal to Noise Determinations

Standard Mode

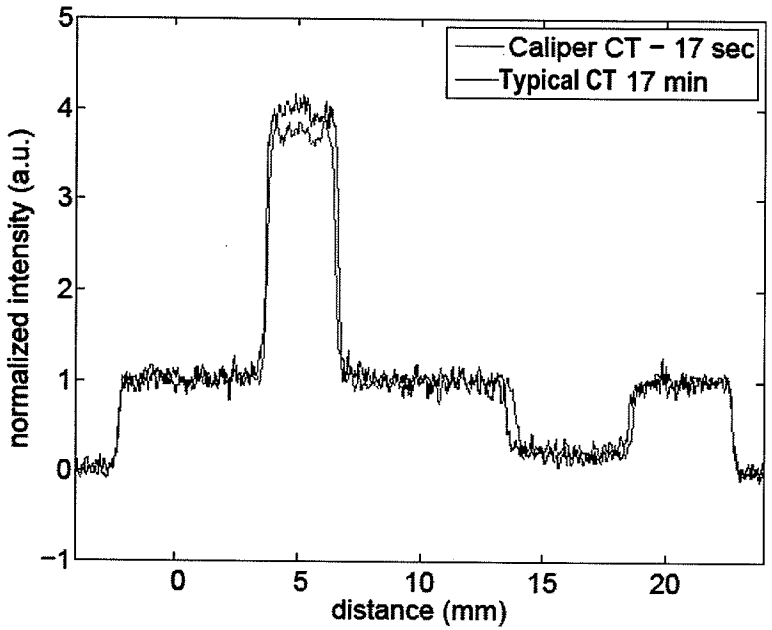

Fine Mode

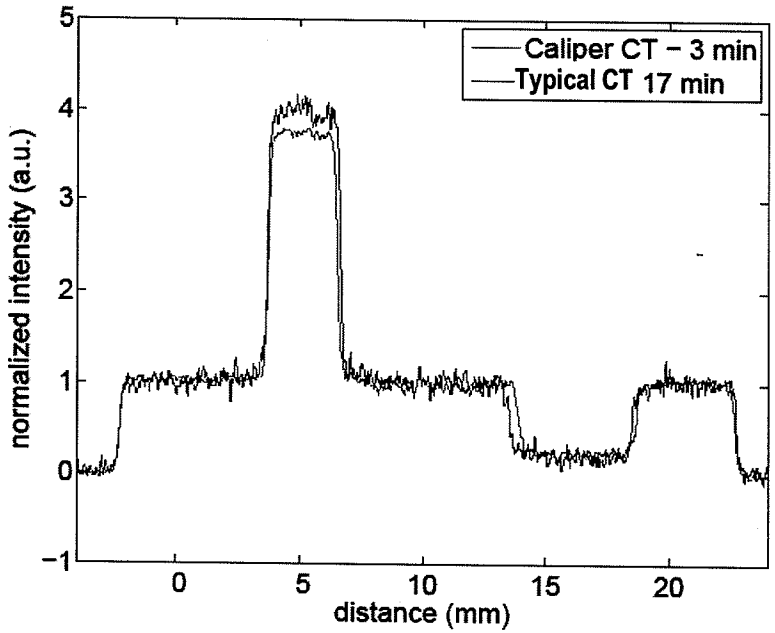

- QuantumFX fine vs standard scan time should small attenuation in signal modulation
- Shorter scan times for equivalent signal to noise

QuantumFX µCT

Signal to Noise Determinations

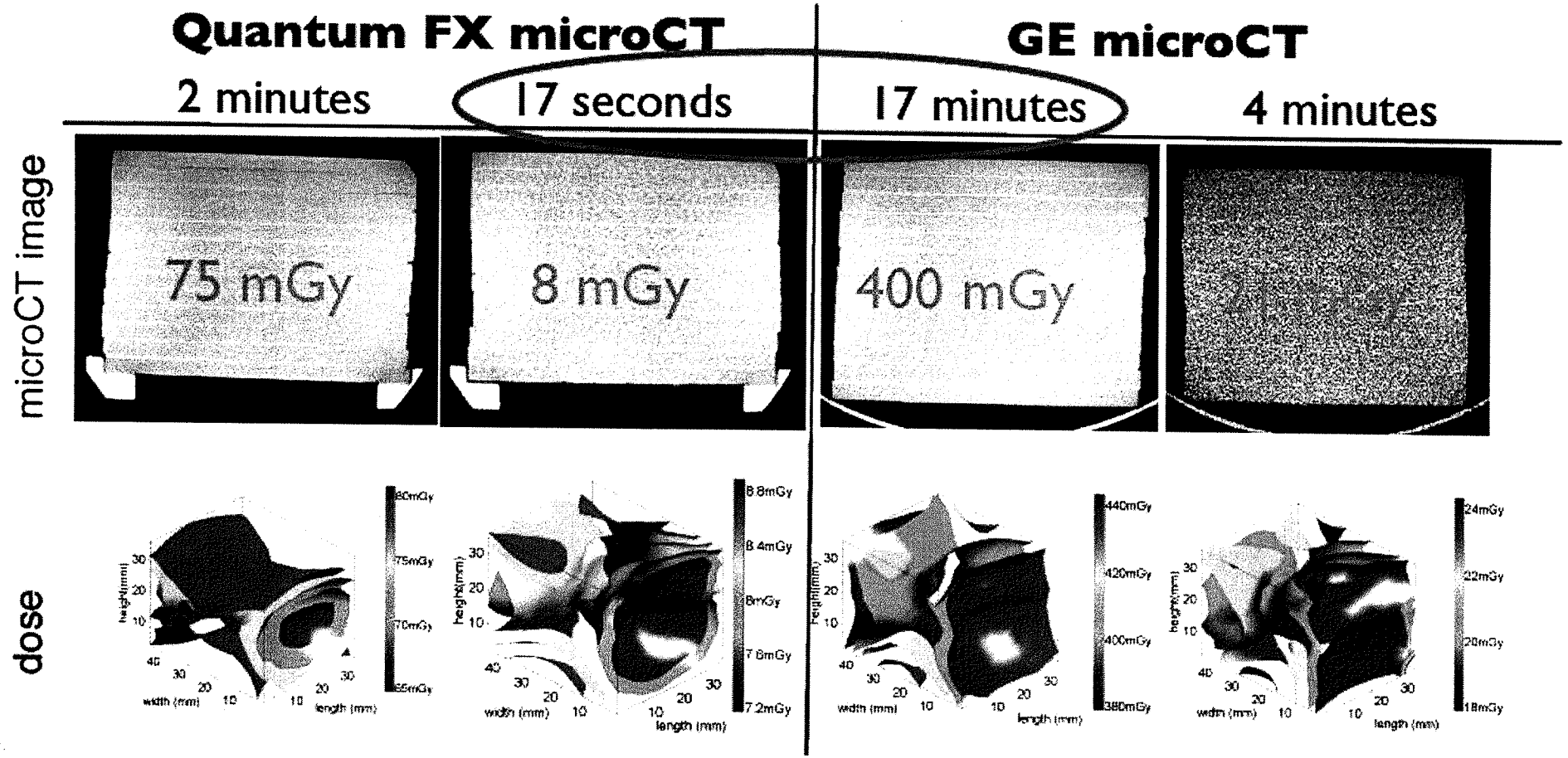

Planar Time Course
CC10-Tag expression in alveoli

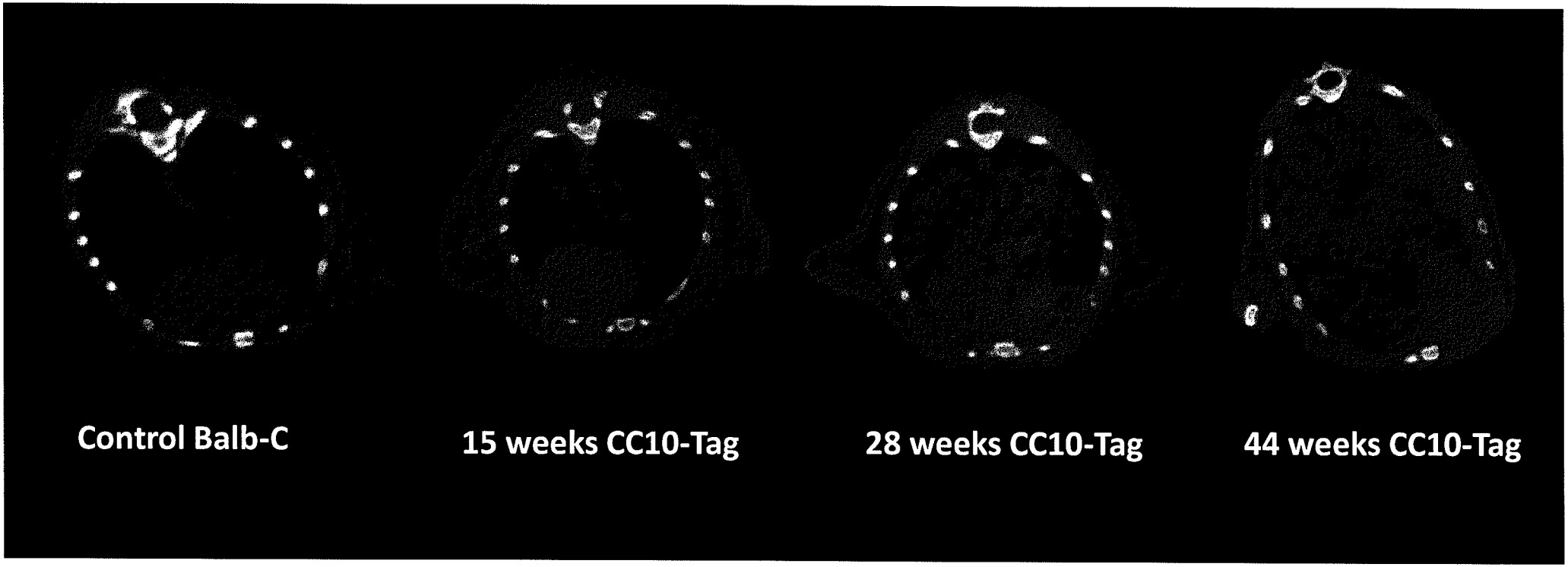

3D Video Time Course

*Segmentation View

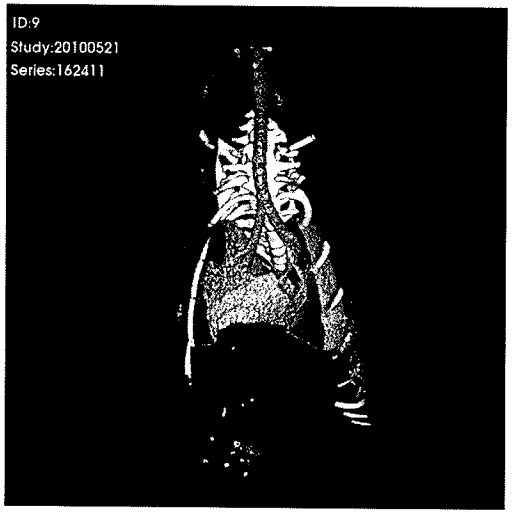

Control Balb-C

15 weeks CC10-Tag

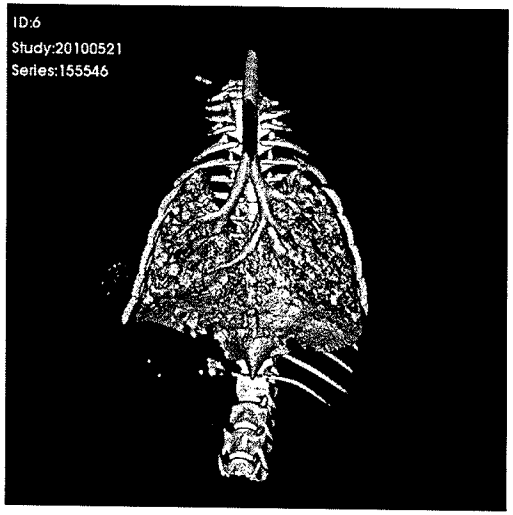

28 weeks CC10-Tag

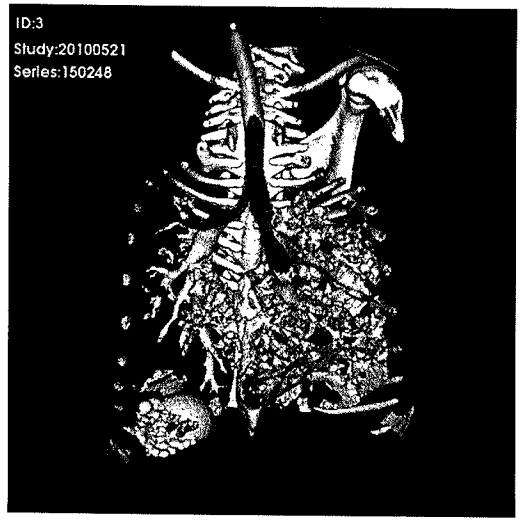

44 weeks CC10-Tag

*Pink=Tissue, Blue=Air, White=Bone

Monitoring MDA-MB-231 Tumor Metastases with Osteolytic Activity with BLI and CT

Day18 Day22 Day39 Day44

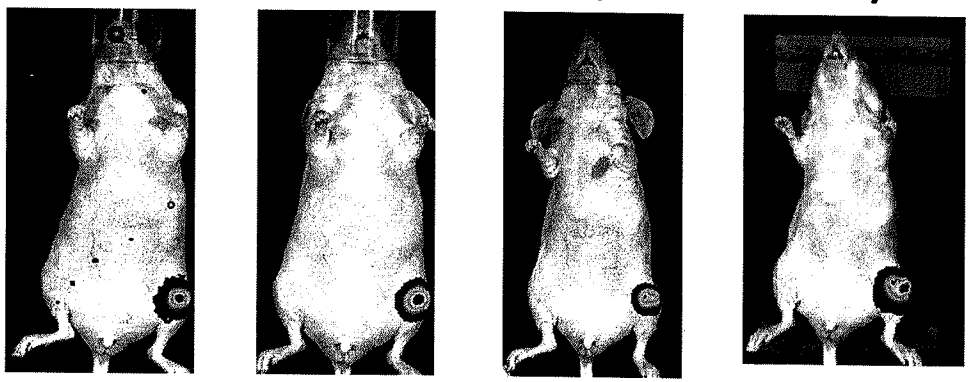

Day18 Day22 Day44

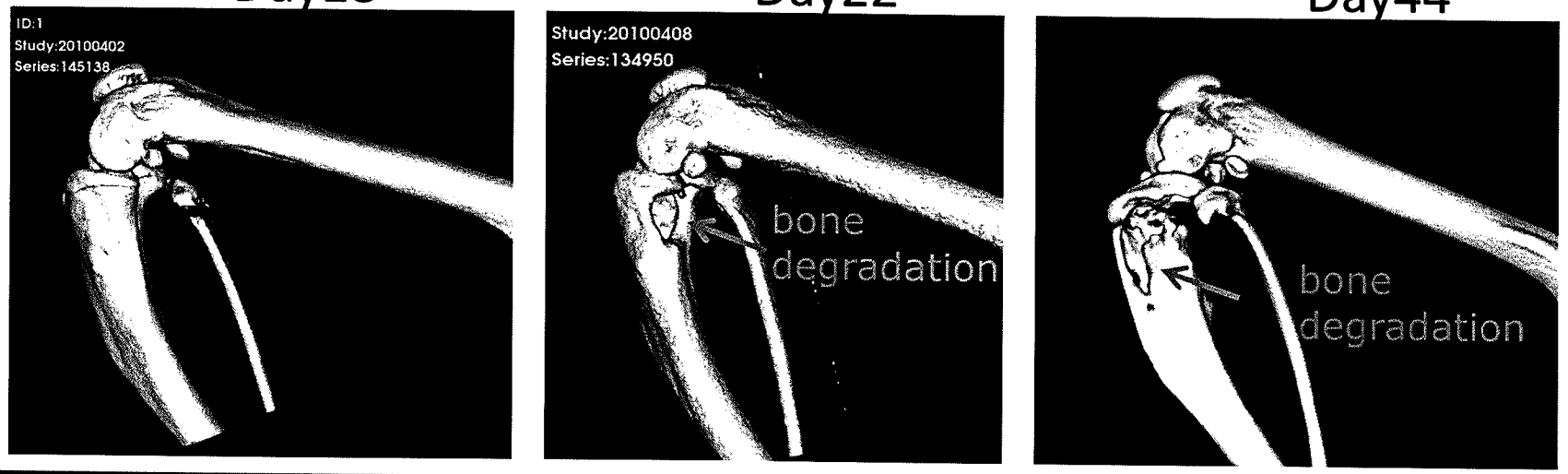

in vitro in vivo

Monitoring Tumor Progression and Osteolytic Lesion of MB231-D3H2LN-Luc with IVIS Spectrum and uCT

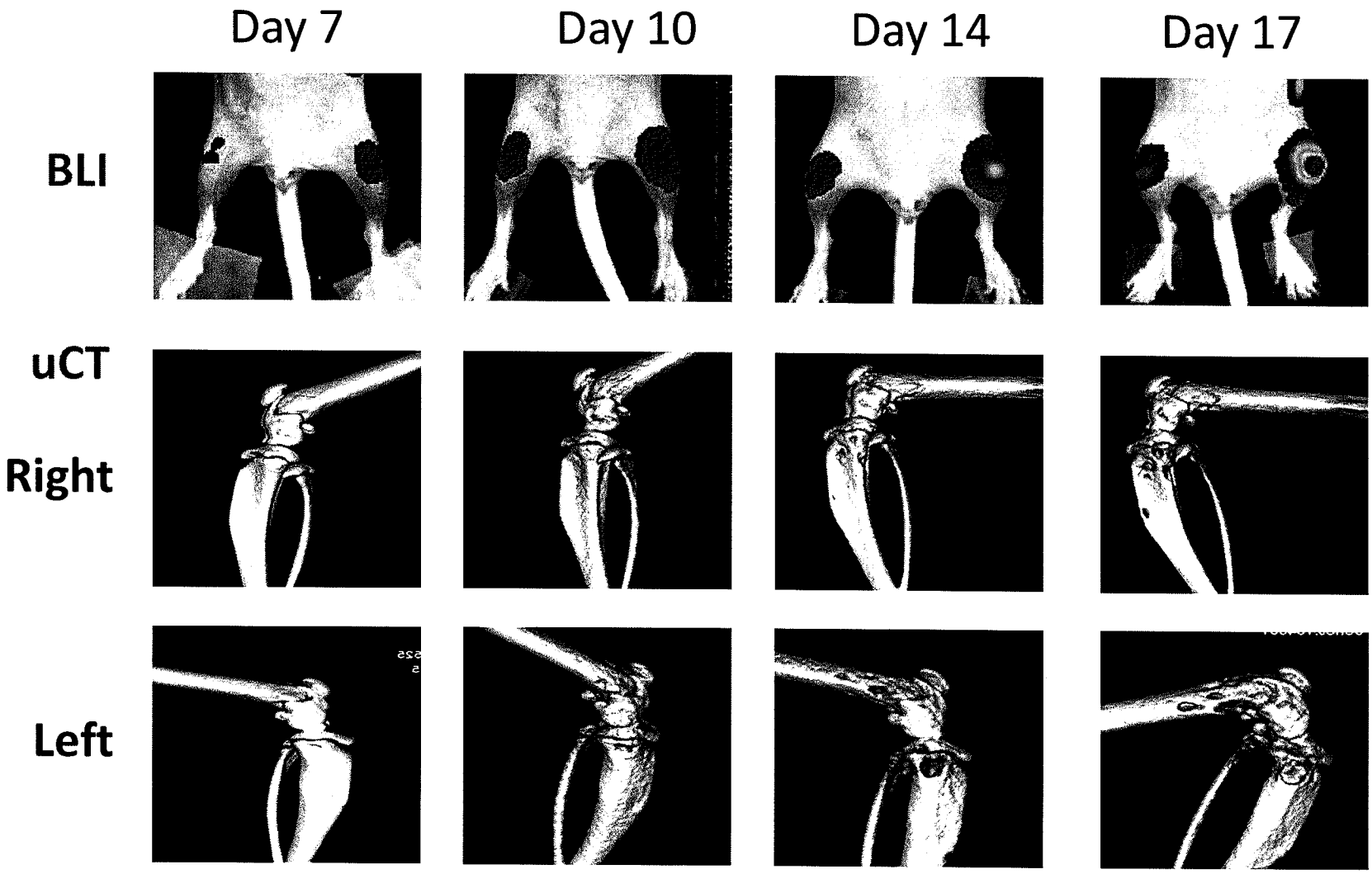

QuantumFX μCT

Contrast Agents

Soft tissue imaging and tumor measurement using contrast agent and 3D reconstruction.

Animal tumor model system
- 2 x 10^6 PSN-1 cells
- Balb/c mice
- Imaged day 15
- Clinical contrast agent

Imaging parameters
- 18 second can time
- 20μ resolution
- 5~8 mGy dosage

Tumor volume results:
- CT volume 17.78 mm3
- Excised volume 15.82 mm^3
- Multiple time points measured

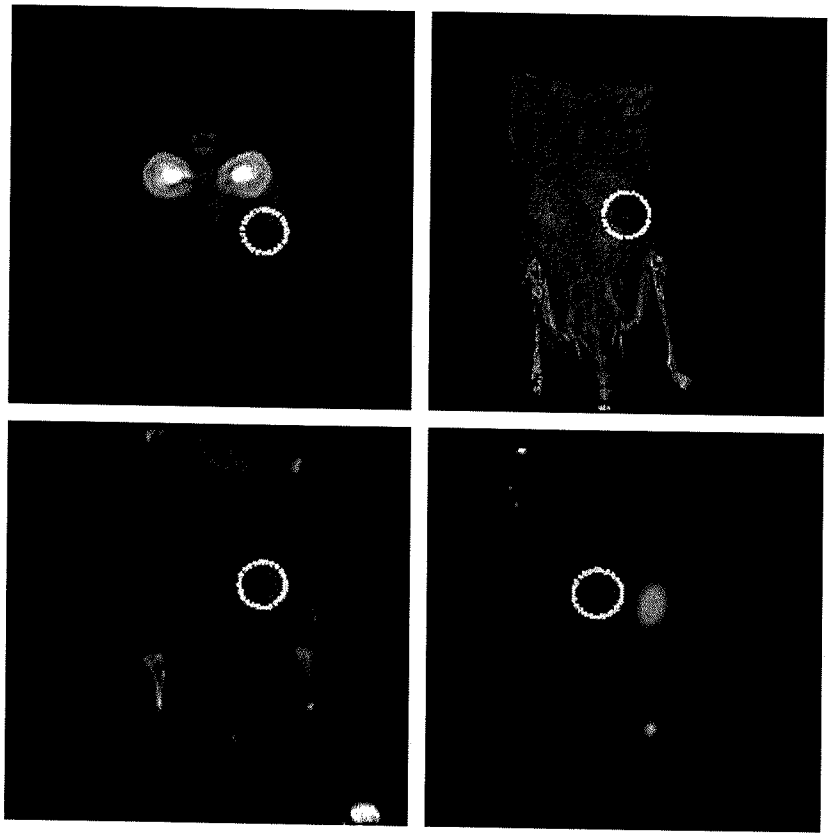

QuantumFX µCT

Contrast Agents

CT tumor measurement correlates with excised tumor volume determination

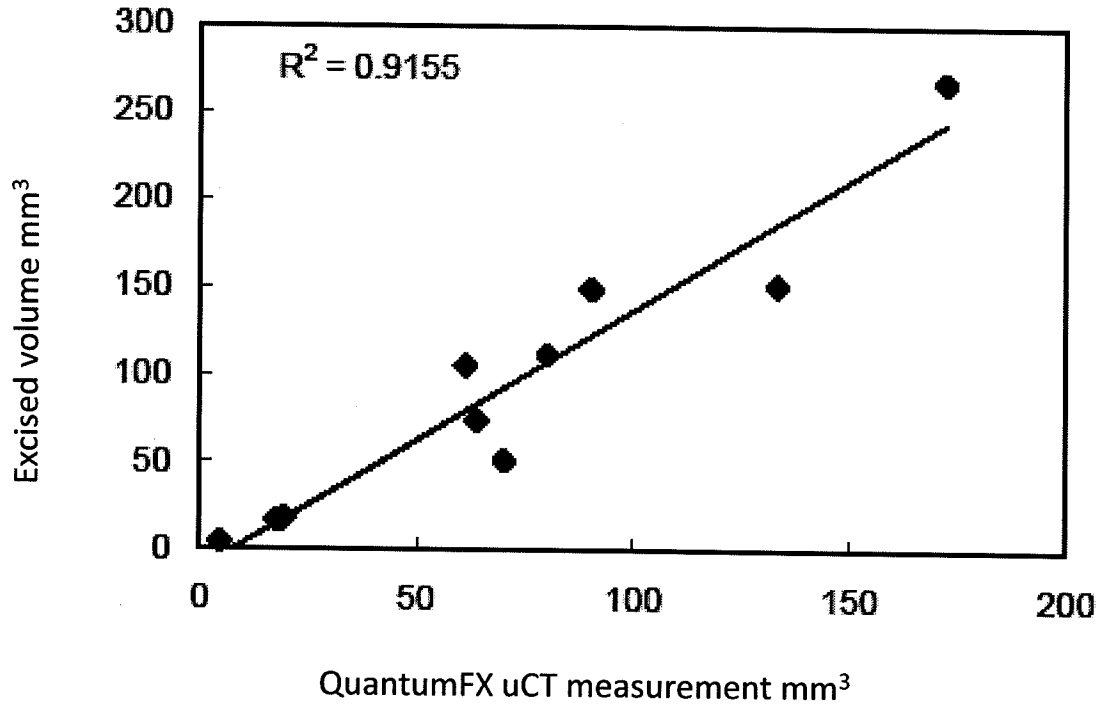

QuantumFX µCT

IVIS Co-registration

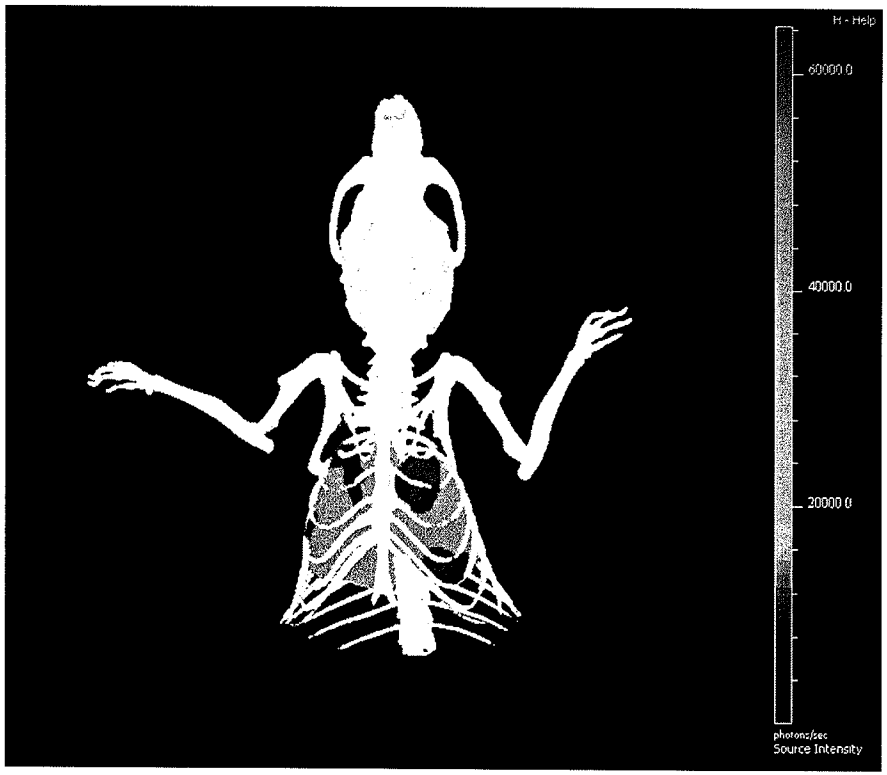

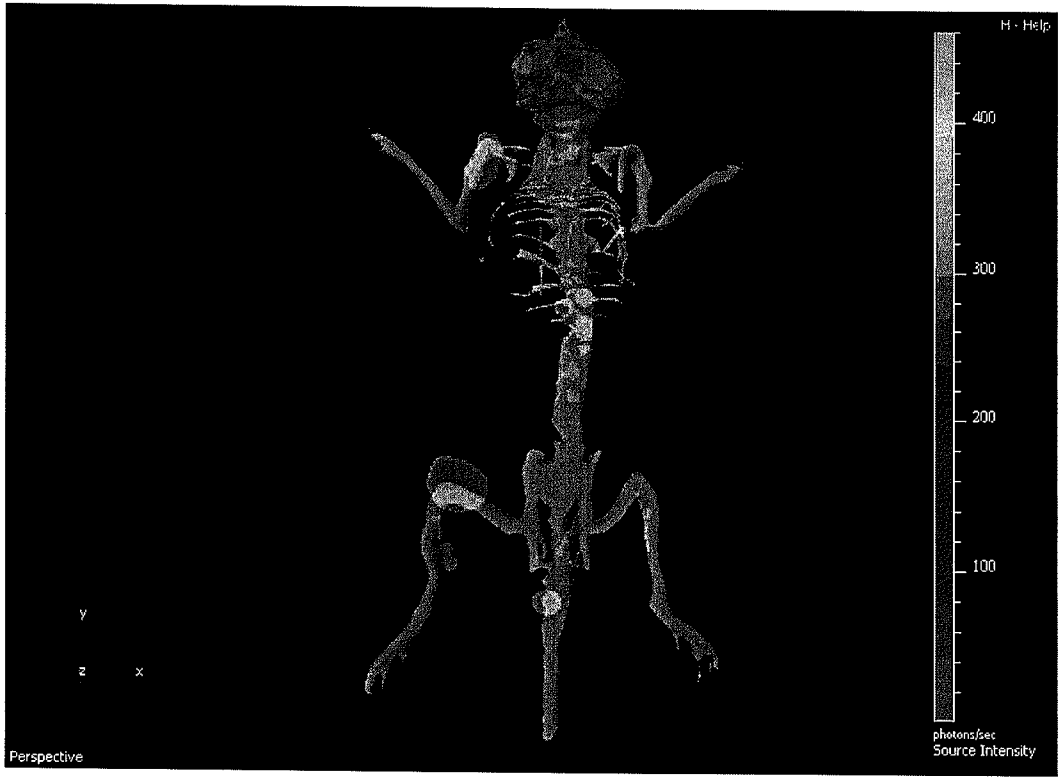

Transferring from IVIS Spectrum to imaging instruments of other modalities

Optical

Transfer bed will be available this summer

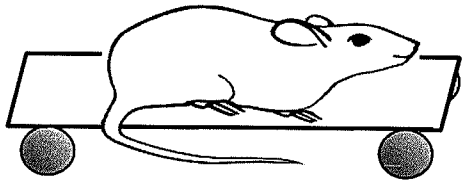

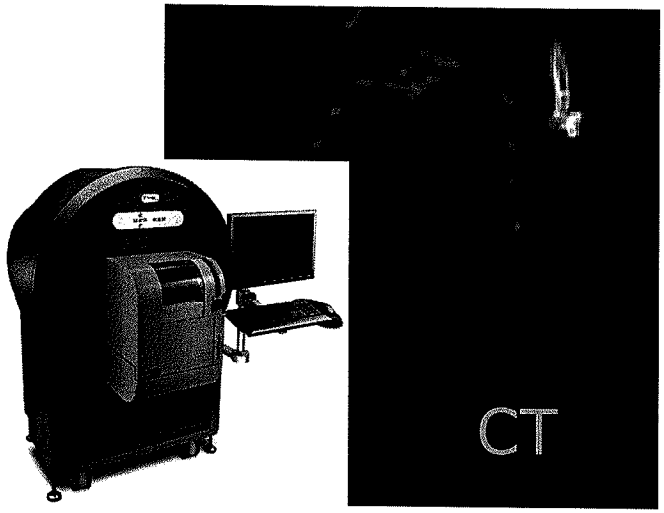

Bed is compatible with a number of commercially available systems

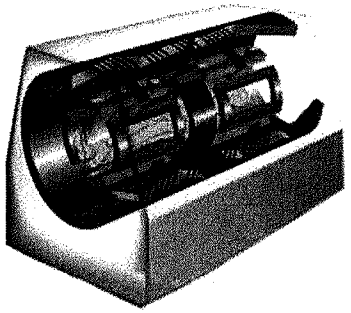

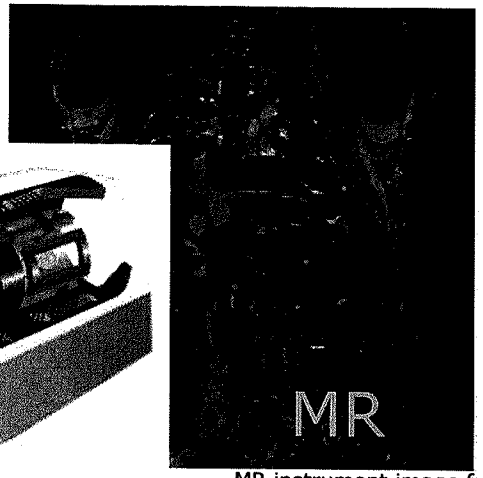

MR instrument image from http://vefir.mh.is/emjul/efni/nemverk/nemv-v07/geislun/MRI.htm

IVIS | CT Co-Registration

Tools for Co-registration

Animal Transfer Stations for 3D Multi-Modal Imaging

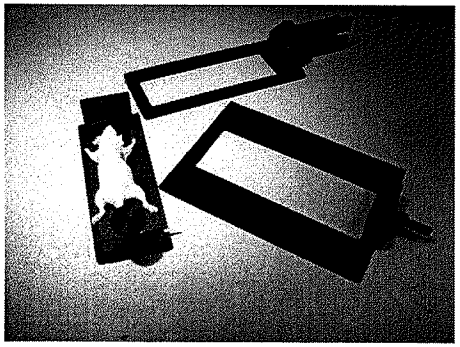

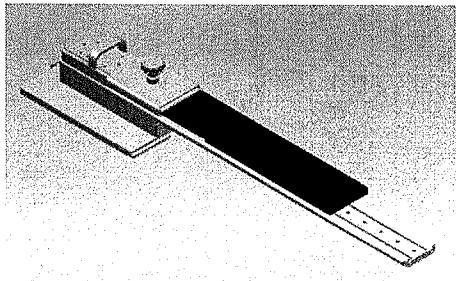

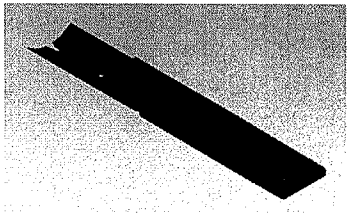

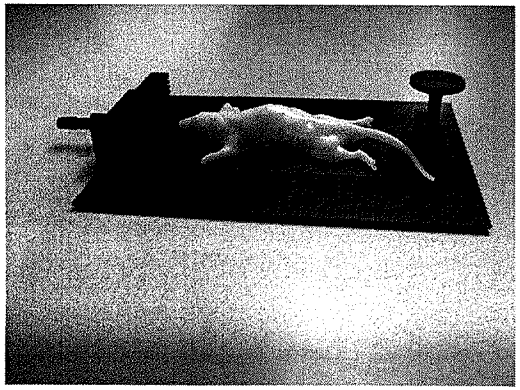

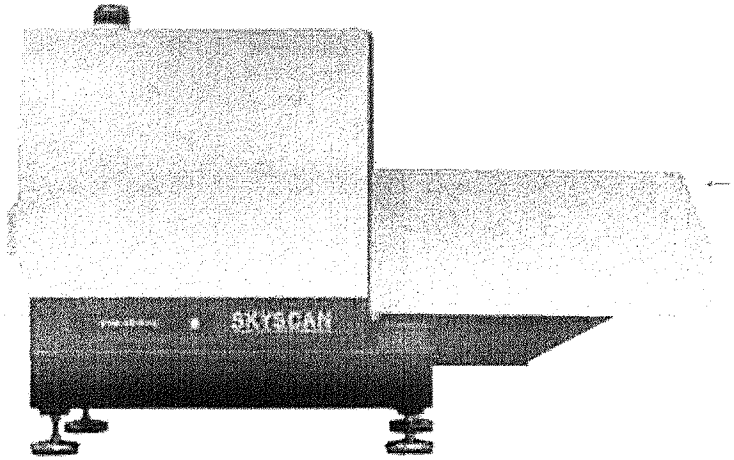

Adaptors Available for Multiple Vendors
Enquire with your local representative

Bioluminescent 3D reconstruction registered with volumetric CT data

MDA-MB-231 Tumor Metastases with Osteolytic Activity ,Day 44

Raw Image Data

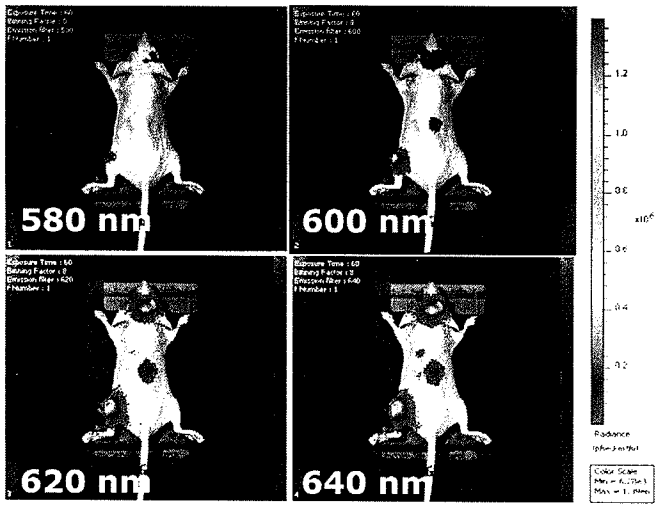

580 nm + 600 nm

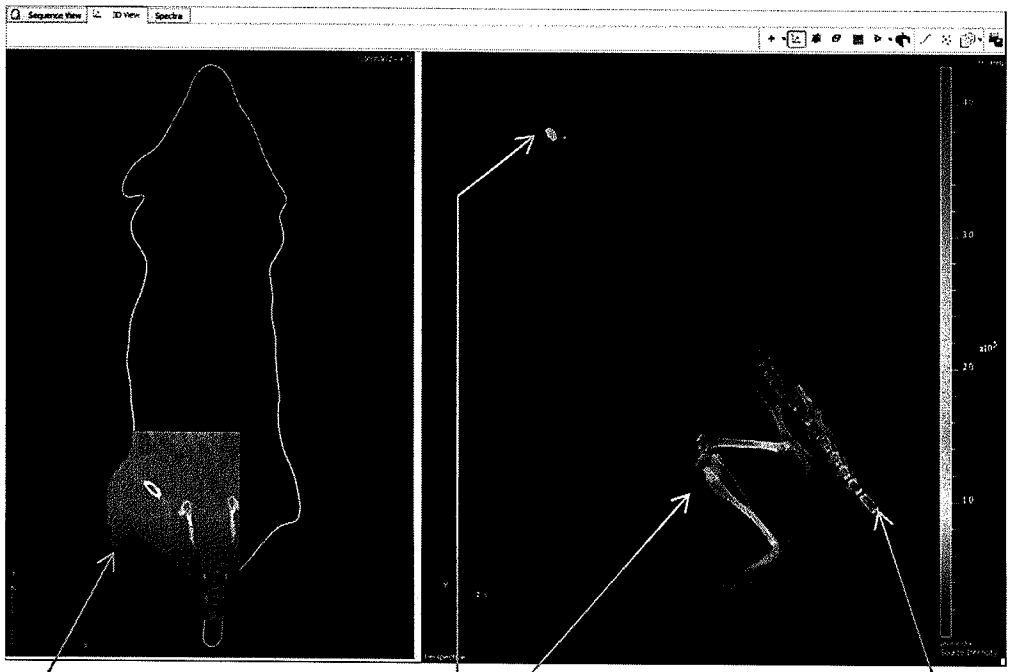

CT slice data

Bioluminescence 3D Reconstruction

Volumetric CT data


Bone degradation
Perspective

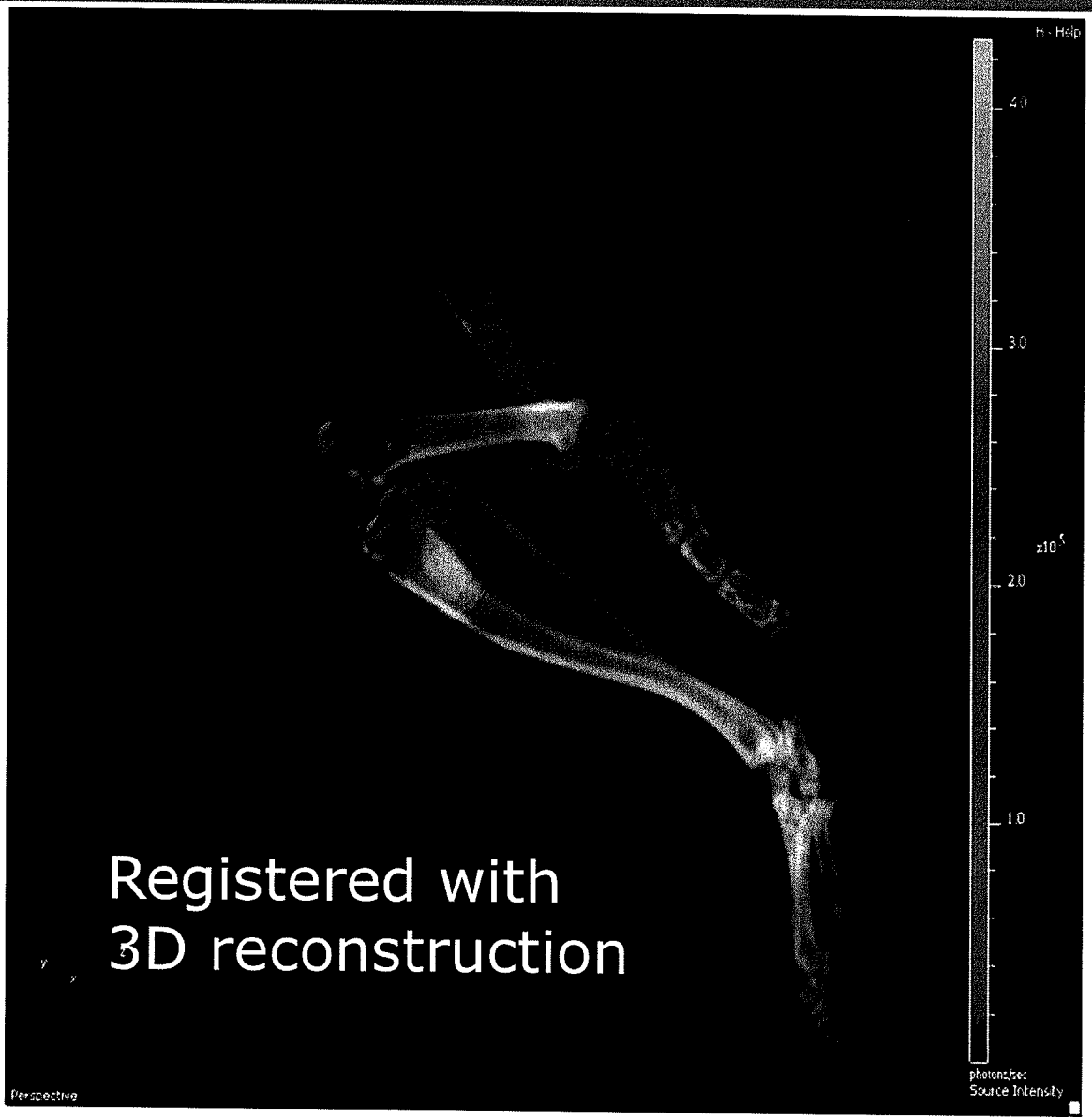

Registered with
3D reconstruction

Liver uptake of Cy5.5

Raw Image Data
Exc 675 nm / Em 720 nm

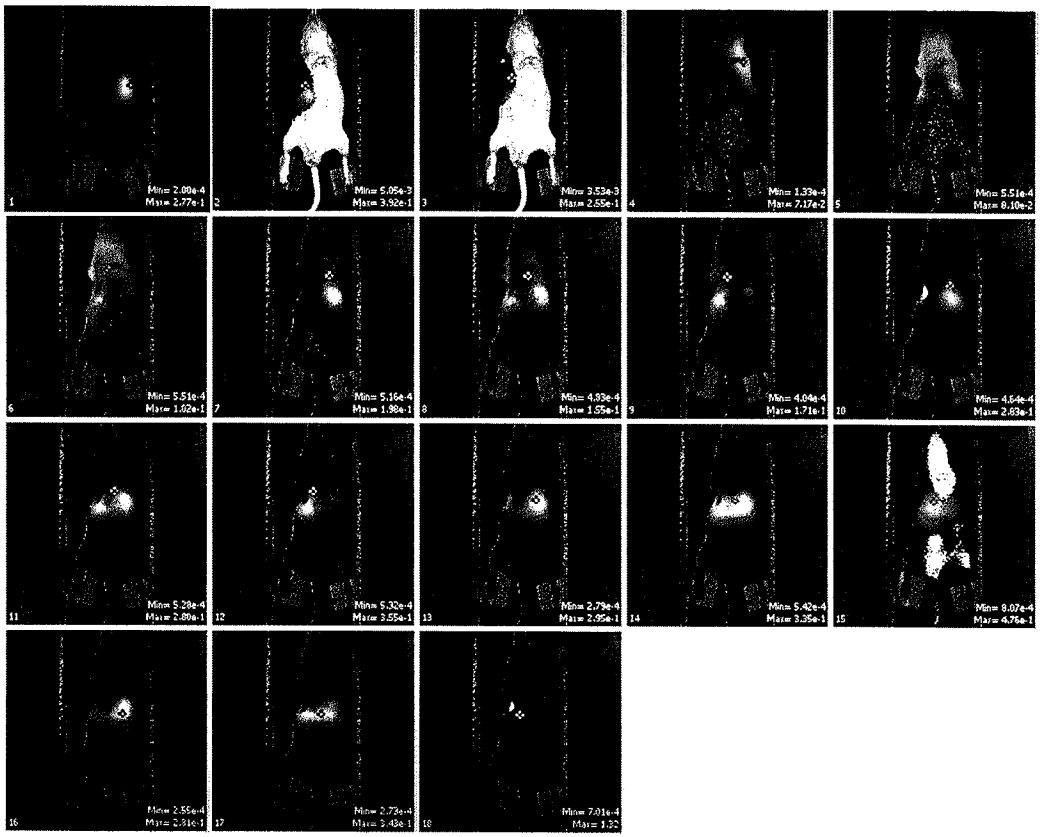

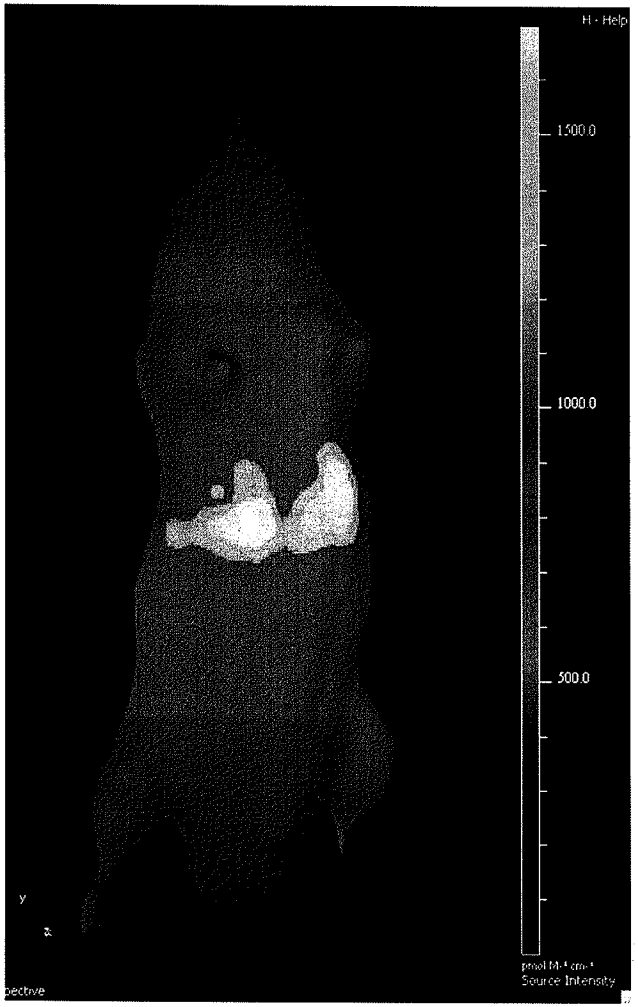

Quantum FX CT data Registration to Structured light surface

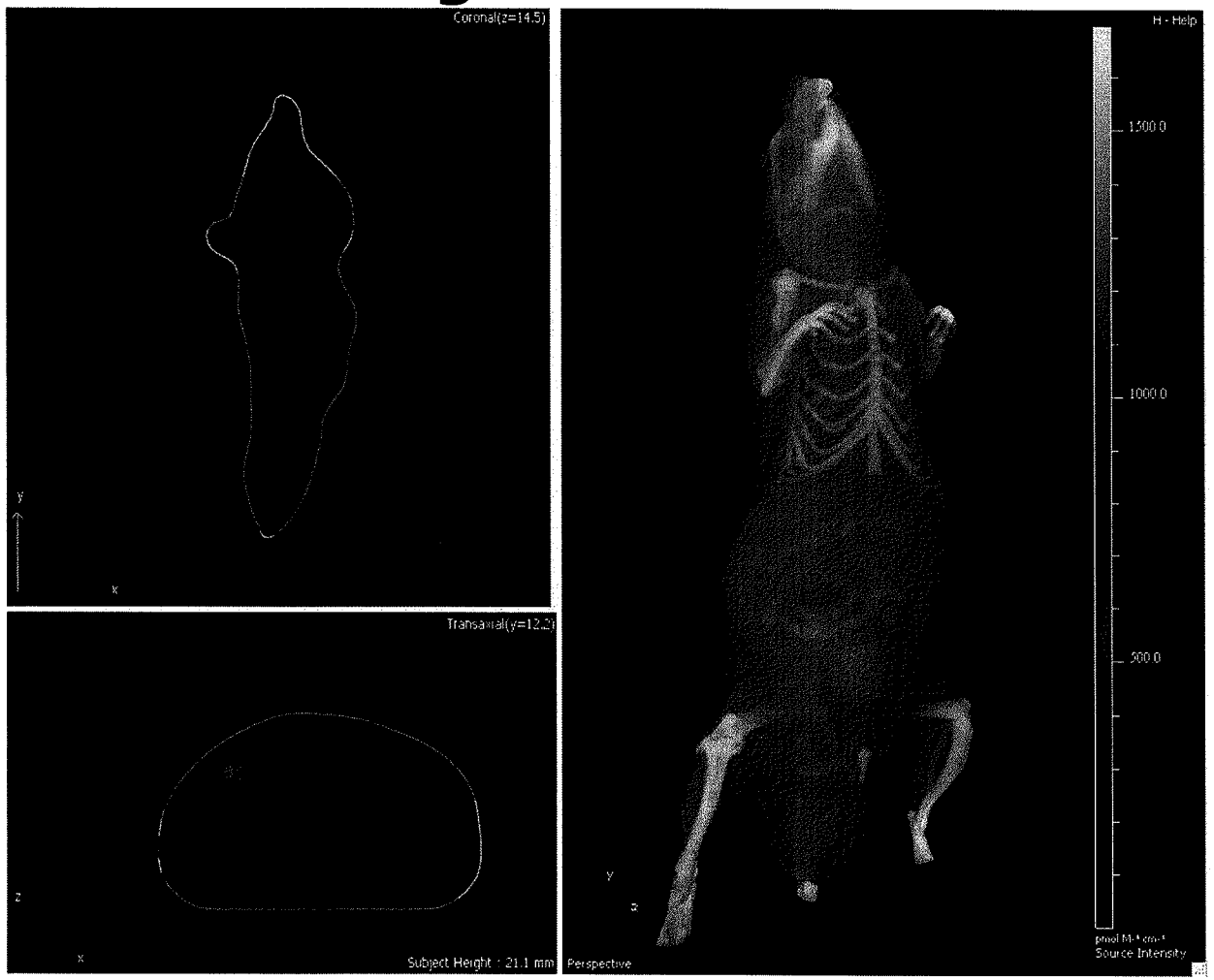

CT volume data intensity adjustment highlights skeleton

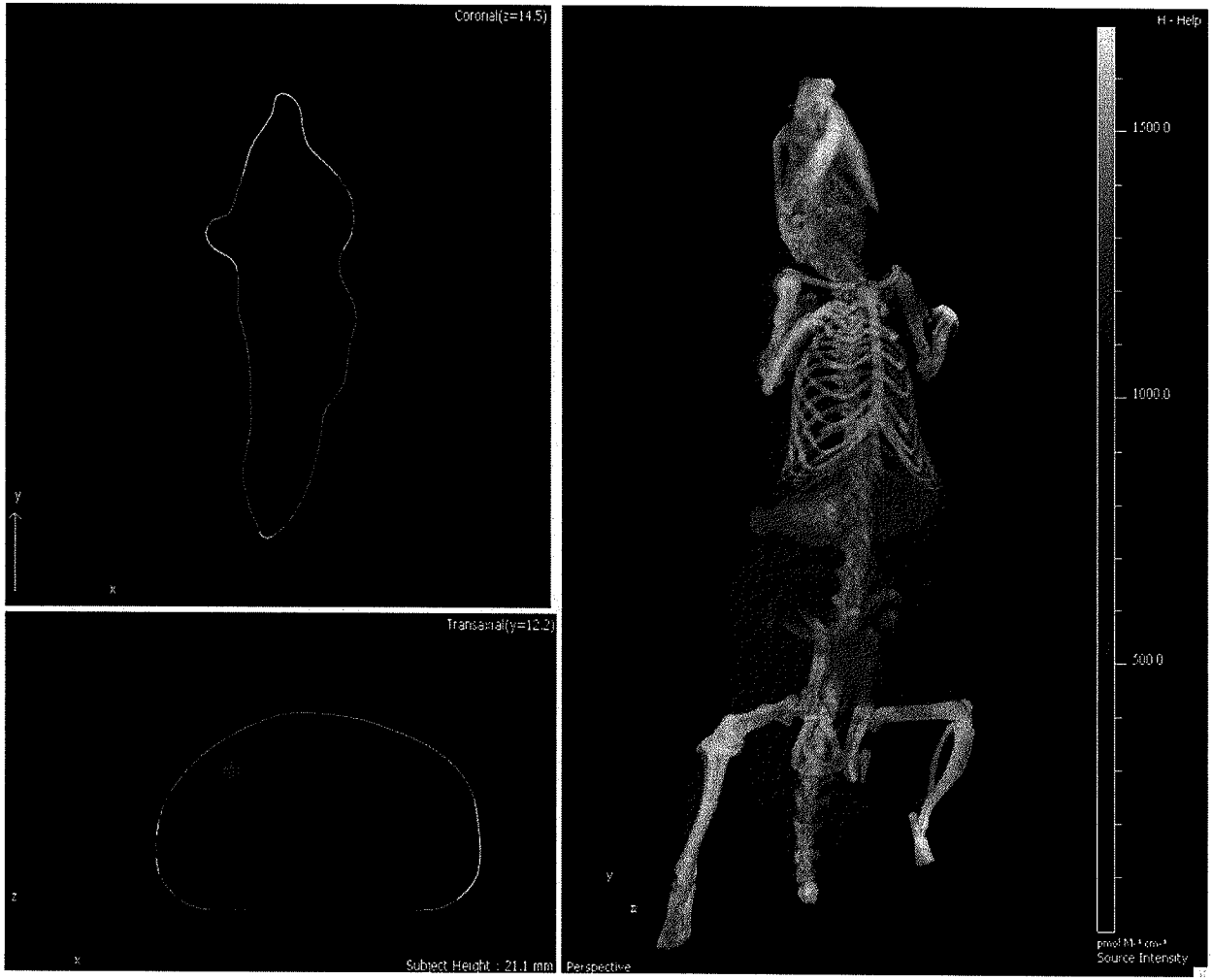

Quantum FX CT data Registration with Cy5.5 distribution reconstruction

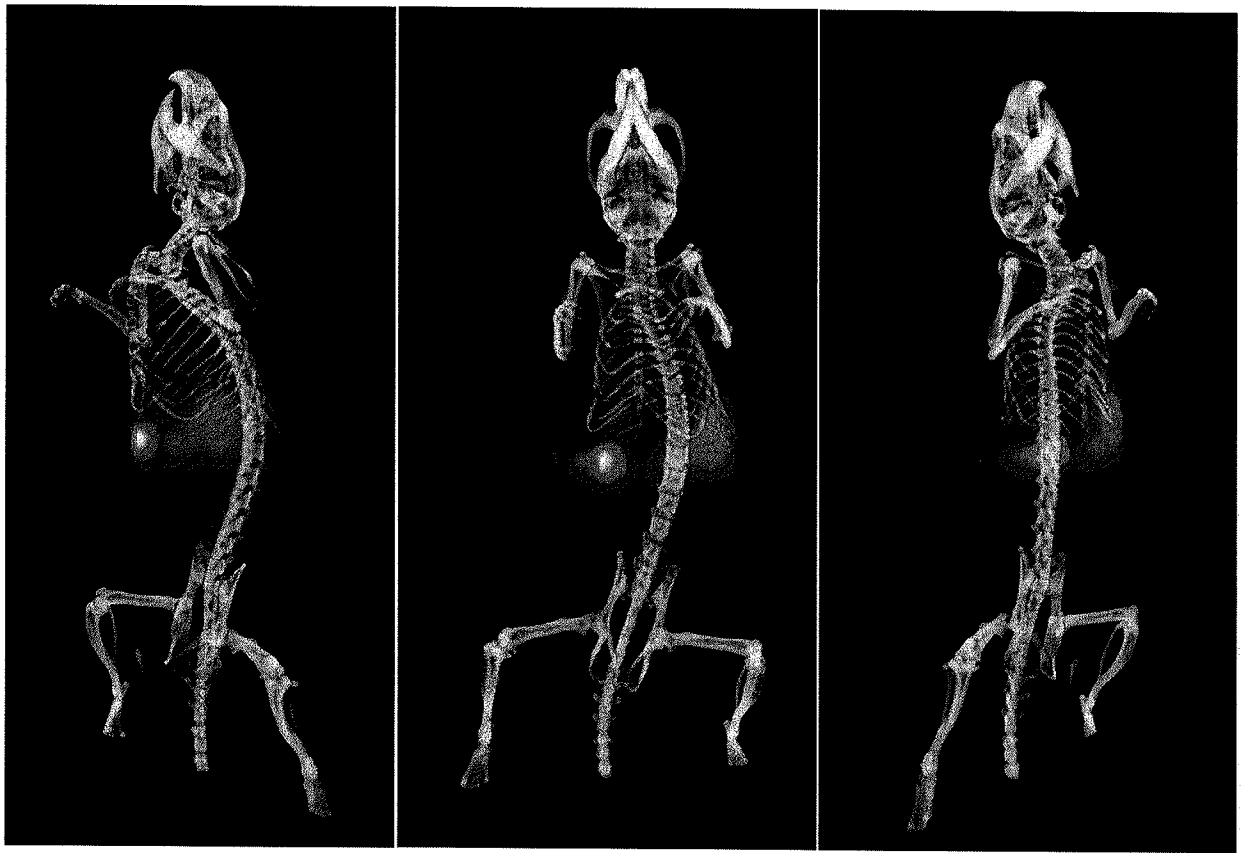

3D Anatomical Information

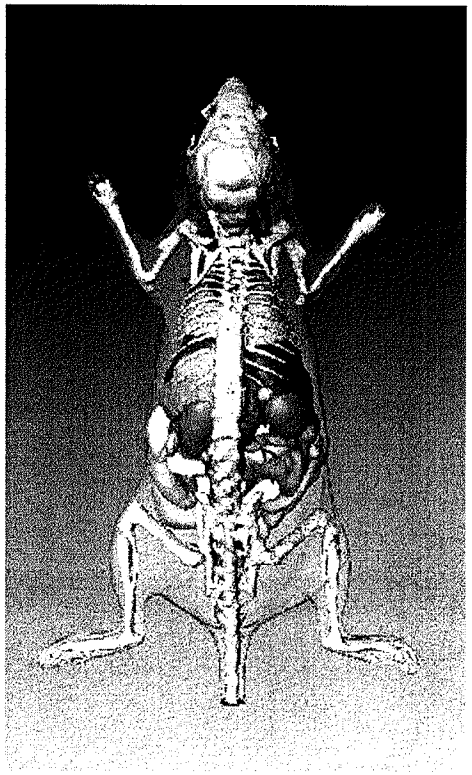

Living Image
Organ Atlas

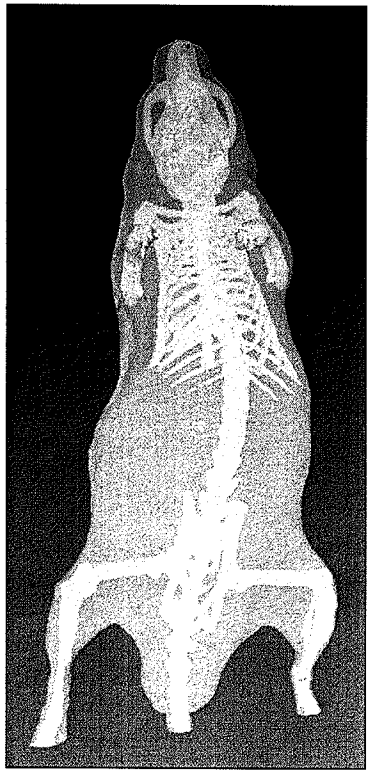

CT/MR-segmented
Isosurfaces

CT

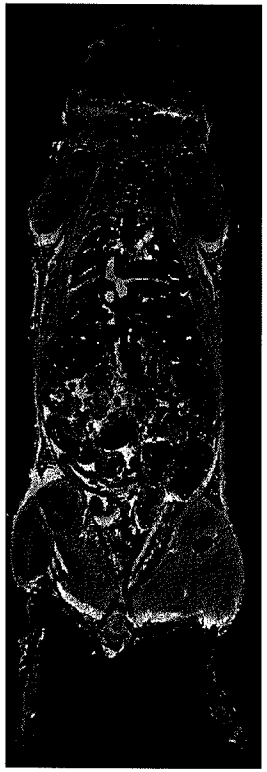

MRI

└Volumetric Data┘

3D Multi-Modality Tools

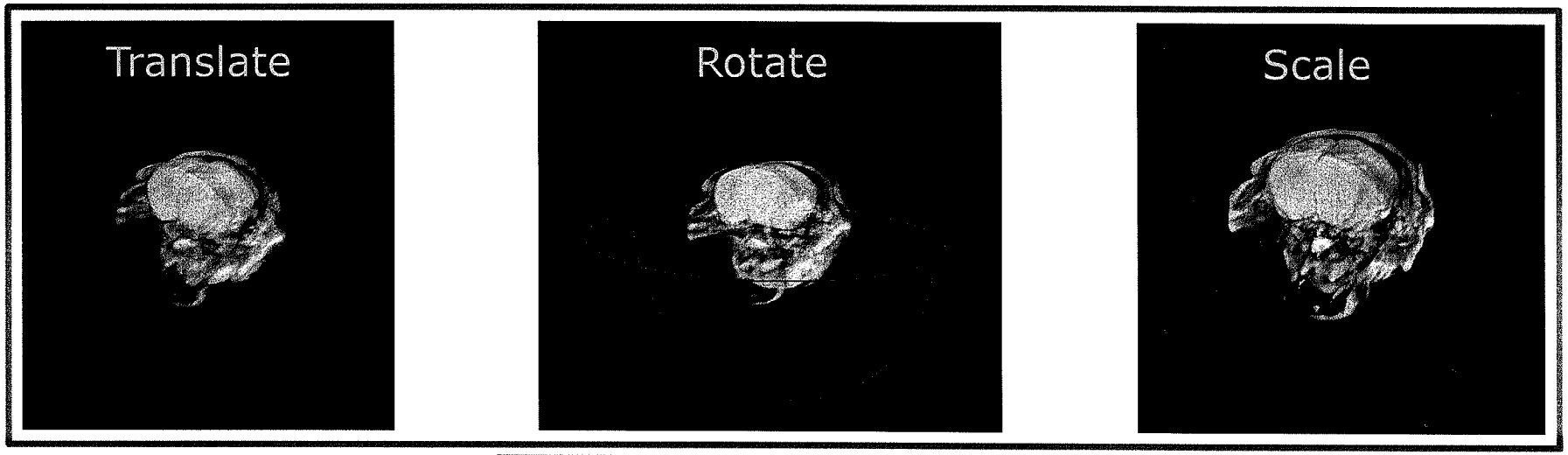

- Import CT/MR data from any system

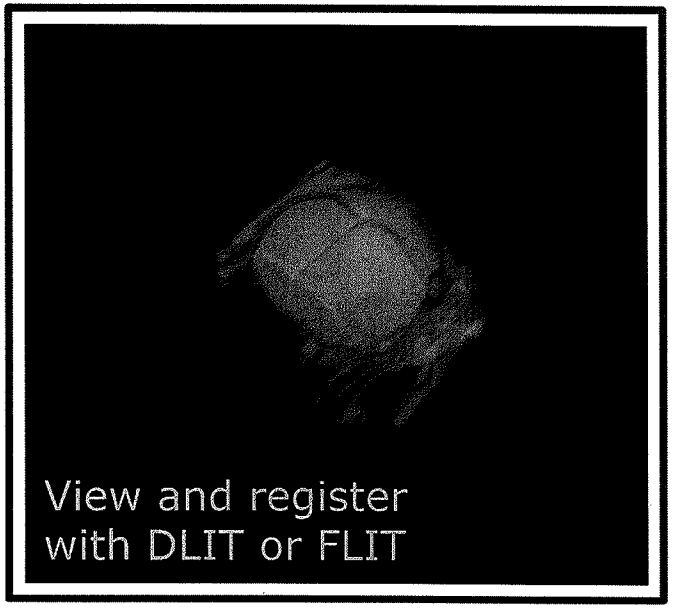

MR volumetric data registered to Bioluminescence 3D reconstruction

GFAP-luc expression due to prion disease

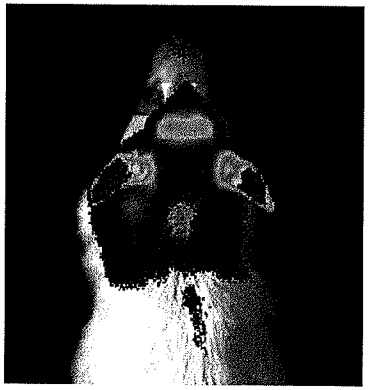

Raw Data

600 nm image

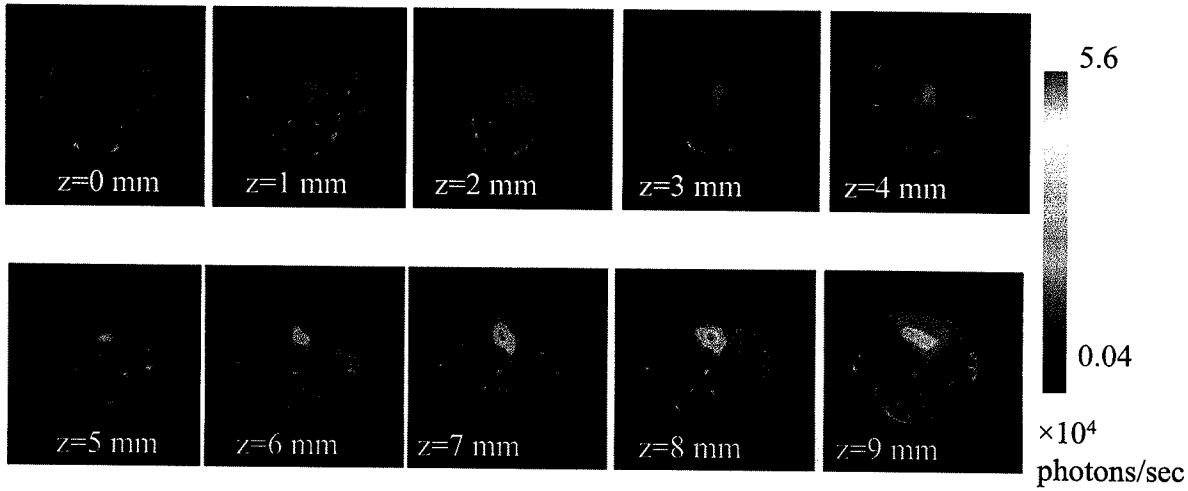

Volumetric MR data

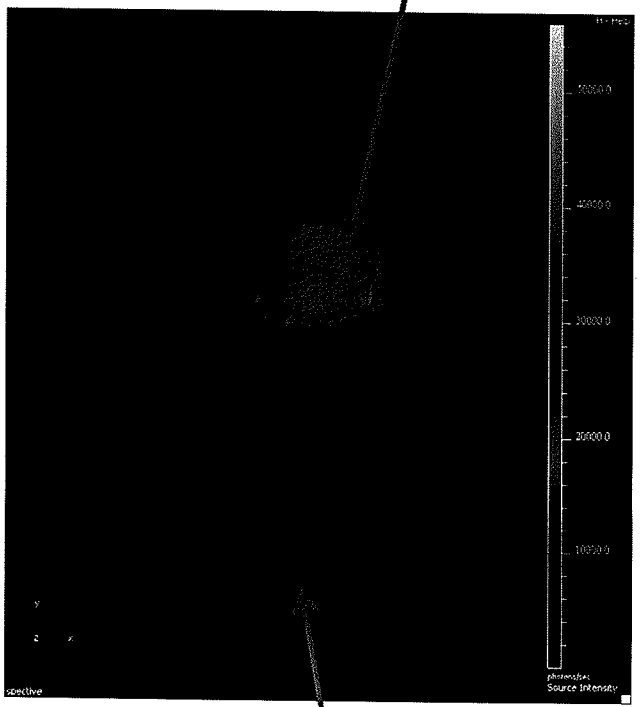

Mouse surface

Metabolism Analysis:

- Fat composition and mapping

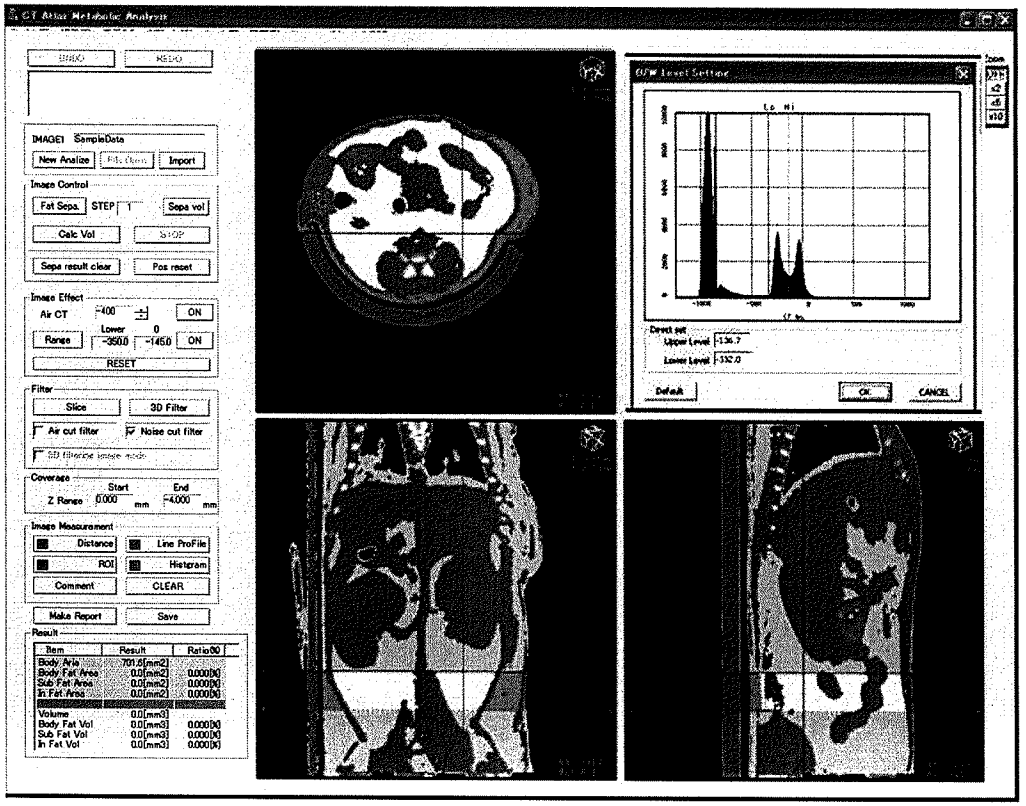

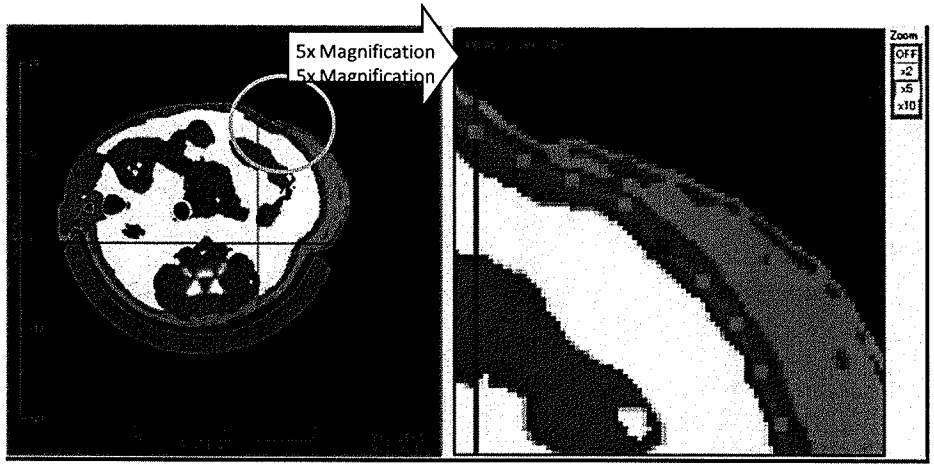

Quantum Micro *CT*

uCT Software

Instrument comes standard with acquisition, reconstruction and basic morphological measurement tools.

Analytical software options:

- Metabolic mapping to show body fat
- 3D alignment to compare bone growth pattern
- Bone mineral density analysis tools
- IVIS co-registration software and kit.

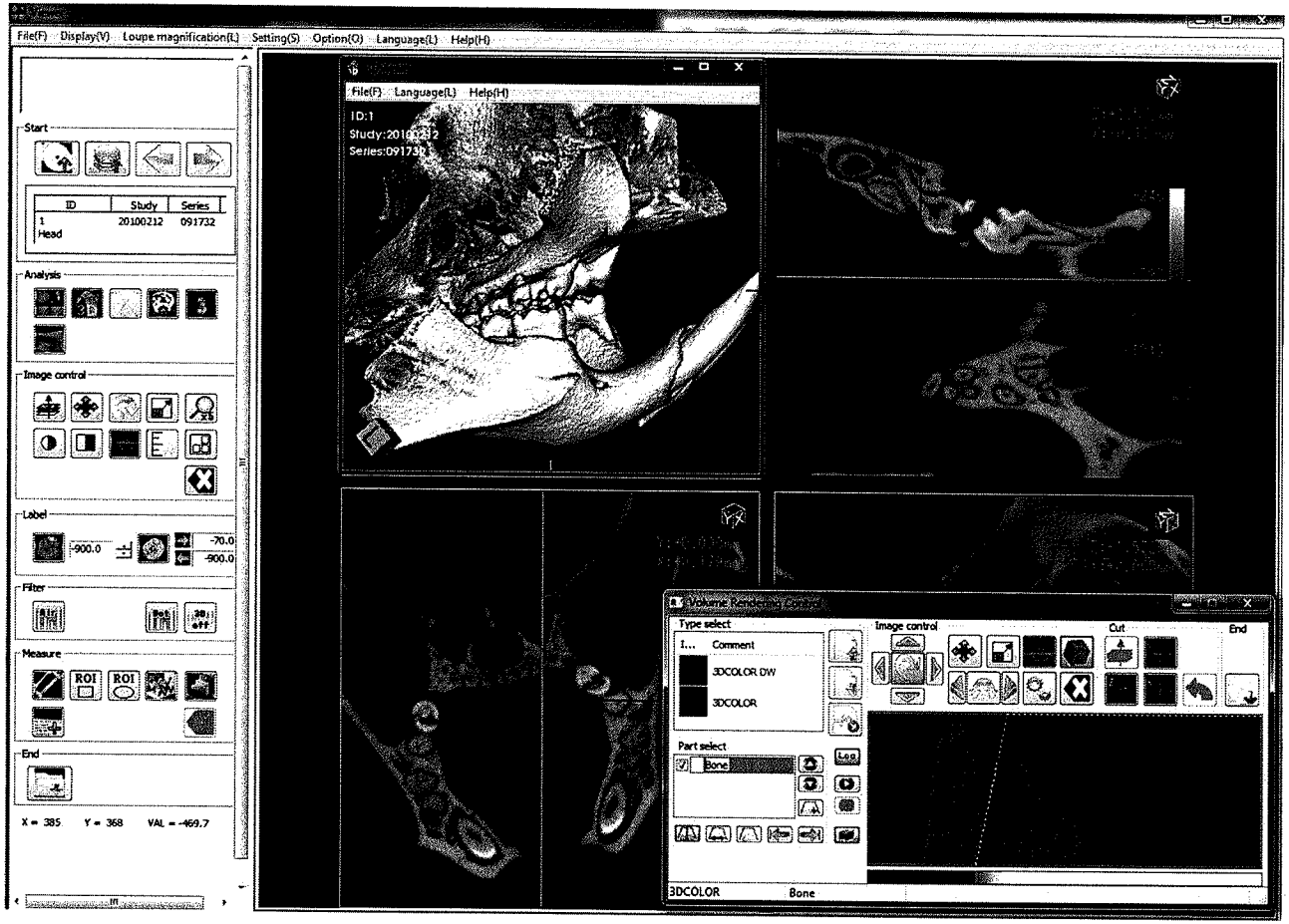

IVIS UNIVERSITY

http://www.caliperls.com/products/optical-imaging

IVIS University Tech Center: Join for free and download the latest Tech notes, Imaging Protocol and Webinar recordings.

IVIS University User Blog: Online user forum to ask questions or post your latest advancement in optical imaging.

Stay Connected and Updated: As an IVIS user, follow the latest new optical techniques and instrument add-on features!

Basic and Advanced Training Courses: Caliper now offers a range of courses on optical imaging techniques for all level of users. Get a better understanding of the principles of fluorescence and bioluminescence small animal imaging or if you need to refresh your skills in spectral unmixing of multiple fluorescence sources, 3D source localization and quantitation.

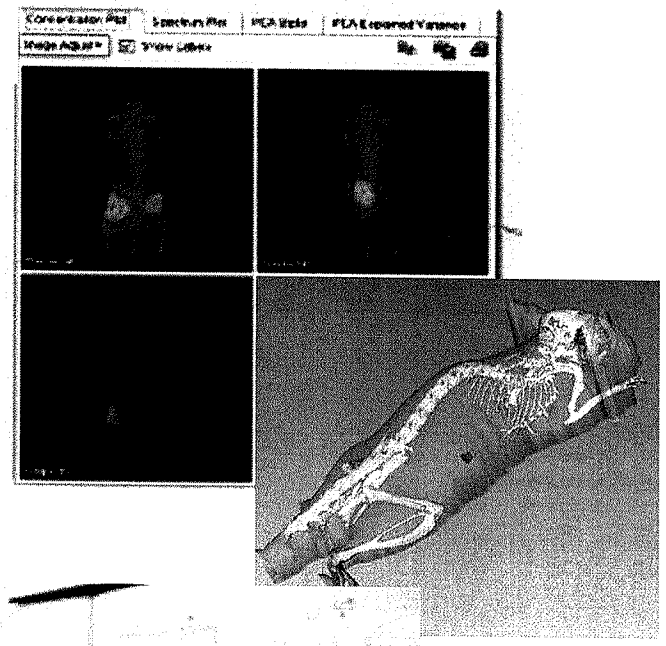

IVIS® University

Hopkinton, MA 01748
P 919-678-0255
elizabeth.bowman@caliperls.com